UNIVERSITAT POLITÈCNICA DE CATALUNYA

Programa de Doctorat:

AUTOMÀTICA ROBÒTICA I VISIÓ

Tesis Doctoral

CONTRIBUTION TO THE STUDY AND DESIGN OF ADVANCED CONTROLLERS. APPLICATION TO SMELTING FURNACES

Juan Manuel Ojeda

Director:

Josep M. Fuertes i Armengol

Juliol de 2013

Dedication

I would like to dedicate this thesis to my wife, who daily contributes to the familiy's support, and to my sons Juan Manuel, Alvaro Juan y Juan Alonso. It is also dedicated to the memory of my father who consecrated his life to the family and to my mother for her endles love.

Acknowledgements

I wish to start this section to first and foremost thank God for being my strength and guide in the writing of this thesis. I would to express my thanks to my thesis advisor, Dr. Josep M. Fuertes i Armengol, and his wife Dr. Eulàlia Griful i Ponsati. This thesis would not have been completed without their expert advice and unfailing patience to correct mistakes of previous versions. I am also grateful to the Spanish Agency for International Development Cooperation. This institution has supported this research in the sometimes-difficult circumstances in which it has been written. Finally, I would like to express my special thanks to my wife who constantly encouraged me to pursue this project, even when bad things has been happened.

Abstract

In this doctoral thesis, contributions to the study and design of advanced controllers and their application to metallurgical smelting furnaces are discussed. For this purpose, this kind of plants has been described in detail. The case of study is an Isasmelt plant in south Peru, which yearly processes 1.200.000 tons of copper concentrate. The current control system is implemented on a distributed control system. The main structure includes a cascade strategy to regulate the bath temperature. The manipulated variables are the oxygen enriched air and the oil feed rates. The enrichment rate is periodically adjusted by the operator in order to maintain the oxidizing temperature. This control design leads to large temperature deviations in the range between 15°C and 30°C from the set point, which causes refractory brick wear and lance damage, and subsequently high production costs.

The proposed control structure is addressed to reduce the temperature deviations. The changes emphasize on better regulate the state variables of the thermodynamic equilibrium: the bath temperature within the furnace, the matte grade of molten sulfides ($\%Cu$) and the silica ($\%SiO_2$) slag contents. The design is composed of a fuzzy module for adjusting the ratio oxygen/nitrogen and a metallurgical predictor for forecasting the molten composition. The fuzzy controller emulates the best furnace operator by manipulating the oxygen enrichment rate and the oil feed in order to control the bath temperature. The human model is selected taking into account the operator' practical experience in dealing with the furnace temperature (and taking into account good practices from the Australian Institute of Mining

and Metallurgy). This structure is complemented by a neural network based predictor, which estimates measured variables of molten material as copper (%Cu) and silica ($\%SiO_2$) contents. In the current method, those variables are calculated after slag chemistry assays at hourly intervals, therefore long time delays are introduced to the operation.

For testing the proposed control structure, the furnace operation has been modeled based on mass and energy balances. This model has been simulated on a Matlab-Simulink platform (previously validated by comparing real and simulated output variables: bath temperature and tip pressure) as a reference to make technical comparisons between the current and the proposed control structure.

To systematically evaluate the results of operations, it has been defined some original proposals on behavior indexes that are related to productivity and cost variables. These indexes, complemented with traditional indexes, allows to assess qualitatively the results of the control comparison. Such productivity based indexes complement traditional performance measures and provide a fair information about the control efficiency.

The main results is that the use of the proposed control structure presents a better performance in regulating the molten bath temperature than using the current control system (forecasting of furnace tapping composition is helpful to reach this improvement). The mean square relative error of temperature error is reduced from 0.72% to 0.21% (72%) and the temperature standard deviation from 27.8°C to 11.1°C (approx. 60%). The productivity indexes establish a lower consumption of raw materials (13%) and energy supply (29%).

Resumen

En esta tesis doctoral, se discuten contribuciones al estudio y diseño de controladores avanzados y su aplicación en hornos metalúrgicos de fundición. Para ello, se ha analizado este tipo de plantas en detalle. El caso de estudio es una planta Isasmelt en el sur de Perú, que procesa anualmente 1.200.000 toneladas de concentrado de cobre. El sistema de control actual opera sobre un sistema de control distribuido. La estructura principal incluye una estrategia de cascada para regular la temperatura del baño. Las variables manipuladas son el aire enriquecido con oxígeno y los flujos de alimentación de petróleo. La tasa de enriquecimiento se ajusta periódicamente por el operador con el fin de mantener la temperatura de oxidación. Este diseño de control produce desviaciones de temperatura en el rango entre $15°C$ y 30°C con relación al valor de consigna, que causa desgastes del ladrillo refractario y daños a la lanza, lo cual encarece los costos de producción.

La estructura de control propuesta está orientada a reducir las desviaciones de temperatura. Los cambios consisten en mejorar el control de las variables de estado de equilibrio termodinámico: la temperatura del baño en el horno, el grado de mata ($\%Cu$) y el contenido de escoria en la sílice ($\%SiO2$). El diseño incluye un módulo difuso para ajustar la proporción oxígeno/nitrógeno y un predictor metalúrgico para estimar la composición del material fundido. El controlador difuso emula al mejor operador de horno mediante la manipulación de la tasa de enriquecimiento de oxígeno y alimentación con el fin de controlar la temperatura del baño del aceite. El modelo humano es seleccionado teniendo en cuenta la experiencia del operador en el control de la temperatura del horno (y considerando el principio de buenas prácticas

del Instituto Australiano de Minería y Metalurgia). Esta estructura se complementa con un predictor basado en redes neuronales, que estima las variables medidas de material fundido como cobre (%Cu) y el contenido de sílice ($\%SiO2$). En el método actual, esas variables se calculan después de ensayos de química de escoria a intervalos por hora, por lo tanto se introducen tiempos de retardo en la operación.

Para probar la estructura de control propuesto, la operación del horno ha sido modelada en base a balances de masa y energía. Este modelo se ha simulado en una plataforma de Matlab-Simulink (previamente validada mediante la comparacin de variables de salida real y lo simulado: temperatura de baño y presión en la punta de la lanza) como referencia para hacer comparaciones técnicas entre la actual y la estructura de control propuesta.

Para evaluar sistemáticamente los resultados de estas operaciones, se han definido algunas propuestas originales sobre indicadores que se relacionan con las variables de productividad y costos. Estos indicadores, complementados con indicadores tradicionales, permite evaluar cualitativamente los resultados de las comparativas de control. Estos indicadores de productividad complementan las medidas de desempeño tradicionales y mejoran la informacin sobre la eficiencia de control.

El resultado principal muestra que la estructura de control propuesta presenta un mejor rendimiento en el control de temperatura de baño fundido que el actual sistema de control. (la estimacin de la composicin del material fundido es de gran ayuda para alcanzar esta mejora). El error relativo cuadrático medio de la temperatura se reduce de 0,72% al 0,21% (72%) y la desviación estándar de temperatura de 27,8 ° C a 11,1° C (aprox. 60%). Los idicadores de productividad establecen asimismo un menor consumo de materias primas (13%) y de consumo de energía (29%).

Resum

En aquesta tesi doctoral, es discuteixen contribucions a l'estudi i disseny de controladors avançats i la seva aplicació en forns metal lúrgics de fosa. Per a això, s'ha analitzat aquest tipus de plantes en detall. El cas d'estudi és una planta Isasmelt al sud del Perú, que processa anualment 1.200.000 tones de concentrat de coure. El sistema de control actual opera sobre un sistema de control distribuit. L'estructura principal inclou una estratègia de cascada per regular la temperatura del bany. Les variables manipulades són l'aire enriquit amb oxigen i els fluxos d'alimentació de petroli. La taxa d'enriquiment s'ajusta periòdicament per l'operador per tal de mantenir la temperatura del procés. Aquest disseny de control produeix desviacions de temperatura en el rang entre 15 $^{\circ}C$ i 30 $^{\circ}$ C amb relació al valor de consigna, que causa desgastos en el totxo refractari i danys a la llana, la qual cosa encareix els costos de producció.

L'estructura de control proposta està orientada a reduir les desviacions de temperatura. Els canvis consisteixen en millorar el control de les variables d'estat d'equilibri termodinàmic: la temperatura del bany al forn, el grau de mata ($\%Cu$) i el contingut d'escòria en la sílice ($\%SiO_2$) . El disseny inclou un mòdul difs per ajustar la proporció oxigen/nitrogen i un predictor metal lúrgic per estimar la composició del material fos. El controlador difús emula el millor operador de forn mitjanant la manipulació de la taxa d'enriquiment d'oxigen i el alimentació per tal de controlar la temperatura del bany de l'oli. El model humà és seleccionat tenint en compte l'operador 'experiència en tractar amb la temperatura del forn (i tenint en bones pràctiques del compte de l'Institut Australià de Mineria i Metallúrgia). Aquesta

estructura es complementa amb un predictor basat en xarxas neuronals, que estima les variables mesures de material fos com coure (%Cu) i contingut de sílice ($\%SiO_2$). En el mètode actual, aquestes variables es calculen després d'assajos de química d'escòria a intervals per hora, per tant llargs retards s'introdueixen a l'operació.

Per provar l'estructura de control proposat, l'operació del forn ha estat modelada basant-balanos de massa i energia. Aquest model s'ha simulat en una plataforma de Matlab-Simulink (prèviament validat mitjanant la comparació de variables de sortida real i allò fingit: bany de pressió temperatura i punta) com a referència per fer comparacions tcniques entre l'actual i l'estructura de control proposta.

Per avaluar sistemàticament els resultats d'aquestes operacions, s'han definit algunes propostes originals sobre indicadors que es relacionen amb les variables de productivitat i costos. Aquests indicadors, complementats amb indicadors tradicionals, permet avaluar qualitativament els resultats de les comparatives de control. Aquests indicadors de productivitat complementen les mesures d'acompliment tradicionals i milloren la informació sobre l'eficiència de control.

El resultat principal mostra que l'estructura de control proposta presenta un millor rendiment en el control de temperatura de bany fos que l'actual sistema de control. (L'estimació de la composició del material fos és de gran ajuda per assolir aquesta millora). L'error relatiu quadràtic mitjà de la temperatura es redueix de 0,72% al 0,21% (72%) i la desviació estàndard de temperatura de 27,8 ° C a 11,1 ° C (aprox. 60%). Els indicadores de productivitat s'estableixen així mateix un menor consum de matèries primeres (13%) i de consum d'energia (29%).

Contents

Chapter 1

Introduction

1.1 Motivation

The main objective of industrial control systems is to keep controlled variables within acceptable ranges (or closely follow certain references). The minimization of output variations under process disturbances highlights the control effectiveness. This aspect is helpful to attain a consistent productivity, and therefore a suitable operation cost.

This situation is specially relevant in extractive metallurgy and in the field of mineral processing, due to market competitiveness and to scarcity of mineral resources. It is well recognized (and reported) by control practitioners, that control reliability and safety can be only achieved by having a robust and solid regulatory lower level.

The control assessment is mainly focused on the variability of process variables, and cover performance characteristics constraints or user specified benchmarks without regarding explicitly the production process. Therefore this criterion is usually unsatisfactory to determine the impact on the process efficiency and how can it affect the productivity.

The control assessment can be improved by using adequate indexes, although this issue is related to control structure and design methodologies, which have been the focus of considerable efforts in the mining industry. This aspect has motivated the present academic research in order to contribute to this field of the

study.

1.2 Problem statement

1.2.1 Context of the problem

This research is focused on the copper smelting process and complementary activities like concentrate handling and oxygen production. Typical core ores contain between 0,5% and 2% of copper in form of sulfides. The most common source is the chalcopyrite ($CuFeS_2$). The raw material is crushed and ground to get the copper mineral grains.

This process of comminution is a previous step before the Cu is isolated in a flotation circuit. The crushed ore along with water is mixed with lime slurry into ball mills. This mixture is further crushed by a rotating drum to obtain a fine powder, which is discharged to flotation cells. In this system, blown air and foaming agents are added to create a froth.

The copper mineral is selectively attached by the air bubbles and risen to the cell surface, where the floated Cu-mineral particles are agglomerated. The resulting enriched concentration becomes between 20 - 30% of copper. The concentrated material is carried to the belt system for its transport into the Isasmelt furnace.

This technology is addressed to smelt copper concentrate. The pyrometallurgical process allows to separate copper from iron and sulfur. This separation is performed in a slag bath. In the Isasmelt mechanism this phase presents two reaction sites in one vessel (independent each other), one for fast oxidation and other for slow reduction.

The oxidizing reaction produces a molten sulfide containing 50 - 70% copper, slag and gases. The chalcopyrite concentrate and added fluxes react with the dissolved magnetite ($Fe_2O_3.FeO$), which is formed by oxidizing the fayalalite slag (FeO). The required oxygen for this reactions is delivered through a top submerged lance.

As a result, the copper matte and slag are periodically tapped and mechanically settled, while gases from smelting are treated to be converted in sulfuric

acid. The resulting matte (65% Cu) is sent to conventional converting and the residuary slag (0.7% Cu) is discarded. The critical variables are the oxygen enrichment rate, the molten temperature, the matte grade and the slag composition.

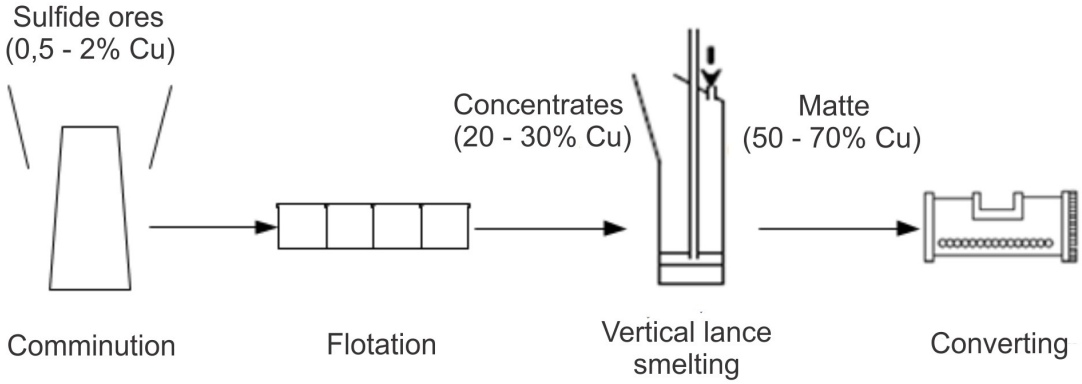

Figure 1.1: Main processes for extracting copper from sulfide ores

1.2.2 Limitations and complexity

The metallurgist defines the type and quantity of raw materials that will be blended and added to the furnace. The mass and energy balance of every concentrate bin and fluxes determines the feed recipe composition. This standard combination is entered into the distributed control system, so that the control operator can set smelting values at the panel control (see figure 1.2).

The smelting process within the Isasmelt furnace is carried out at temperatures between 1180°C and 1190°C. The heat required to sustain the thermodynamic reactions is given by the sulfur content of the copper concentrate (95%). The energy supplement to keep a heat balance is sourced from coal and eventually from oil.

The bath temperature is regulated by a cascade control strategy (see figure 1.3) The schema includes a PID controller as the primary loop. The output signal (by comparing set point and process values) is transmitted to the main control. This controller remotely fixes the respective set-points of the inner components. That means the single PID control blocks of oxygen, blown air and oil.

Figure 1.2: Smelting setpoints

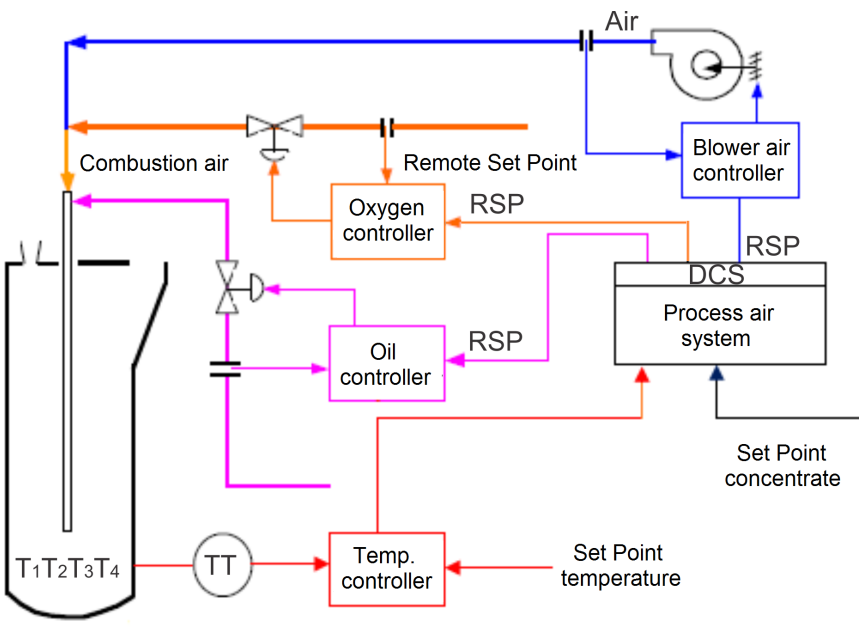

Figure 1.3: Cascade control schema

The temperature is firstly controlled by adjusting the oxygen-enrichment rate ($\%O_2$) in the combustion air ($\dot{w}_{air}$) (represented in 1.1). The oxygen mass flow ($\dot{w}_{O_2}$) is calculated by the concentrate, coal and oil requirements (1.2). Coal is also used for coarse regulation of the temperature ($\pm 20°C$) and fuel oil is applied for fine temperature control ($\pm 5°C$).

$$\dot{w}_{air} = \frac{\dot{w}_{O_2}}{\%O_2} \tag{1.1}$$

$$\dot{w}_{O_2} = k_1 \dot{w}_{conc} + k_2 \dot{w}_{coal} + k_3 q_{oil} \tag{1.2}$$

Temperature variations are common during copper smelting not only due to multiple compounds and chemical reactions, but also to slow time constants and long time delays. The operation design creates temperature deviations about 30°C on average. This event causes an operator over-activity and leads to poor performance control (figure 1.4).

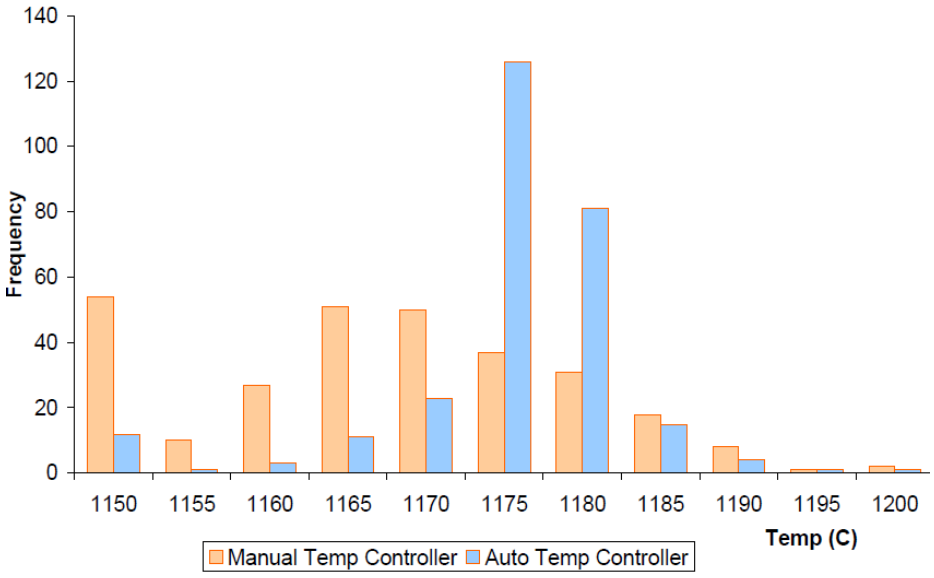

Figure 1.4: Temperature automatic control - 2007

The optimal furnace operation is dependent upon the operator skills to regulate the bath temperature and additional intensive properties at the thermodynamic equilibrium state (the silica factor, the matte grade and the SO_2 pressure).

Unfortunately such manual regulation becomes ineffective to keep these variables within their adequate operation range.

Large temperature deviations affect the life of refractory furnace lining and submerged injection lance, for example if is too high, brick wear increases (see figure 1.5) and lance life decreases (see figure 1.6). The over-temperature trips can produce plant shut downs.

Figure 1.5: Brick wear just prior to removal

The product quality is also affected by the temperature control. In effect, the matte grade is controlled by the ratio of the amount of O2 added via the Lance to the amount of feed material. If the feed materials composition is constant, then more oxygen will increase the matte grade, and less oxygen will decrease the matte grade (see figure 1.7).

1.2.3 Controller performance

Controller performance monitoring and assessment are critical in such applications. There are stochastic and deterministic methods to analyze this control behavior. The common methods involve a comparison of control features to some

Figure 1.6: Lance tip wear

Figure 1.7: Slag sample

standard. This metric relates stability, time response and variance to a specific patron.

This task is performed through shear number of loops on distributed control systems (DCSs) but mainly using fewer resources to reach the same level of service. There are several software packages to easily and accurately obtain controller quality metrics and to monitor all aspects of their control loops, and this data is available on the DCS or plant registers.

These techniques ideally cover special requirements such as follows: independence of disturbance or set-point spectrum, plant testing or process dynamics, able to be automated, adequate metrics to identify performance issues. This kind of methods do not cover explicitly economic aspects. Although, advanced process control projects present the achievable variance in economic terms.

This methodology is generally based on the variance of process variables and this variability is related to a monetary value. A performance function defines either profit or loss in comparison to an optimal operation point. However, this approach is not representative enough to determine its impact on the process efficiency.

Common assessment criteria compare the controller performance to zero variance in reaching setpoints. This metric links the deviation of controller performance to a minimum variance controller as benchmark comparison. Alternative methods propose the use of performance indexes, as the ratio of the best achievable variance to the controlled variable under evaluation.

However, such methods require accurate process and disturbance models, without regarding the economic approach of advanced control projects knowledge. A performance function only requires a process insight and expert knowledge without regarding the economic impact on the production facility. This is an industry current problem at the time to decide a control strategy.

A primary difficulty of controller performance monitoring is the shear number of loops to be monitored - a typical large processing operation consists of hundreds of control loops, often operating under varying conditions. The majority of the controllers use the PID algorithm, but there may also be advanced multivariable model-based controllers and other application specific controllers.

In the past decades there has been a considerable effort on developing adequate

indexes for these tasks, but this effort has been mainly focused on operating conditions Jelali [2010]. Any controller performance methodology must separate out the effects of plant disturbances (which are external to the controller) from tuning, equipment problems, and out-of-service issues.

1.2.4 Research questions

To sum up, the main problem of current control assessment can be described by the following questions:

How to formulate and solve control problems of complex processes (with non-linearity and long time-delays) as pyro-metallurgical processes, considering the molten bath temperature control within an Isasmelt copper smelting process as a case study?

- Which methodology is suitable to design a control structure?
- Which techniques and control structures are adequate to regulate those metallurgical processes?
- How to assess the controller performance in such processes?
- Which kind of index is more representative to this question?

1.3 Objectives

The general objective of this thesis is to contribute to the study and design of control systems in pyro-metallurgical processes, using fuzzy logic and neural network techniques. This contribution will be specifically applied to regulate the molten bath temperature in the copper smelting process.

- To establish a control system to regulate the molten bath temperature in the copper smelting process.
- To study and design a control structure to this complex process. The methods and techniques should achieve desired responses in real scenarios such as the case application.

- To establish adequate methods for the controller performance assessment.
- To introduce suitable indexes for assessing control and process performance.

1.4 Methodology

Once determined the scope of the research based on the problem statement, a deductive approach has been applied to establish the hypotheses by using advanced control methodologies. The state of the art review has included conventional PID and advanced control theory, specifically fuzzy based control applications in thermal processes, and also artificial intelligence techniques, model predictive control and controller performance assessment.

The case of study is a smelter located in South Peru, whose operation data is used to contrast the research hypothesis (observing periods run from December 15th to 30th, 2007; December 15th to 30th, 2008 and during June 2010). From these results, inductive reasoning works the other way, moving from the specific observations to detect patterns and regularities, which finally end up developing some general conclusions.

The contributions of this research can be applied in a similar way to different thermal processes. This is a broad generalization of control theory to complex processes. This research has been developed at the following stages:

1. Data are collected to provide information about the copper smelting process. This information is gathered by direct observation and questionnaires to the process responsible. The schema includes a description of the Isasmelt furnace operation, production plans, maintenance and failure statistics.

2. Information handling covers analysis, description, indexing, classification, cataloging, condensation, storage and bibliographies. It has also received expert advice on key issues of intelligent systems and control theory. Finally, the results reported have been published in engineering journals in the final-year research dissertation.

3. Isasmelt plant modeling:

(a) Description of the Isasmelt process.

(b) Metallurgical process modeling.

(c) Main technical specifications.

(d) Furnace simulation.

4. Development of an advanced control system using fuzzy techniques and neural networks.

5. Testing and discussion of results:

   The results are obtained by comparing the current and the advanced control structure. Comparisons are performed by using an OPC server, so that process variables from the current furnace operation are manipulated by controllers on the simulated model. In this evaluation, performance and productivity based indexes are analyzed.

   (a) off-line testing of the current conventional and advanced controllers.

   (b) On-line testing of control structures using performance and productivity indexes.

1.4.1 Hypotheses

The research variables are the thermodynamic equilibrium parameters, control structure design, controller performance assessment, performance based index, productivity based index, advanced controller, pyro-metallurgical process (mining industry).

The hypotheses are as follows:

- Complex thermal processes can be improved by using advanced control techniques.
- The study and design of metallurgical processes are critical issues to establish a suitable control system.
- Productivity based indexes provide fair information about operating controllers in such complex processes.

- Performance based indexes at the supervisory layer are complementary to productivity based indexes.

1.4.2 Thesis structure

The content of this thesis is structured as follows:

Chapter 2 presents the literature review of metallurgical process modeling, fuzzy based control theory and related performance assessment methods, which are central themes of this research. This survey is complemented by the theoretical background of modern furnace processes and control performance assessment, as well as economic analysis of such techniques.

Chapter 3 describes the smelting mechanism of copper sulfide concentrates, which occurs within the Isasmelt furnace. This process has been mathematically modeled based upon first order heat/mass balance equations. Then, after modeling this plant for control purposes, the dynamics of the molten bath temperature is analyzed. This analysis enables a comprehension of the temperature behavior, which leads to the plant transfer function.

Chapter 4 details the current control system, composed of the following components: the temperature control subsystem, the oxygen control subsystem, the tip pressure control subsystem and the actuator subsystem. This description includes the main control parameters and their operation features. This chapter concludes with closing remarks.

After that, chapter 5 presents the proposed control structure to regulate the furnace bath temperature. The properties of thermodynamical equilibrium are analyzed for helping to improve control features. This approach includes a fuzzy controller for adjusting the oxygen enrichment rate, a predictive module for forecasting the tapping composition (matte grade of copper and SiO2 in the slag) and the tip pressure control.

In chapter 6, the furnace simulation based on the mathematical model is validated by comparing simulated output variables (bath temperature and tip pressure) and real plant data. The current and proposed control structure are discussed in detail, considering their performance in dealing with the molten bath temperature. In testing both control systems, error lectures with respect to the

temperature set point are initially considered as main index. The results are also compared by using productivity based indexes. This comparison analysis is complemented by single productivity indexes, such as tonnes of smelted concentrate per ton of coal and per liter of oil.

Chapter 7 presents the conclusions and summarizes the main contributions, and give some advices for further research. The conclusions are based on concluding remarks at end each chapter. After this section the most important references are presented, which have been consulted in carrying out this investigation.

Finally complementary material is in the appendix.

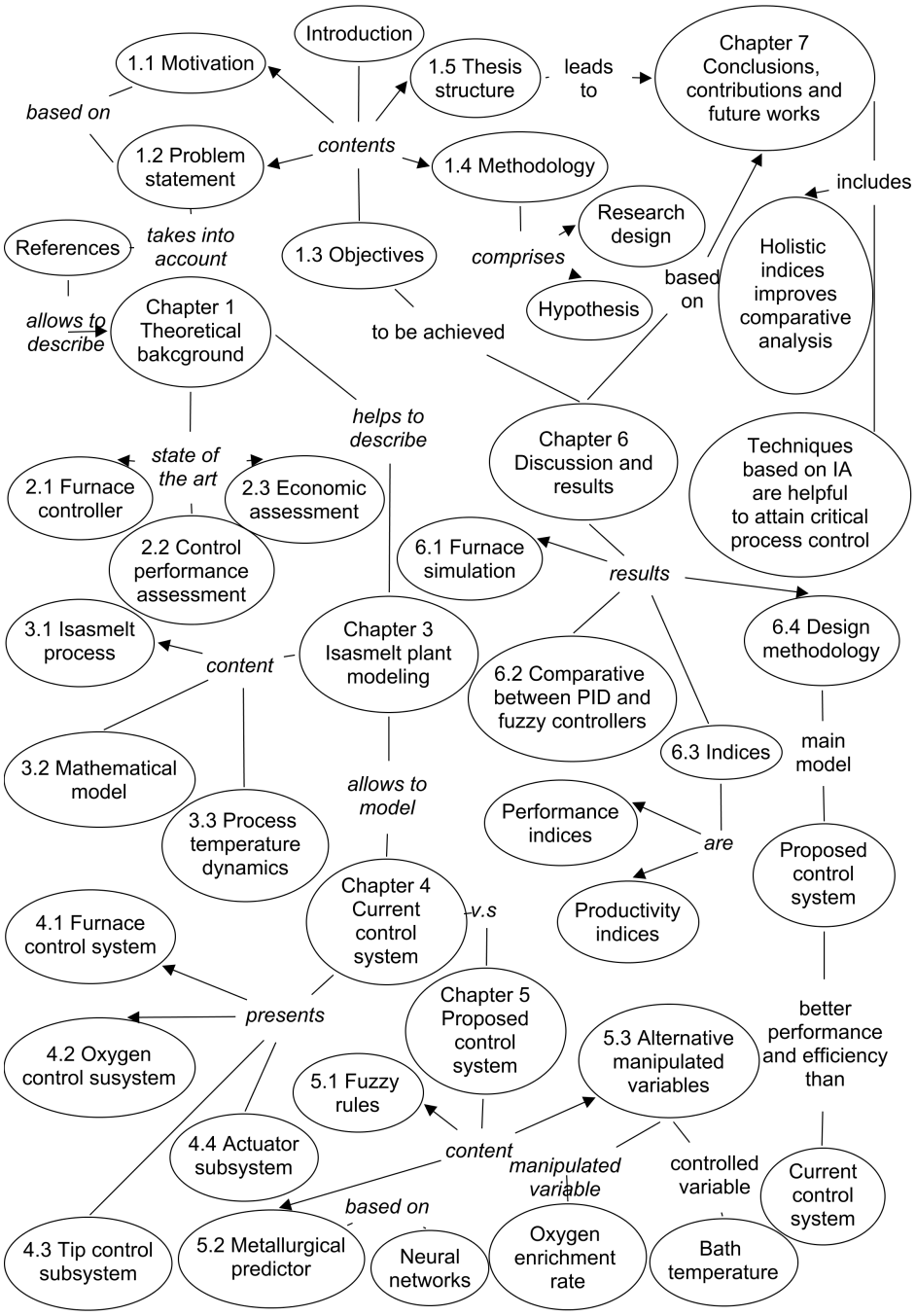

Figure 1.8: Thesis structure

Chapter 2

Theoretical background

The aims of this chapter is to present the theoretical background of control systems and their application in the extractive metallurgy. This approach is complemented by the fuzzy control theory, the analysis of indexes of performance and current methods to link those measures with an economic assessment.

This approach begins with an introductory synopsis of the automation in the mining industry. Its also presented the modern furnace technologies. Likewise, the features of modern copper smelting process are dealt with in detail. It then follows a brief review of system identification methods.

This analysis is used to build the mathematical model of the copper smelting process. The model allows to simulate the dynamics of furnace, which is used to analyze control and usual structures. The last two sections are focused on the fuzzy control theory and the methods for control assessment.

2.1 Furnace process control

Process control is long established in the copper mining industry. In the 1950s single loop pneumatic controller was a common part of their processes. In the early 1970s automatic control systems were introduced in flotation circuits and in concentrator operations McKee [1999], and became common in pyrometallurgical processes.

The smelting furnaces exhibited injecting control mechanisms through sub-

merged tuyeres (by Noranda and Teniente Converter) or injection lances (by Isasmelt) to increase smelting rates by bath agitation King [2007]. All the modern processes aim at a rapid oxidation of chalcopyrite with oxygen enriched air to produce a high-grade matte.

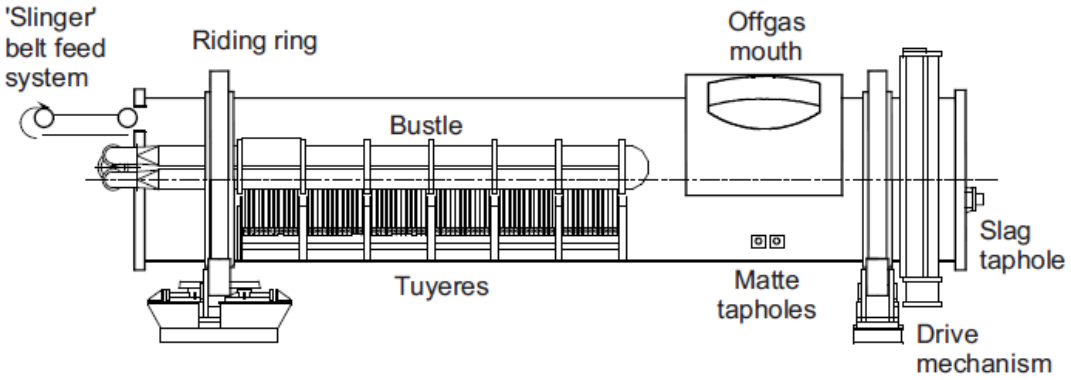

Figure 2.1: Noranda smelting furnace (Schlesinger et al. [2011])

This reaction is instantaneously produced at the oxidizing site, which takes place in the slag phase simultaneously with matte and gas phases. In other words, the thermodynamic equilibrium is achieved when matte, slag and gas coexist within the furnace at the same time. These technologies have driven up the copper grades of mattes (from molten material).

In Noranda process, the matte composition is controlled by adjusting the ratio of total oxygen to concentrate feed rate (2.1). The oxygen is provided by blowing enriched air through tuyeres, which are submerged into the slag. This means that the matte grade (70-74%Cu) is linearly dependent on such ratio. This mechanism allows a rapid increase of Cu concentration in the slag.

$$\%Cu_{matte} = \frac{total\ O_2\ input\ rate}{solid\ feed\ input\ rate} \tag{2.1}$$

The matte/slag temperature is controlled by adjusting the ratio (2.2) and may be so controlled by regulating the ratio (2.3) of the tuyeres blast Zapata [2007].

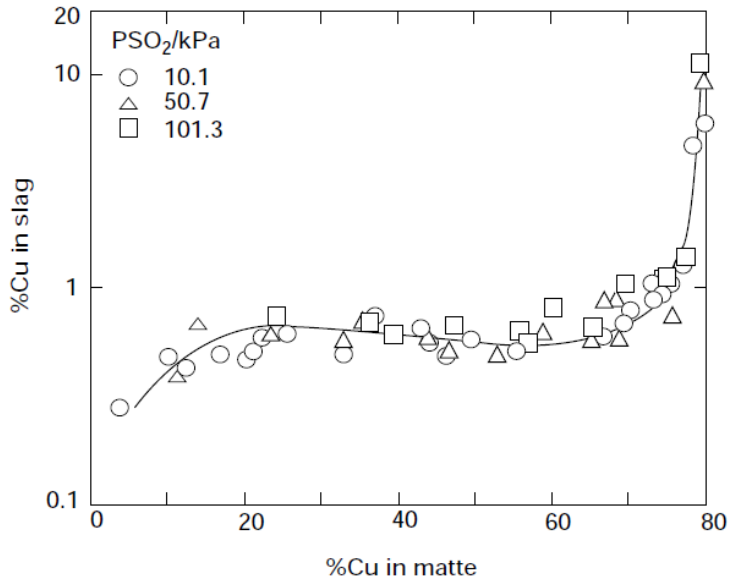

Figure 2.2: Solubility of copper in fayalite slags at 1300°C in equilibrium with mattes of increasing grade (Roghani et al. [2000])

$$T_{matte/slag} = \frac{hydrocarbon\ combustion\ rate}{solid\ feed\ mixture\ input\ rate} \tag{2.2}$$

$$T_{matte/slag} = \frac{N_2\ input\ rate}{O_2\ input\ rate} \tag{2.3}$$

Teniente smelting shares some features with Noranda process: the oxygen enriched air injection and concentrate feeding through tuyeres, and similar matte grade (70-74%). The matte composition is controlled by adjusting the ratio (2.4) and the slag temperature is controlled by the revert feed rates and blast oxygen enrichment level Morrow and Gajaredo [2009].

$$\%Cu_{matte} = \frac{O_2\ input\ rate}{concentrate\ feed\ rate} \tag{2.4}$$

However, the Isasmelt furnace was originally developed for primary lead smelting, this technology has been widely used for smelting copper sulfide concentrates. The process is based on the top-down submerged Sirosmelt lance, which provides the oxygen enriched air instead of using conventional tuyeres.

2.1.1 Process modeling

The thermodynamic of the Isasmelt process for copper matte production was first modeled by Nagamori Nagamori et al. [1994]. This computer model was derived to simulate the behavior of the minor elements Zn, Pb, As, Sb, and Bi as well as the major elements Cu, Fe, Si, O, and S within the furnace.

This model established two independent reactions sites in the bath slag phase, that means a fast oxidation from chalcopyrite and siliceous flux, and slow reduction with lump coal. The BASIC based computer program is comprised of some 820 equations and four iterative loops, but the main equations are written as follows.

$$H_{in} = \sum_{i} n_i(a_i + b_i T_i) \tag{2.5}$$

$$H_{in} = H_{sl} + \sum_{j} (a_j n_j) + T_p \sum_{j} (b_j n_j) \tag{2.6}$$

$$T_p = \frac{\left[H_{in} - H_{sl} - \sum_{j} (a_j n_j) \right]}{\sum_{j} (b_j n_j)} \tag{2.7}$$

where H_{in} is the total enthalpy of the input system, T is the temperature of the furnace feed and n is the number of moles of each species. The subscript summation (i) represents 23 input substances and the subscript summation (j) refers to 25 output substances.

The thermodynamical model was developed to scale up the pilot plant with a capacity of 15 tons/hour for full-scale Isasmelt furnaces. This study enables a comprehension of the thermodynamic process at matte smelting temperatures, specifically the behavior of minor elements like antimony and arsenic.

The interest in their activity is the common presence of such impurities in copper ores. Their elimination to produce high-purity products has been the focus of successive researches Nagamori [2001], Coursol and Stubina [2005], Chen et al. [2010].

However this model enables a systematic evaluation of the operating condition, the smelting mechanism is based on Aksoy equilibrium. This reaction sequence

given in (2.8) has been reconsidered by the current approach (2.9).

$$2CuFeS_2 + 2,5O_2 \rightarrow Cu_2S + FeS + FeO + 2SO_2 \tag{2.8}$$

$$\begin{aligned} 6CuFeS_{2(s)} + 18Fe_3O_{4(l)} \rightarrow 54FeO_{(l)} + 7SO_{2(g)} + 3Cu_2S_{(l)} \\ +2FeS_{(l)} + 4FeO_{(l)} \end{aligned} \tag{2.9}$$

In the interim Mount Isa Mines undertook an advanced control project to improve the Isasmelt temperature control. The mathematical modeling of this system is based on first-principles and black box techniques MacLeod et al. [1995]. This model contains gross simplifications and assumptions which are their major limitations. In this work, it is assumed that the mass of the gas and vapour products is negligible, however represents close to 50% of the amount mass.

In a similar way this equation affects the dynamic energy balance. Although this approach has been addressed to describe the temperature behavior this only occurs over a limited range.

In general there are three perspectives on modeling copper smelting process: first principle, gray box and black box approaches. The first principle technique refers to models based on physical and chemical laws, e.g. mass and energy balances, thermodynamic equilibrium, chemical reaction kinetics or mass and heat transport phenomena.

In the gray and black box approaches the model is as a result of empirical descriptions. The gray box approach is the combination of white box based on internal analysis, while black box describes a model in terms of its input, output and transfer characteristics without internal observation.

2.1.2 Process simulation

The purpose of the process simulation is to understand the plant operation. The application is performed based on the mathematical model, which can cover steady state and dynamic situations. There are commercial simulation softwares in this field (ANSYS, FLUENT, ABACUS and PHOENIXS), as well in thermodynamic (HSC and METADATA) and properly metallurgical systems (Aspen Plus, METSIM and Speedup).

Furthermore the computational fluid dynamic (CFD) modeling is specially meaningful to represent copper metallurgy processes. This kind of software is useful to describe diverse metallurgical processes, in special multiphase systems which includes aluminum reduction cells, ferro-silicon metal production, tapping and metal refining or metal casting Johansen [2003].

Likewise, the splash generation in bath smelting furnaces is also simulated by CFD modeling techniques Pan and Langberg [2010]. These characterization is helpful for designing a control structure.

2.1.3 Control structure

The control of modern copper smelter generally runs on distributed control systems (DCSs). The architecture is composed of sub-systems controlled by one or more controllers, which are supported by networks for communication and monitoring. The structure is generally composed of lower level loops Cockerell et al. [1999]. This structure can encompass single control loops and multivariable/advanced control loops (feed-forward, cascade, batch, ratio, selective and fuzzy control).

In such control loops a primary controller regulates process variables by sending signals to a controller of a different loop that impacts the process variables of the primary loop. These techniques require careful analysis and clear understanding of the process Moon and Lee [2007]. The objective is mostly to attain stable operation using a low grade of resources and higher production rate.

The thermal state of the furnace heart is a key determinant for the hot metal quality, fuel consumption and productivity. This variable is carefully monitored and controlled. In blast furnaces the lecture is taken after analyzing the silicon content in the hot metal.

This analysis is performed by some techniques like neural networks, evolutionary networks, partial least squares, state space or support vector machines.

This aspect is one of the most studied phenomena. This process is commonly used to produce pig iron (hot metal) in iron and steel plants. The mathematical models for this operation are based on mass, momentum, heat balances or reaction kinetics equations.

The progress in this field covers 1-D model, 2-D gas flow model, 2-D total model, multi-flow or four-fluid model (gas, liquid, solid and fines), 3-D unsteady state model and recently advanced total models like DEM (Discrete Element Method) Ueda et al. [2010].

The lack of objective information from metallurgical production in electric arc furnaces enables the use of some non-intensive artificial intelligence calculi namely fuzzy modeling, qualitative and semi-qualitative modeling, neuro-computing and genetic algorithms utilization Pokorny and Buzek [2003].

Fuzzy based controller has been used in the steel making area to weigh alloy metal into electric arc furnace and implemented Lee et al. [2008] and similar applications Dussud et al. [1998].

There are also integrating approaches which combine conventional and fuzzy control called hybrid controllers. This kind of application was introduced to the temperature control of glass melting furnace. The linear part of the temperature dynamic (crown temperature) is controlled by a PI controller and the nonlinear part (bottom temperature) by a fuzzy system, which are combined in a cascade strategy Moon and Lee [2003].

In this structure, some elements are necessary for the successful process control in mineral and metallurgical plants: people and control/process knowledge, tools and instruments, the technology and support management, technology transfer. Although this approach reduces the temperature standard deviation, this occurs over a limited range and specific plant operating conditions Thwaites [2007].

2.2 Fuzzy controllers

Fuzzy logic systems are usually classified into three types: pure fuzzy logic systems, Mamdani's fuzzy system and Takagi and Sugeno's fuzzy systems Patil and Kolte [2008]. The basic configuration of fuzzy systems consists of classical IF -THEN rules and the fuzzy inference engine. The pure fuzzy system uses this set of rules, also called fuzzy rule base, for building a fuzzy map.

The mapping from the fuzzy rule base in the input universe of discourse $U \subset R^n$ leads to the output universe of discourse $V \subset R$. The logic principle of

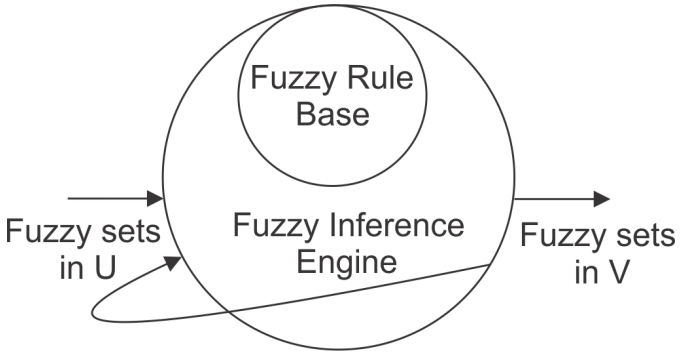

Figure 2.3: Schema of pure fuzzy system

IF - THEN rules are described as follows:

$$R^l : \ IF \ x_1 \ is \ F_1^l \ and \ ... \ and \ x_n \ is \ F_n^l \ , THEN \ u \ is \ G^l \tag{2.10}$$

where F_i^l and G^l are fuzzy sets, $x = (x_1, ..., x_n)^T \in U$ and $u \in V$ are input and output variables respectively, and $l = 1, 2, ...M$.

Mamdani's model presents a basic structure of fuzzy control system, fuzzyfier at the input and defuzzyfier at the output of the pure fuzzy system, knowledge base and inference engine. Real-valued variables are described by mapping crisp points in U to fuzzy sets in U (fuzzyfier), and by mapping fuzzy sets in V to crisp points in V (defuzzyfier), as is shown in figure 2.4.

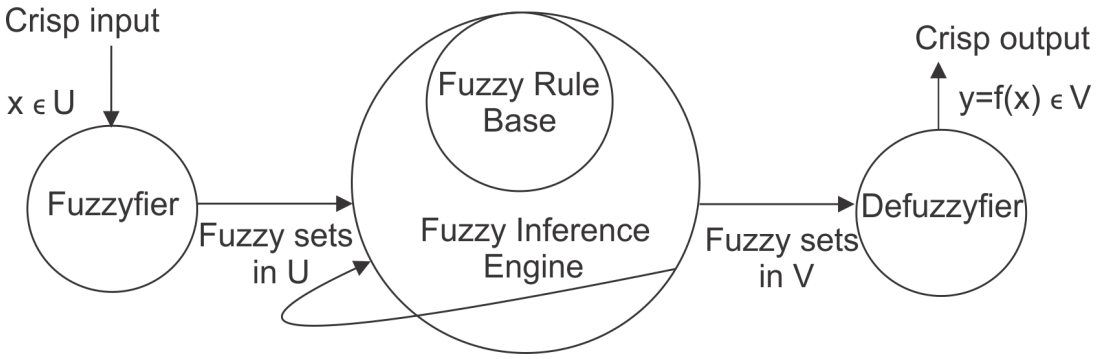

Figure 2.4: Schema of Mandani's fuzzy system

Finally, Takagi and Sugeno's system describes a global nonlinear system in terms of a set of local linear models, connected by fuzzy membership functions.

In T - S fuzzy model the conclusions are denoted by functions instead of fuzzy sets (space UxV); that mathematically means:

$$If\ x_1\ is\ A_{r1}\ and\ x_2\ is\ A_{r2}\ ...and\ x_n\ is\ A_{rn}\ then\ u = f_r(x_1, x_2\ ..., x_n)$$

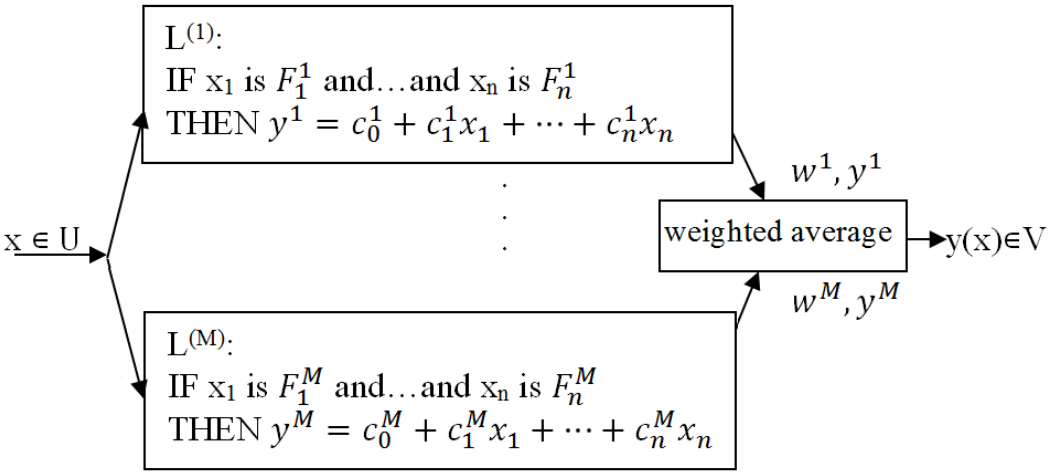

Figure 2.5: Schema of Takagi and Sugeno's fuzzy system

Fuzzy controller is commonly addressed to regulate complex and nonlinear processes, like heating furnaces or similar thermal processes. The features of fuzzy controller enables its application on the industry, because of its flexibility, long lag and simplicity. The engineering applications should enhance conventional control systems Liu et al. [2009], Zenghuan et al. [2010], Lei et al. [2009].

In some cases, algorithms are helpful to improve fuzzy control designs Yun et al. [2009] as the particle swarm optimization technique to tuning temperature factors Zhi et al. [2009]. This method presents variants as the hybrid fuzzy-PID controller, which combines the simplicity of PID structure and the fuzzy ability of handling nonlinearities and uncertainties Jing and Xuesong [2010].

This design presents comparative advantages with respect to pure fuzzy controllers Milans et al. [2011], because overcomes deficiencies of each other Hui et al. [2010]. This method has been successfully applied in a regenerative rotary reheating furnace yong Su and Wen [2010] and in a reduction furnace to optimize the recovery of nickel Ramírez et al. [2004].

In similar way neural fuzzy control is a combination of fuzzy control and neural network. That means, fuzzy reasoning is performed applying neural network techniques. The rules are identified and membership functions learned by neuro-learning algorithms Mitra and Hayashi [2000].

This kind of control scheme also includes tuning parameters in neuro-fuzzy controller via genetic algorithms Wang et al. [2004] or tuning PID controllers via fuzzy neural networks Shen [2001] or adaptive neuro-fuzzy control Li and Lee [2003]. The industrial applications indicate that this system has a high control precision and good reliability Hong et al. [2006].

The Takagi Sugeno's fuzzy based control is an alternative to regulate furnace operations. T - S control methods are based on simple local models. The local structure presents feedback controllers and are combined to obtain a global controller so that global stability with/without various performance indexes of the closed-loop fuzzy control system is guaranteed Feng [2006].

2.3 Control performance assessment

The control performance assessment is addressed to analyze the behavior of controlled loops under changes in the system. A typical control system can be formed by sheer number of control loops, and therefore requires an adequate maintenance for keeping them well tuned.

Performance metrics according to Jelali [2010] share common features, some of which are sensitivity to detuning and detect process model mismatch or equipment problems with independence of disturbances, objectivity and accuracy, easily computation, realistic and achievable. However, the main disadvantage of mostly indexes is the difficulty to convert the metrics into economic measures.

The evaluation methods are usually classified into stochastic and deterministic categories. The stochastic index refers to the variance (or the deviation standard) of the controlled variable or control error. The stochastic based index most commonly studied is the minimum variance controller calculation. This index is based on the variance of the process output, which is compared as a benchmark to the minimal theoretically achievable variance control (MVC) Harris [1989], Yea and Chen [2005]. In turn, deterministic methods include classic performance

measures (i.e. rise time, settling time, overshoot).

2.3.1 Minimum variance indexes

The minimum variance index methods enable to evaluate controller responses by analyzing the process data of controlled variables; this means, the dispersion measure (variability) around the set-point of a well-known control model. However, this method is unable to distinguish such output variations from process disturbances Cano-Izquierdo et al. [2012].

The MVC index method can be described using a CARMA model (2.11).

$$A(q^{-1})y(t) = q^{-d}B(q^{-1})u(t) + C(q^{-1})\varepsilon(t) \tag{2.11}$$

In this model, it is assumed that $A(q)$, $B(q)$ and $C(q)$ are polynomials in q^{-1} of order n, m and p respectively, so that all poles and zeros are inside the unit circle for discrete time.

$$A(q^{-1}) = 1 + a_1q^{-1} + a_2q^{-2} + ... + a_nq^{-n} \tag{2.12}$$
$$B(q^{-1}) = b_0 + b_1q^{-1} + b_2q^{-2} + ... + b_mq^{-m} \tag{2.13}$$
$$C(q^{-1}) = 1 + c_1q^{-1} + c_2q^{-2} + ... + c_pq^{-p} \tag{2.14}$$

where $d > 1$ is defined as the process time delay, expressed as an integer multiple of the sampling interval T_s and $\epsilon(t)$ as a random zero-mean sequence with finite variance, that mathematically means $E\{\varepsilon(t)\} = 0$ and $E\{\varepsilon(t)^2\} = \sigma^2$.

The diophantine equation in 2.15 is used to estimate the model output d steps ahead.

$$E_d(q^{-1})A(q^{-1}) + q^{-d}F_d(q^{-1}) = C(q^{-1}) \tag{2.15}$$

where:

$$E_d(q^{-1}) = 1 + e_1q^{-1} + e_2q^{-2} + ... + e_{d-1}q^{-d+1} \tag{2.16}$$
$$F_d(q^{-1}) = f_0 + f_1q^{-1} + f_2q^{-2} + ... + f_{n-1}q^{-n+1} \tag{2.17}$$

Then, the minimum variance of the error between the set point and the actual output at the time $(t+d)$ is estimated by

$$\underset{u(t)}{Min}\left\{J(t)\right\} = \underset{u(t)}{Min}\, E\left\{y(t+d)^2\right\} \tag{2.18}$$

$$\underset{u(t)}{Min}\, E\left\{\left(\frac{F_d(q^{-1})}{C(q^{-1})}y(t) + \frac{q^{-d}B(q^{-1})E_d(q^{-1})}{C(q^{-1})}u(t) + E_d(q^{-1})\varepsilon(t+d)\right)^2\right\} \tag{2.19}$$

The minimum of the function 2.20 is achieved when the $y(t)$ and $u(t)$ terms are set to zero, therefore the MVC law is

$$u(t) = -\frac{F_d(q^{-1})}{q^{-d}B(q^{-1})E_d(q^{-1})}y(t) \tag{2.20}$$

In consequence, the MVC function becomes

$$\underset{u(t)}{Min}\, E\left\{y(t+d)^2\right\} = E\left\{E_d(q^{-1})\varepsilon(t+d)\right\} \tag{2.21}$$

And is finally given by the expression

$$\sigma\left[1 + \sum_{i=1}^{d-1} e_i^2\right] = \sigma_\varepsilon^2\left[\sum_{i=1}^{d-1} e_i^2\right] = \sigma_{MV}^2 \tag{2.22}$$

The MVC index is estimated by comparing the system-output variance σ to the output variance index σ_{MV}^2. Those index values range within the interval $[0, 1]$. The values close to 1 indicate a good control with respect to the theoretically achievable output variance. The values close to 0 mean a poor control performance.

A closed loop block diagram in standard form is presented in figure 2.6. The output measurement $y(t)$ is a direct function of the disturbance $D(t)$.

2.3.2 Performance indexes for steady state operation

In the case of steady state operation, an useful index is the permanent error (PE), calculated by comparing the set-point and the measured process value S-L.Jämsä-Jounella et al. [2002]. This index is recursively calculated as follows:

$$PE_i = \gamma PE_i + (1-\gamma)p_i \tag{2.23}$$

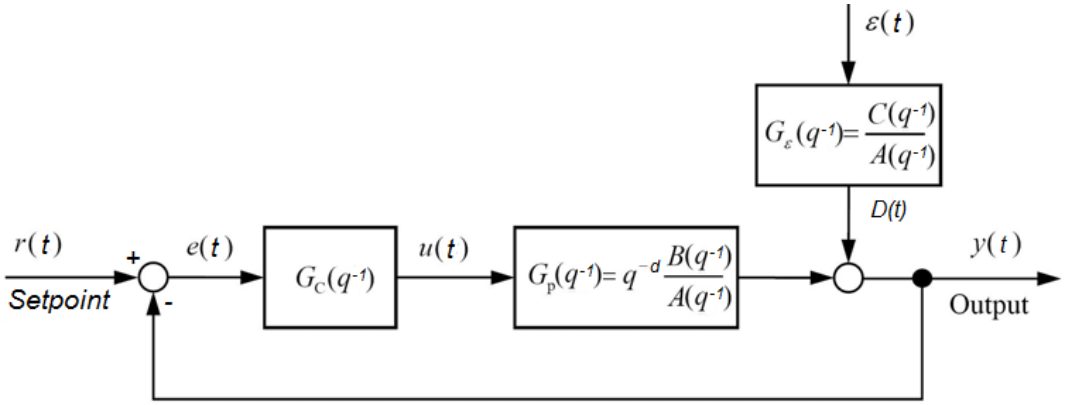

Figure 2.6: Minimum variance controller

where γ is the forgetting factor and $PE_i - 1$ is the previous value of the index.

$$p_i = \begin{cases} -1, e_i < e_{\text{lim}} \\ 0, -e_{\text{lim}} < e_i < e_{\text{lim}} \\ 1, e_i < e_{\text{lim}} \end{cases} \tag{2.24}$$

The forgetting factory is calculated as follows:

$$\gamma = 1 - \frac{1}{5\tau} \tag{2.25}$$

where τ is a specific time constant given by a process cycle.

2.3.3 Deterministic performance indexes

Deterministic indexes are based on step changes in set points or load disturbances to evaluate the control performance. The monitoring is performed during a specific time period, the length of which is used as criteria to describe how well the process responds to changes in the system.

The set-point response criteria are based on a single point of the response function. Such performance metrics are helpful for specifications of starting design and control loops tuning. The basic indexes are the rise time (t_r), the settling

time (t_s), the decay ratio (c/a), the overshoot ($\alpha = 100a/b$) and the steady-state error (see figure 2.7).

However, indexes as rise time and settling time are not enough descriptive separated from the process dynamics, Swanda and Sebog (1999) introduced procedures for calculating normalized indexes. This method enables to obtain non-dimensionless indexes for a rise time and settling time. The normalized metrics relates the rise time and settling time to an approximation of a time constant τ. The dimensionless indexes for a rise time and settling time can therefore be expressed as follows:

$$SPD = \frac{t_{rise}}{\tau} \tag{2.26}$$

and

$$TIME = \frac{t_{setling}}{\tau} \tag{2.27}$$

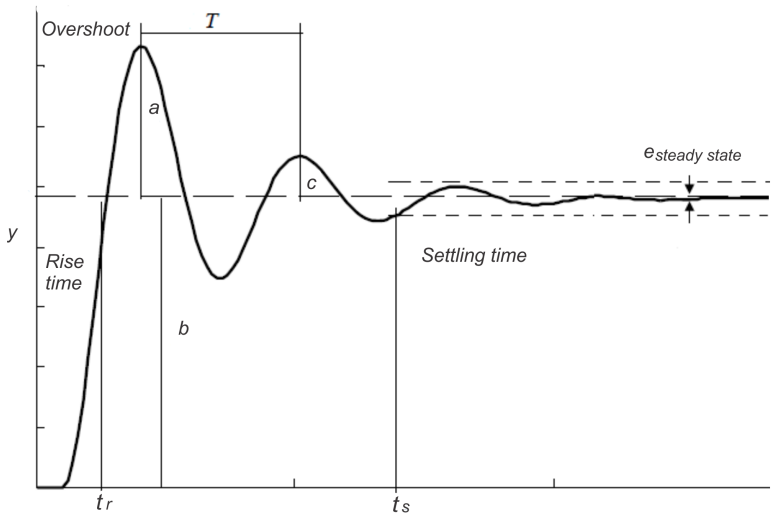

Figure 2.7: Basic indexes

In addition to basic performance indexes, there are traditional metrics based on the error criteria. The cumulative deviation of the controlled variable from specific set-points are determined by simple integration. A performance index to

monitoring large deviations error, which causes great control degradation is the Integral of the Squared Error (ISE). This index is mathematically given by

$$ISE = \int_0^\infty [sp(t) - pv(t)]^2 dt = \int_0^\infty e^2 dt \tag{2.28}$$

where $sp(t)$ is the set-point, $pv(t)$ is the process value and e is the single error.

An index to detect process oscillations around the set-point is the Integral of Absolute Error (IAE). This metrics provides information of the performance controller as linear function with the deviation magnitude.

$$IAE = \int_0^\infty |sp(t) - pv(t)| dt = \int_0^\infty |e| dt \tag{2.29}$$

Likewise, an alternative method to detect oscillations is the IAE_i index, calculated taking into account IAE values from successive set-point crossings of the process value.

$$IAE_i = \int_0^{t_i} |sp(t) - pv(t)| \, dt \tag{2.30}$$

where t_i are the times of successive set point $sp(t)$ crossing $pv(t)$. This index can detect load disturbances, which occur when the value of the IAE_i crosses the predefined value of IAE_{lim}. This bound term is mathematically given by

$$IAE_{\text{lim}} = \frac{e_{\text{lim}} t_{dis}}{4} \tag{2.31}$$

where t_{dis} the duration of a single load disturbance that can be calculated if the frequency of the process is known. Additionally the size if the overshoot can be estimated by measuring the amplitude of the oscillation.

$$AMP = \frac{y_{pv,\max} - y_{pv,\min}}{\Delta y_{sp}} \tag{2.32}$$

where $y_{pv,\max\,/\,\min}$ are the maximum and minimum values of the process measurement after a rise time and Δy_{sp} is the magnitude of the set point change.

Long-term differences from the set point due to continuous oscillations or sluggish controller tuning were chosen to be monitored by calculating the integral of the time-weighted absolute error (ITAE).

$$ITAE = \int_0^{\tau} t\,|y_{pv}(t) - y_{sp}(t)|dt \tag{2.33}$$

which emphasizes long-term deviations.

Stochastic variations around the set point value were selected for detection, e.g. by monitoring the integral of the squared error (ISE),

$$ISE_i = \gamma.ISE_{i-1} + (1-\gamma)[y_{pv}(t) - y_{sp}(t)]^2 \tag{2.34}$$

which highlights the largest deviations. These variations may be too short-term to be detected by oscillation detection procedures, but they can be detected effectively with the ISE. The calculation can be carried out on-line by using a recursive algorithm.

An index denoted as ISU can be used as a measure of how much the control action changes. It is similar to the index ISE

$$ISU_i = \gamma.ISU_{I-1} + (1-\gamma)[u(k) - u(k-1)]^2 \tag{2.35}$$

2.3.4 Performance index for disturbance rejection

Disturbance rejection was chosen to be detected by the idle index. The index is defined by

$$I = \frac{t_{pos} - t_{neg}}{t_{pos} + t_{neg}} \tag{2.36}$$

where the following procedures are updated every sampling instant:

$$lt_{pos} = \begin{cases} t_{pos} + h & \text{if}\Delta u\Delta y > 0, \\ t_{pos} & \text{if}\Delta u\Delta y \leq 0, \end{cases} \tag{2.37}$$

$$t_{neg} = \begin{cases} t_{neg} + h & \text{if}\Delta u\Delta y > 0, \\ t_{neg} & \text{if}\Delta u\Delta y \leq 0, \end{cases} \tag{2.38}$$

and h is the sampling period. The index is bounded to the interval [-1,1]. A positive value of I close to 1 means that the control is sluggish and negative value of I close to -1 is obtained in a well-tuned control loop.

2.3.5 Performance index for valve monitoring

Undesirable performance of a control loop may also result from an inadequate actuator sizing, and not only from poor controller tuning. Therefore an index was developed to monitor the valve capacity. The value of he index describes the time t_{vc} that a valve opening is greater than 90% or smaller than 10% with respect to the time needed to carry out the set point change.

The valve capacity index can therefore be calculated as

$$VC = \frac{\int_0^\tau t_{vc} dt}{\tau} \tag{2.39}$$

where

$$t_{vc} = \begin{cases} 0, x \in [0, 1...0, 9] \\ 1, x < 0, 1 \vee x > 0, 9 \end{cases} \tag{2.40}$$

and x is the valve opening. Values close to zero indicate a correct actuator sizing, and values close to one are a sign of a deficient valve sizing.

2.4 Concluding remarks

In this chapter, the state of the art in the fields of furnace control, performance assessment and productivity is reviewed. The references about furnace control establishes diverse mechanisms in regulating copper smelting processes through submerged tuyeres (by Noranda and Teniente Converter methods) or injection lances.

This analysis includes process modeling and simulation as well as the control structure and the fuzzy theory. However, Nagamori's model enables a systematic evaluation of the Isasmelt process, the reaction mechanism has been reconsid-

ered by current approaches. This model could be improved using first principles techniques and stored data from the real plant.

The control techniques based on fuzzy logic and neural network theory, successfully applied in thermal processes, provide a pragmatic alternative to control pyro-metallurgical processes. The relative simplicity of such engineering solutions facilitates its application to unstable processes, and affect production profits of mining industry.

On the other hand, current indexes to evaluate the control performance are not enough to determine the impact on the process efficiency and how it can affect the process productivity. That means, such indexes are addressed to evaluate design features and operating performance without regarding directly economic aspects of the system.

In this chapter, different performance indexes and their applicability have been presented. In particular minimum variance indexes and performance indexes for steady state operation and deterministic indexes. Such performance indexes can hardly link process variables to monetary values. Therefore it is necessary to define either productivity based indexes (around a specific operating point).

Chapter 3

Isasmelt plant modelling

In this chapter, the copper smelting process within an Isasmelt furnace is modeled. This representation is used to analyze the relation between manipulated variables (concentrate and fluxes) and the controlled output (bath temperature). This analysis covers smelting mechanisms, chemical reactions and thermodynamic properties.

The results of this analysis have allowed to understand the system behavior. The smelting process could have been mathematically modeled and therefore simulated. This simulation will be later used to make analytical comparisons between the current control system and the modified control system design.

3.1 Isasmelt process

The Isasmelt furnace is a tall vertical cylinder supported on a concrete base and covered by a roof from boiler-tube panels. The height of the stationary vessel is 17 m. and its internal diameter is 5,5 m. The furnace is lined with 0,45 m. of chrome-magnetite refractory bricks plus a backing revetment. That means the tapering diameter is approximately 4,4 m (see figure 3.1).

The main component of this system is a single submerged combustion lance, which is lowered into the furnace through a hole in the roof. The vertically aligned steel barrel has an internal diameter between 0,3 and 0,5 m and is 12- 16 m high. This device allows to directly inject oxygen enriched air and oil below the surface

of the slag bath.

Figure 3.1: Isasmelt furnace before being operated

3.1.1 Smelting process

In the smelting process, the furnace is fed by a homogeneous mixture of copper concentrate ($\dot{w}_{conc}$) (containing about 10% moisture), fluxes such as silica ($\dot{w}_{sil}$) and coquina, coal ($\dot{w}_{coal}$), reverts and water ($\dot{w}_{H_2O}$). It is just considered the addition of silica flux (instead of adding silica and coquina) in order to simplify the operating model.

The feed system is composed of conveyor belts with three storage bins for the concentrate and five additional bins for silica flux, limestone, coal, reverts and recycle dust (see figure 3.2). The concentrate is proportionally mixed with the rest of raw materials onto the paddle mixer conveyor. Furthermore water is added (if required) before being delivered to the furnace chute.

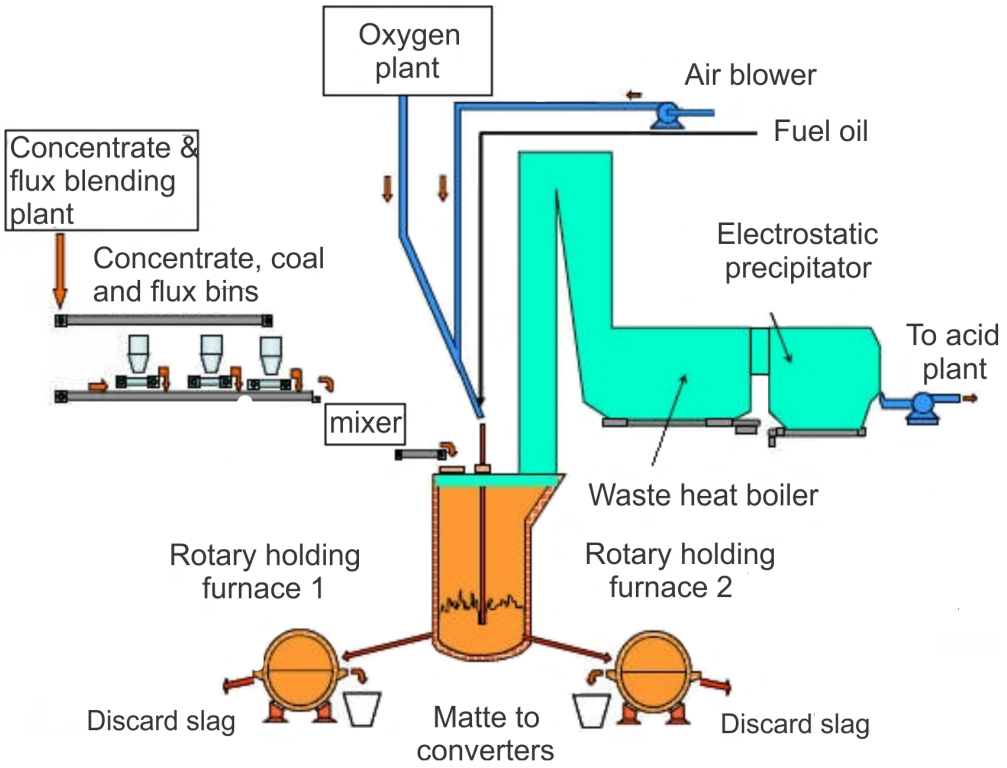

Figure 3.2: Isasmelt copper smelter flow sheet

The concentrate contains on average less than 27% of copper. Its composition is periodically assayed to obtain a high-grade commercial matte of about 60% Cu. This analysis is also necessary to calculate the oxygen demand. The resulting flow rate is maintained by adding industrial oxygen ($\dot{w}_{oxy}$) to the blown air (q_{air}), resulting in enriched air ($\dot{w}_{air}$) with 60% - 70% of oxygen Arthur and Hunt [2005b].

This process yields a sulphide phase commonly called matte (mixed copper-iron sulphide), a slag phase (iron oxide and silica), and offgas phase (mostly sulfur dioxide, nitrogen, water vapour, and carbon dioxide) ($\dot{w}_{gas}$). The molten phases ($\dot{w}_{tap}$) present a significant difference in density, thereby the matte sinks to the bottom and the slag floats on top (see figure 3.3).

The molten material is discharged into the RHF furnace in a semi-continuous process or batch, which allows mechanical settling of matte and slag. The matte obtained by this process is rich in copper, whereas slag is discarded usually after a copper recovery stage. The sulfur dioxide off-gas from smelting are treated to

be converted into sulfuric acid.

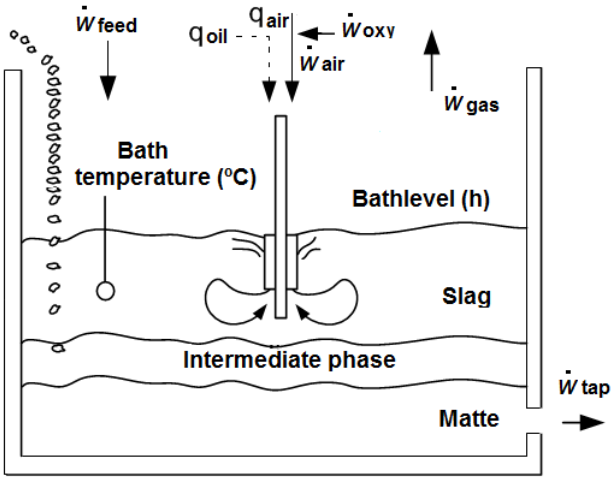

Figure 3.3: Simplified model of the Isasmelt furnace

3.1.2 Chemical reactions

The basic chemical reactions are expressed by the stoichiometric oxidation of pure chalcopyrite ($CuFeS_2$) and also pyrite (FeS_2) with oxygen-enriched air. The current copper smelting technology is aimed to obtain a rapid oxidation of chalcopyrite. This reaction requires oxygen enriched air to achieve a high-grade of copper matte

$$2\mathrm{CuFeS_2}{+}2.5\mathrm{0_2} \rightarrow \mathrm{Cu_2S} + \mathrm{FeS} + \mathrm{FeO} + 2\mathrm{SO_2} \tag{3.1}$$

The iron oxide is neutralized by SiO_2 to form fayalalite slag (3.2) Kho [2006]. The matte, slag and gases are simultaneously produced by Cu_2S and FeS at the oxidizing reaction site. Therefore all three phases are considered to be in equilibrium; that means, the state properties of phases do not change with time.

$$4\mathrm{CuFeS_2}{+}5\mathrm{O_2}{+}\mathrm{SiO_2} \rightarrow 2(\mathrm{Cu_2SFeS}) + 4\mathrm{SO_2} + (2\mathrm{FeO.SiO_2}) \tag{3.2}$$

The reaction mechanism occurs at two independent sites in the slag phase: one for fast oxidation and the other for slow reaction. In the oxidizing reaction, the chalcopyrite unlike the pyrite (3.3) does not react directly with the oxygen.

Figure 3.4: Concentrate smelting

The sulfur from the concentrate is oxidized by the oxygen from the magnetite (3.4).

$$6CuFeS_2 + 18Fe_3O_4 \rightarrow 54FeO + 7SO_2 + 3Cu_2S + 2FeS + 4FeO \tag{3.3}$$

$$18Fe_3O_4 \leftarrow 54FeO + 9O_2 \tag{3.4}$$

The excess of sulfur is used as fuel to maintain the process heating. The smelting reactions form matte containing copper sulfide and iron-silicate slag. The residual off-gas with high concentration of sulfur are then oxidized into sulfur dioxide (3.5). The partial pressure of SO_2 participates fully in matte-slag reactions.

$$FeS_{2(l)} + 5/2O_{2(g)} \rightarrow FeO_{(l)} + 2SO_{2(g)} \tag{3.5}$$

The magnetite is formed by the iron oxide (FeO) from the slag and the injected oxygen (3.6). This process is governed by oxygen flow which is introduced through the top submerged lance; furthermore FeO is neutralized with SiO_2 flux to form fayalalite slag (3.7). However, a high level of magnetite (around 18%) in slag is also indicative of achieving a matte grade [1] of 60% to 65%.

[1]The higher the copper content of the matte, the greater the amount of iron that is rejected

$$54FeO_{(l)} + 9O_{2(g)} \rightarrow 18Fe_3O_{4(l)} \tag{3.6}$$

$$4FeO_{(l)} + 4SiO_{2(s)} \rightarrow 4FeO.SiO_{2(l)} \tag{3.7}$$

The increment of matte grade produces an inevitable rise of copper loss to slag and high risk of magnetite accretion. This problem becomes especially acute when the bath slag is subsequently treated by settling in an electric or rotary furnace, where the solid magnetite may precipitate out together with the suspended matte. The oxygen regulation is a way to avoid this issue.

In the reduction step the slag is partially reduced by introducing slow reacting lump coal. This compound regulates the magnetite build-up: the carbon slightly forms ferrous oxide releasing carbon dioxide (3.8), which is also spontaneously produced by reacting with the oxygen (3.9). To sum up, this process assure a high medium-grade matte and a slag low in magnetite and copper.

$$Fe_3O_4(s) + CO_{(g)} \rightarrow 3FeO_{(l)} + CO_{2(g)} \tag{3.8}$$

$$CO_{(g)} + 0,5O_{2(g)} \rightarrow CO_{2(g)} \tag{3.9}$$

3.1.3 Thermodynamic analysis

The thermodynamic equilibrium takes place at the oxidizing reaction site. At the steady state conditions coexist matte, slag and gas phases. The main components (C) of the Isasmelt smelting process are copper, iron, oxygen, silica and sulfur Nagamori et al. [1994]. The degrees of freedom to specify the equilibrium are given by the Gibbs phase rule.

According to this rule it is required 4 process variables to maintain this equilibrium (P = C + 2 - F= 5 + 2 - 3 = 4). These conditions are specified by the temperature [°C], the oxygen content in lance air, the matte-grade [%Cu], the slag composition [$r = Fe/SiO_2$] and the partial pressure of sulfur dioxide [$p = S0_2$].

The model specifications at the equilibrium point are given as follows:

The target matte grade is estimated in 62% ± 1.0% to minimize copper losses to slag (less than 0,7%). The matte and slag composition are controlled by chemical analysis. The molten samples are taken after a smelting discharge (see 3.5).

into the slag

When the matte grade is deviated from the expected value after 3 consecutive tests, the operator modifies the ratio of air in the process control system.

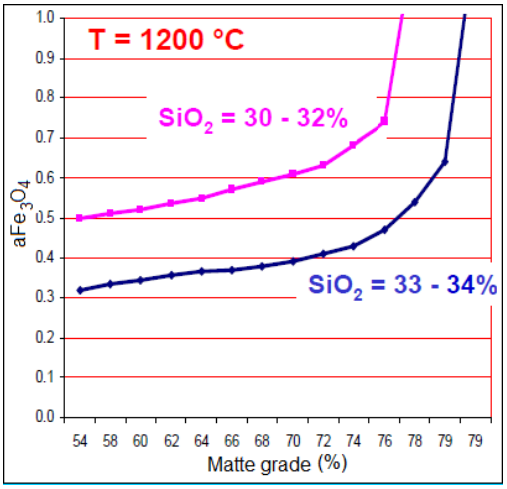

Figure 3.5: Matte grade diagram

In a similar way, the ratio SiO_2/Fe is set in (0.83 ± 0.1) to achieve an adequate silica content in the slag. This factor ensures an optimum matte/slag phase separation and an adequate viscosity coefficient. When this ratio is deviated from the target value, the operator corrects the silica factor to achieve suitable fluxes to the smelting process.

The temperature on the Isasmelt furnace normally fluctuates as the bath rises (tap hole closed) and falls (tap hole open). The bath temperature is maintained between 1175°C and 1185°C in order to safe the refractory lining of the furnace and moreover achieve adequate viscosity to minimize slag copper losses and to avoid precipitation of magnetite within the separation furnace.

The SO_2 partial pressure is ranged to ($\approx 0.32atm$). This property is directly linked to the level of oxygen enrichment to the process air and the chemical composition of the concentrate. The magnetite content of the slag produced in thermodynamic equilibrium with the above related parameters is estimated at $\approx 8.5\%$ (see 3.6).

The standard free energy for the formation of copper and iron sulfides at 1250°C are relatively similar. The formation of the oxides is much more negative for the iron oxide meaning that iron oxide is much more stable than copper oxide.

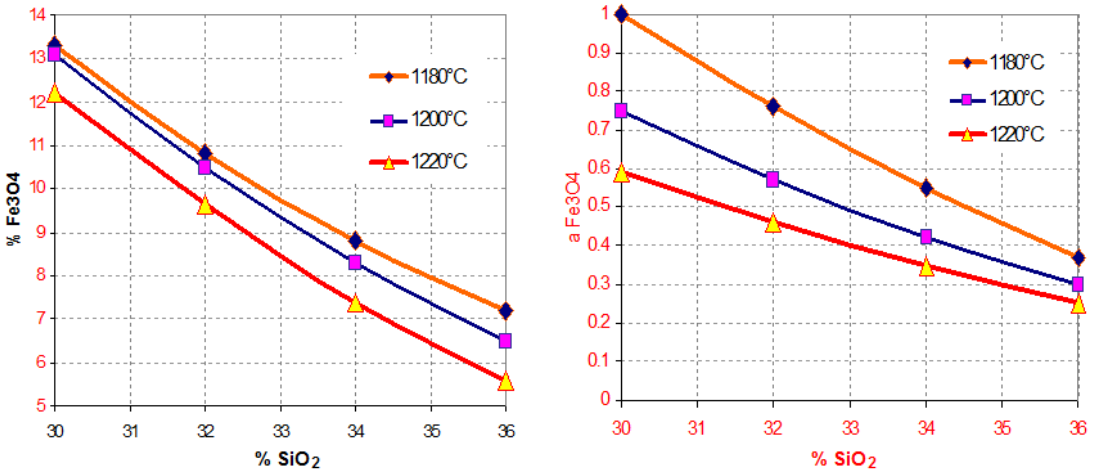

Figure 3.6: Slag-magnetite diagram

This means that when the matte is oxidized during matte smelting, iron sulfide is preferentially oxidized into iron oxide.

$$4Cu_{(l)} + S_{2(g)} \rightarrow 2Cu_2S_{(l)} \qquad \Delta G^\circ = -160,3kJ \quad (3.10)$$

$$2Fe_{(s)} + S_{2(g)} \rightarrow 2FeS_{(l)} \qquad \Delta G^\circ = -135,8kJ \quad (3.11)$$

$$4Cu_{(l)} + O_{2(g)} \rightarrow 2Cu_2O_{(l)} \qquad \Delta G^\circ = -111,3kJ \quad (3.12)$$

$$2Fe_{(s)} + O_{2(g)} \rightarrow 2FeO_{(l)} \qquad \Delta G^\circ = -328,9kJ \quad (3.13)$$

3.2 Mathematical process modelling

The smelting process has been mathematically modeled based on first-principles (i.e. the mass and energy balance). There has been designed a basic model using stored data from a real plant. The process modelling has included an extended model to represent the furnace bath temperature, which has been simulated in order to validate the mathematical models.

The tags to identify the process variables in the DCS of the real plant are detailed in table 3.1.

Table 3.1: Tags for parametric estimation on DCS

Variable	Sensor
Oxygen flow	FIC103
Blown air	FIC113
Oil flow	FIC113
Bath temperature	TIC354
Concentrate feed	WY049
Coal feed	WY044
Lance position	PIC139

3.2.1 Dynamic mass balance

The dynamic mass balance of molten material (m) within the furnace is given by the expression (3.14). This equation is determined by the inflow rate of raw materials (copper concentrate, fluxes and water) and enriched air, and the outflow rate of products (tapping flow and gases), neglecting the small mass loss due to handling operations (3.15).

$$\frac{dm}{dt} = \dot{w}_{feed} + \dot{w}_{air} - \dot{w}_{tap} - \dot{w}_{gas} - 0,01\dot{w}_{feed} \tag{3.14}$$

$$\frac{dm}{dt} \approx \dot{w}_{feed} + \dot{w}_{air} - \dot{w}_{tap} - \dot{w}_{gas} \tag{3.15}$$

where:

$$\dot{w}_{feed} = \dot{w}_{conc} + \dot{w}_{sil} + \dot{w}_{H_2O} + \dot{w}_{coal} + \dot{w}_{rev} \tag{3.16}$$

Then this equation may be expressed as:

$$\frac{dm}{dt} = \dot{w}_{conc} + \dot{w}_{sil} + \dot{w}_{H_2O} + \dot{w}_{coal} + \dot{w}_{rev} + \dot{w}_{air} - \dot{w}_{gas} - \dot{w}_{tap} \tag{3.17}$$

However, after analyzing historical data from the plant, an equivalence relation between the resulting gas mass of this process (124tph) and the amount of mass of silica, water, reverts, coal and enriched air (125,6tph) is found (3.18). This equivalence of masses also appears in related works Player [1996], Alvear et al. [2010] and in this case specifically allows the equation to be simplified (3.19).

$$\dot{w}_{gas} \approx \dot{w}_{sil} + \dot{w}_{H_2O} + \dot{w}_{rev} + \dot{w}_{coal} + \dot{w}_{air} \tag{3.18}$$

$$124(tph) \approx 125,6(tph)$$

$$\frac{dm}{dt} = \dot{w}_{conc} - \dot{w}_{tap} \tag{3.19}$$

3.2.2 Dynamic energy balance

The dynamic energy balance can be expressed in terms of summations of the input-output energy and the rate of heat generation. The i subscript in 3.20 is given by 1=$conc$, 2=sil, 3=$H_2O_{(l)}$, 4=rev and 5=$coal$; the j subscript is given by 1=h_{reac} if heat is from pyrite decomposition and 2=h_{oil} if heat is due to oil combustion; k is equal to 1=tap, 2=N_2, 3=SO_2, 4=$H_2O_{(g)}$ and the inlet and outlet temperatures of this balance are respectively denoted by T_i and T.

In this balance, it is assumed no heat is lost to the vessel outside and the minimal contributions of $\dot{w}_{O_2}$ and $\dot{w}_{N_2}$ to this process are ignored. The units applied in determining the dynamic energy balance are $\dot{w}$ $[kg/s]$, q_{oil} $[lt/s]$, Cp $[J/kg\text{-}^\circ C]$, m $[kg]$, $T[^\circ C]$ and $h_j[J/s]$.

$$mCp\frac{dT}{dt} = \sum_i \dot{w}_i Cp_i T_i + \sum_j h_j(t) - \sum_k \dot{w}_k Cp_k T \tag{3.20}$$

Then, deriving the left side of equation (3.20)

$$mCp\frac{dT}{dt} + CpT\frac{dm}{dt} = \sum_i \dot{w}_i Cp_i T_i + \sum_j h_j - \sum_k \dot{w}_k Cp_k T \tag{3.21}$$

Substituting equation (3.19) in (3.21) and reordering:

$$mCp\frac{dT}{dt} = \sum_i Cp_i \dot{w}_i T_i + \sum_j h_j - Cp\dot{w}_{conc} T - \sum_{k=2}^{4} Cp_k \dot{w}_k T \tag{3.22}$$

The expression in (3.23) displays the heating components of the process, assuming that the rate of heat generation ($h_1 = \alpha_1 \dot{w}_{O_2}$), due to pyrite decomposition and related reactions, depends on the oxygen factor ($\alpha_1, J/kg$) and the rate of oil combustion ($h_2 = \alpha_2 q_{oil}$) is given by its specific energy consumption ($\alpha_2, J/lt$) MacLeod et al. [1995], Steinboeck et al. [2011].

$$mCp\frac{dT}{dt} = \sum_i Cp_i \dot{w}_i T_i + \alpha_1 \dot{w}_{O_2} + \alpha_2 q_{oil} - Cp\dot{w}_{conc} T - \tag{3.23}$$
$$Cp_{N_2}\dot{w}_{N_2} T - Cp_{SO_2}\dot{w}_{SO_2} T - Cp_{H_2O}\dot{w}_{H_2O} T$$

The model becomes simplified in (3.24) by neglecting the heat contribution of SO_2 and H_2O gases to this process. This expression also includes the equivalence $m = (\rho A)h$, where ρ is the average density of the molten bath, A is the circular section of the furnace and h is the bath height.

$$\frac{dT}{dt} = \frac{1}{Cp(\rho A)h}\left(\sum_i Cp_i \dot{w}_i T_i + \alpha_1 \dot{w}_{O_2} + \alpha_2 q_{oil} - Cp\dot{w}_{conc} T - Cp_{N_2}\, \dot{w}_{N_2} T\right) \tag{3.24}$$

The differential equation in 3.24 can be linearized by the Taylor series expansion at the steady-state operating point $f(\bar{T}_i,\ \bar{\dot{w}}_{O_2}, \bar{q}_{oil},\ \bar{T},\ \bar{\dot{w}}_{conc},\ \bar{\dot{w}}_{N_2})$.

$$\frac{d\mathrm{T}}{dt} = \frac{\partial \bar{f}}{\partial T_i}(T_i - \bar{T}_i) + \frac{\partial \bar{f}}{\partial \dot{w}_{O_2}}(w_{O_2} - \bar{\dot{w}}_{O_2}) + \frac{\partial \bar{f}}{\partial q_{oil}}(q_{oil} - \bar{q}_{oil}) + \tag{3.25}$$
$$\frac{\partial \bar{f}}{\partial T}(T - \bar{T}) + \frac{\partial \bar{f}}{\partial \dot{w}_{conc}}(\dot{w}_{conc} - \bar{\dot{w}}_{conc}) + \frac{\partial \bar{f}}{\partial \dot{w}_{N_2}}(\dot{w}_{N_2} - \bar{\dot{w}}_{N_2})$$

The feeding temperature at initial conditions are approximately constant such that $\mathrm{T}_i = T_i(t) - \bar{T}_i(t) \approx 0$. Then, equation (3.25) becomes simplified as follows.

$$\frac{d\mathrm{T}}{dt} = \frac{1}{Cp(\rho A)h}\left[\alpha_1 \dot{W}_{O_2} + \alpha_2 Q_{oil} - Cp(\bar{\dot{w}}_{conc}\right. \tag{3.26}$$
$$\left.\mathrm{T} + \bar{T}\ \dot{W}_{\mathrm{conc}}) - \mathrm{Cp}_{\mathrm{N}_2}(\bar{\dot{w}}_{\mathrm{N}_2}\mathrm{T} + \bar{T}\ \dot{W}_{\mathrm{N}_2})\right]$$

where $\dot{W}_{O_2}, Q_{oil}, \mathrm{T}, \dot{W}_{\mathrm{conc}}$ and $\dot{W}_{N_2}$ are deviation variables from the base point. The linearized function (3.26) can be written therefore in terms of small increments above such equilibrium point Zhao [2010].

$$\frac{d\Delta T}{dt} = \frac{1}{h}[\gamma_1 \Delta \dot{w}_{O_2} + \gamma_2 \Delta q_{oil} - \gamma_3\ (\bar{\dot{w}}_{conc}\Delta T \tag{3.27}$$
$$+\bar{T}\Delta \dot{w}_{conc}) - \gamma_4(\bar{\dot{w}}_{N_2}\Delta T + \bar{T}\Delta \dot{w}_{N_2})]$$

whith:

$$\gamma_1 = \frac{\alpha_1}{Cp\,(\rho A)},\ \gamma_2 = \frac{\alpha_2}{Cp\,(\rho A)},\ \gamma_3 = \frac{1}{(\rho A)},\ \gamma_4 = \frac{Cp_{N_2}}{Cp\,(\rho A)}$$

The derivative in 3.27 is approximated for small sampling times by the delta operator. This expression is mathematically given by $\lim_{t_s \to 0} \delta\Delta(t) = d\Delta(t)/dt$.

$$\delta\Delta T_k = \frac{\Delta T_{k+1} - \Delta T_k}{t_s} = \gamma_1 \left[\frac{\Delta \dot{w}_{O_2}}{h}\right]_k + \gamma_2 \left[\frac{\Delta q_{oil}}{h}\right]_k - \gamma_3 \left[\frac{\bar{\dot{w}}_{conc}\Delta T + \bar{T}\Delta \dot{w}_{conc}}{h}\right]_k - \gamma_4 \left[\frac{\bar{\dot{w}}_{N_2}\Delta T + \bar{T}\Delta \dot{w}_{N_2}}{h}\right]_k \tag{3.28}$$

where $k = 1, 2, ..., N$ defines the terms at the sampling instant and $t_s = 10s$ is the sampling period (or sampling time) of observational data.

However, the equation 3.28 can be written as a matrix product of the form

$$Y_{Nx1} = F_{Nx4}\Gamma_{4x1} \tag{3.29}$$

where Y is used instead of $\delta\Delta T_k$ as dependent term, F is the matrix of incremental variables (f_{ik}), which are computed from the real plant, and Γ is the matrix of parameters (γ_i).

$$Y = [f_{1k}, f_{2k}, -f_{3k}, -f_{4k}] \begin{bmatrix} \gamma_1 \\ \gamma_2 \\ \gamma_3 \\ \gamma_4 \end{bmatrix} \tag{3.30}$$

Then, the terms of the resulting matrix can be calculated as follows (see appendix 1).

$$\Gamma = (F^T F)^{-1} F^T Y \tag{3.31}$$

The parameters are estimated applying ordinary least squares method (multiple linear regression) in 3.32.

$$\Gamma = \begin{bmatrix} \gamma_1 \\ \gamma_2 \\ \gamma_3 \\ \gamma_4 \end{bmatrix} = \begin{bmatrix} -3,4236 \times 10^{-5} \\ -7,4544 \times 10^{-4} \\ -3,4662 \times 10^{-7} \\ -2,1333 \times 10^{-9} \end{bmatrix} \tag{3.32}$$

The temperature dynamics can be represented in a block diagram as is shown in figure 3.7.

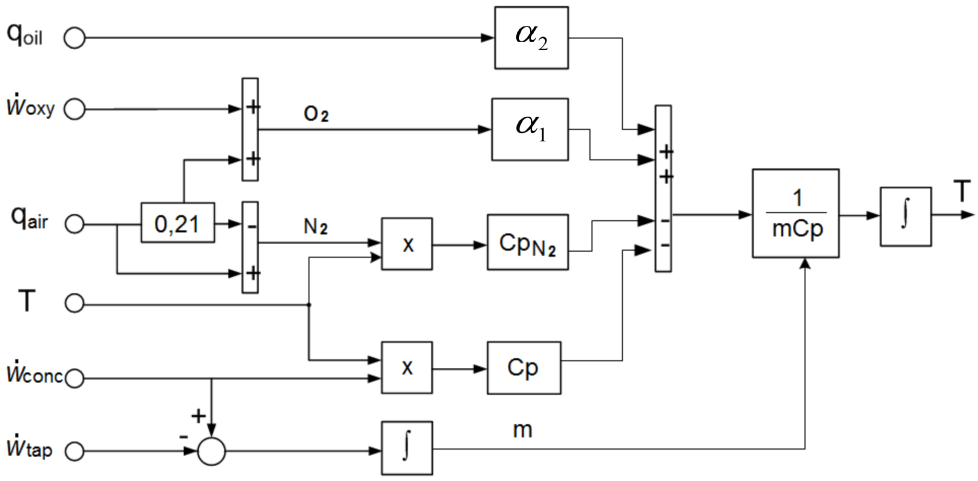

Figure 3.7: Block diagram of the Isasmelt temperature dynamics

3.2.3 Extended process model

In order to analyze the system features of the Isasmelt furnace, it makes sense to build an extended model of the smelting process. This representation adds the coal component to the general thermal function. This means that the coal behavior is also included in the incremental model around the steady state point $(\Delta T, \Delta \dot{w}_{O_2}, \Delta \dot{w}_{coal}, \Delta q_{oil}, \Delta \dot{w}_{conc}, \Delta \dot{w}_{N_2})$.

Then, the modified mathematical expression is linearized using the Taylor expansion.

$$\frac{d\Delta T}{dt} = \frac{1}{h}[\gamma_1 \Delta \dot{w}_{O_2} + \gamma_2 \Delta \dot{w}_{coal} + \gamma_3 \Delta q_{oil} - \gamma_4 \\ (\bar{\dot{w}}_{conc} \Delta T + \bar{T} \Delta \dot{w}_{conc}) - \gamma_5 (\bar{\dot{w}}_{N_2} \Delta T + \bar{T} \Delta \dot{w}_{N_2})] \tag{3.33}$$

The derivative of the temperature is approximated by the delta operator. In this equation, it is used a smaller sampling time ($t_s = 2s$) in order to get more accurate ressults.

$$\delta \Delta T_k = \frac{\Delta T_{k+1} - \Delta T_k}{t_s} \tag{3.34}$$

In a similar way as in the general model, the parametric vectors are calculated using stored data and applying finite difference methods.

$$\delta\Delta T_k = \gamma_1 \left[\frac{\Delta \dot{w}_{O_2}}{h}\right]_k + \gamma_2 \left[\frac{\Delta \dot{w}_{coal}}{h}\right]_k + \gamma_3 \left[\frac{\Delta q_{oil}}{h}\right]_k - \gamma_4 \left[\frac{\bar{\dot{w}}_{conc}\Delta T + \bar{T}\Delta \dot{w}_{conc}}{h}\right]_k - \gamma_5 \left[\frac{\bar{\dot{w}}_{N_2}\Delta T + \bar{T}\Delta \dot{w}_{N_2}}{h}\right]_k \tag{3.35}$$

The resulting values are presented in matrix form (3.36).

$$\Gamma = \begin{bmatrix} \gamma_1 \\ \gamma_2 \\ \gamma_3 \\ \gamma_4 \\ \gamma_5 \end{bmatrix} = \begin{bmatrix} 9,1353 \times 10^{-3} \\ 1,7254 \times 10^{-3} \\ -4,2677 \times 10^{-3} \\ +1,8333 \times 10^{-5} \\ +1,5309 \times 10^{-5} \end{bmatrix} \tag{3.36}$$

The temperature dynamics of the extended model is depicted in a block diagram (see 3.8).

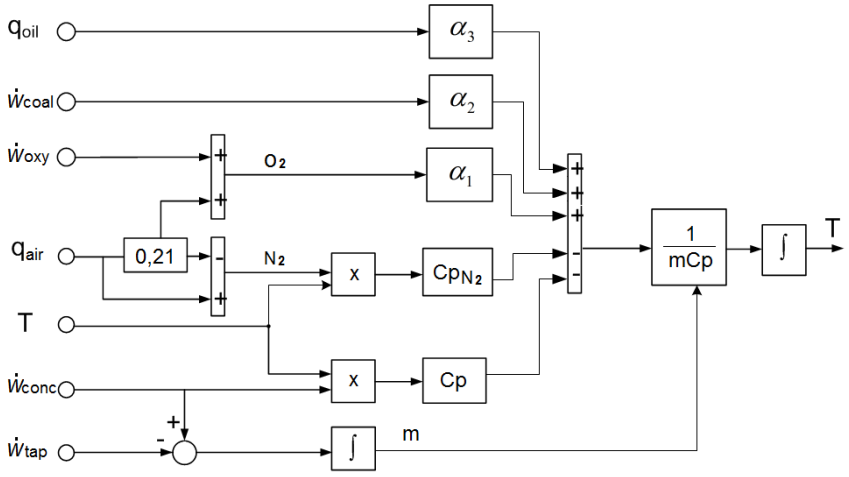

Figure 3.8: Block diagram of the extended temperature dynamics

The thermal behavior by using the extended model is similar to the basic model but have higher computational cost, therefore, the general model will be used in this work. The features of the furnace model are also representative to simulate the control system.

3.3 Thermal process modelling

The life of refractory furnace lining and the product quality are greatly enhanced by the accurate control of the molten bath temperature. This regulation is dependent upon ratio adjustments of nitrogen and oxygen (N_2/O_2). The blown air is enriched with industrial oxygen to reduce amounts of nitrogen and to fulfill the concentrate oxidizing temperature (see 3.9) and (see 3.10).

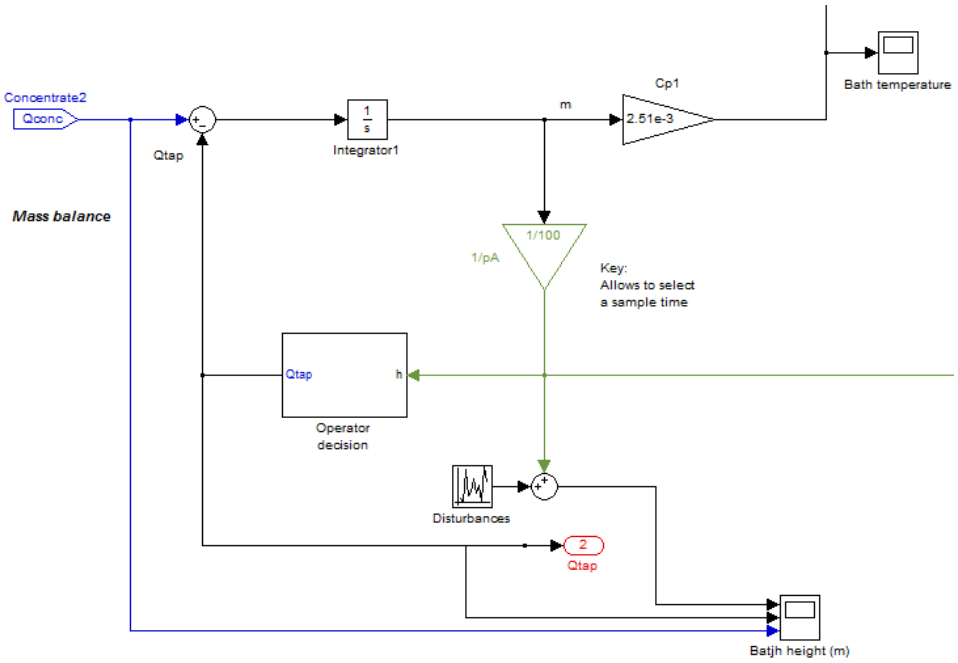

Figure 3.9: Matlab design of mass balance

3.3.1 Temperature dynamics of the Isasmelt furnace

The flow rate of oxygen and nitrogen injected to this process is given in (3.37) and (3.38) respectively.

$$\dot{w}_{O_2} = 0,21q_{air} + \dot{w}_{oxy}, \quad \dot{w}_{N_2} = 0,79q_{air} \tag{3.37}$$

$$\dot{w}_{N_2} = 3,76(\dot{w}_{O_2} - \dot{w}_{oxy}) \tag{3.38}$$

The control logic uses the concentrate, coal and oil rates as a feed forward index to directly set the total oxygen demand (3.39). The oxygen - enriched air

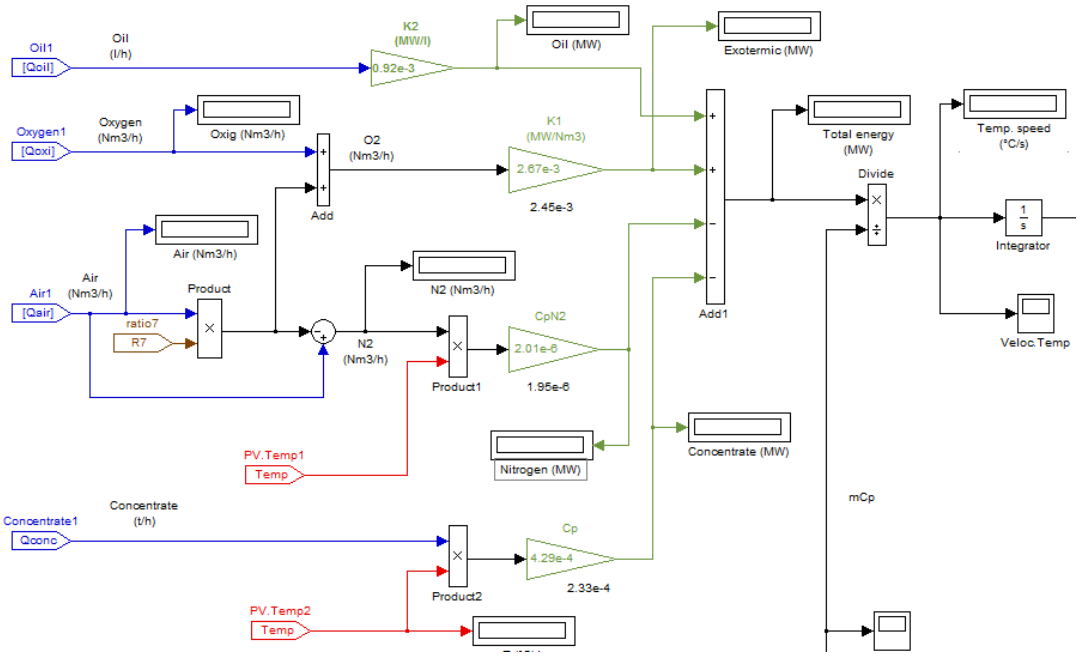

Figure 3.10: Matlab design of energy balance

(3.40) is calculated by dividing the required oxygen for this process by the $\%O_2$ enrichment (3.41).

$$\dot{w}_{O_2} = k_1 \dot{w}_{conc} + k_2 \dot{w}_{coal} + k_3 q_{oil} \tag{3.39}$$

$$\dot{w}_{air} = q_{air} + \dot{w}_{oxy} \tag{3.40}$$

$$\dot{w}_{air} = \frac{\dot{w}_{O_2}}{\%O_2} \tag{3.41}$$

The mathematical model of the plant is obtained by taking the Laplace transform of equation (3.27).

$$\Delta T(s) = \frac{\gamma_1 \Delta \dot{w}_{O_2}}{hs+b} + \frac{\gamma_2 \Delta q_{oil}}{hs+b} - \frac{\gamma_3 \bar{T} \Delta \dot{w}_{conc}}{hs+b} - \frac{\gamma_4 \bar{T} \Delta \dot{w}_{N_2}}{hs+b} \tag{3.42}$$

where

$$b = \gamma_3 \bar{\dot{w}}_{conc} + \gamma_4 \bar{\dot{w}}_{N_2} \tag{3.43}$$

Substituting (3.39) and (3.40) in equation (3.42) results as follows:

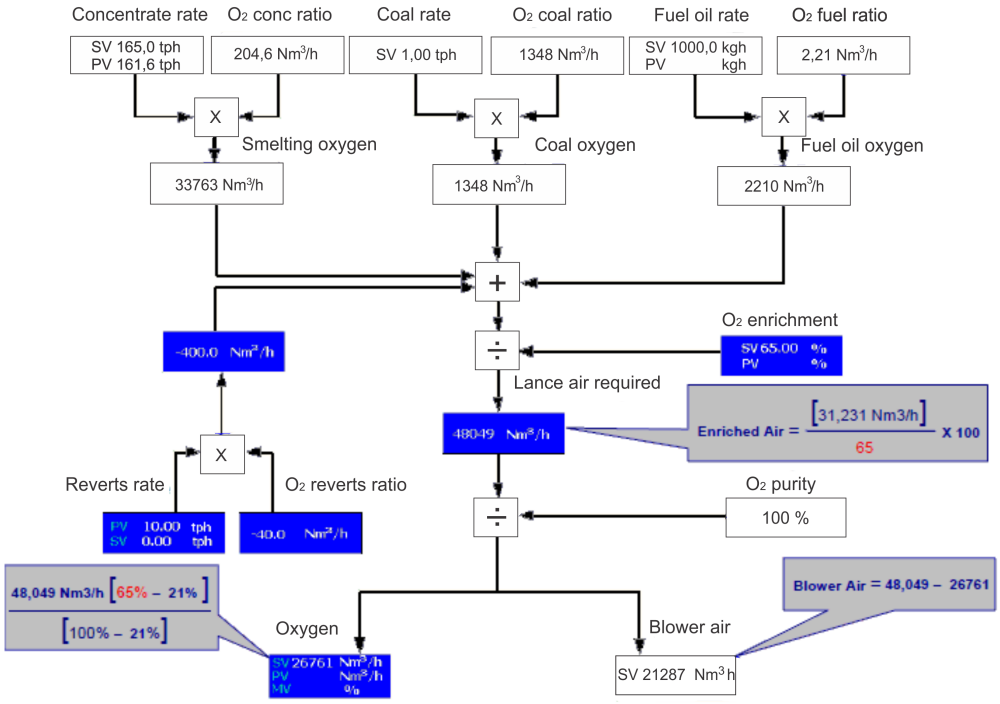

Figure 3.11: Lance air flow requirements

$$\Delta T(s) = \frac{\gamma_1 \Delta \dot{w}_{oxy}}{hs+b} + \frac{0,21K\Delta q_{air}}{hs+b} + \frac{\gamma_2 \Delta q_{oil}}{hs+b} - \frac{\gamma_3 \bar{T} \Delta \dot{w}_{conc}}{hs+b} \tag{3.44}$$

with

$$K = (\gamma_1 - 3,76\gamma_4 \bar{T}) \tag{3.45}$$

3.4 Furnace simulation

In this section, the furnace operation with the current temperature controller is simulated with MATLAB/Simulink. The input variables of this model are the concentrate and coal feed rates (kg/s), the oxygen-enrichment percent (%) and the operation set points; on the other hand, the output variables are the bath temperature (°C) and the tip pressure (KPa).

The furnace simulation is used as a platform to make model comparisons between the current controller and the proposed fuzzy controller, which also represent the temperature dynamics. This simulation model also includes constants

and related parameters, whose values are estimated from the own process according to methods detailed in chapter 4.

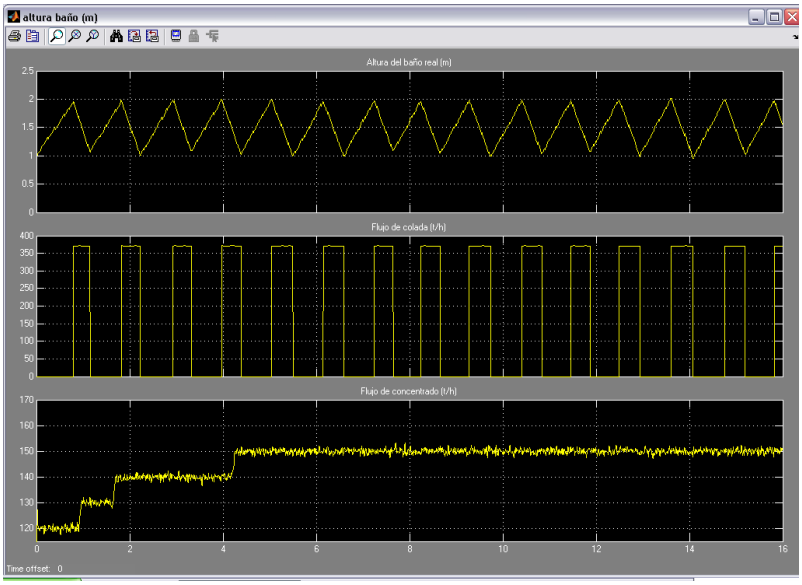

Figure 3.12: Simulated process parameters

The simulation model is performed under normal operating conditions, that cover usual events like concentrate feed (figure 3.12), air/oxygen flow (figure 3.13) and lance tip immersion (figure 3.14).

The following assumptions are considered to carry out furnace simulations:

- Furnace temperature at 1180°C.
- Initial bath level is assumed to be one meter high, to mainly simulate the tip pressure controller.
- Continuous stable flow of air, oxygen and oil.

The results of the model simulation for the bath temperature (see figure 3.15) and tip pressure (see figure 3.16) as shown as follows:

The model validation is possible using historical (stored) data from an Isasmelt copper smelter in Peru (observing eight-hour periods run from December 15^{th} to

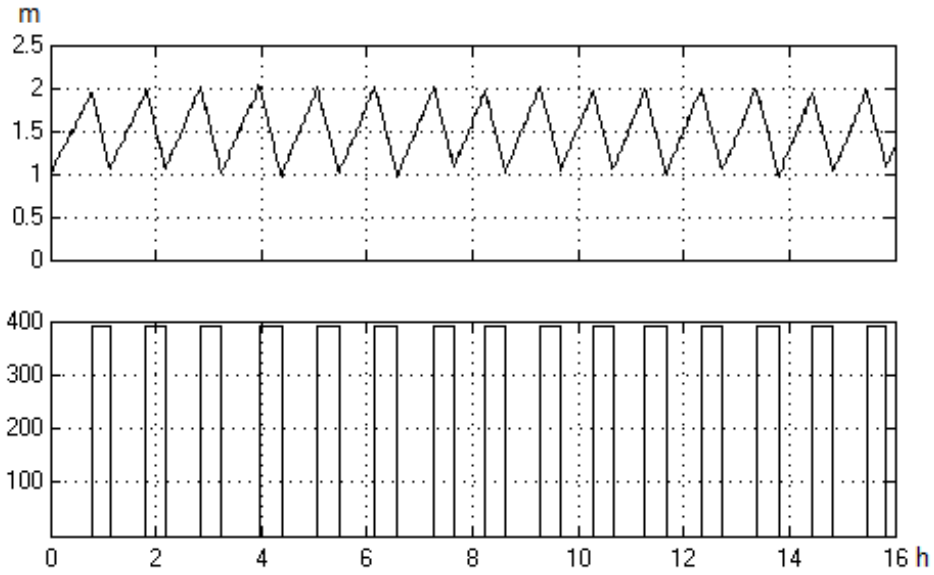

Figure 3.13: Lance position

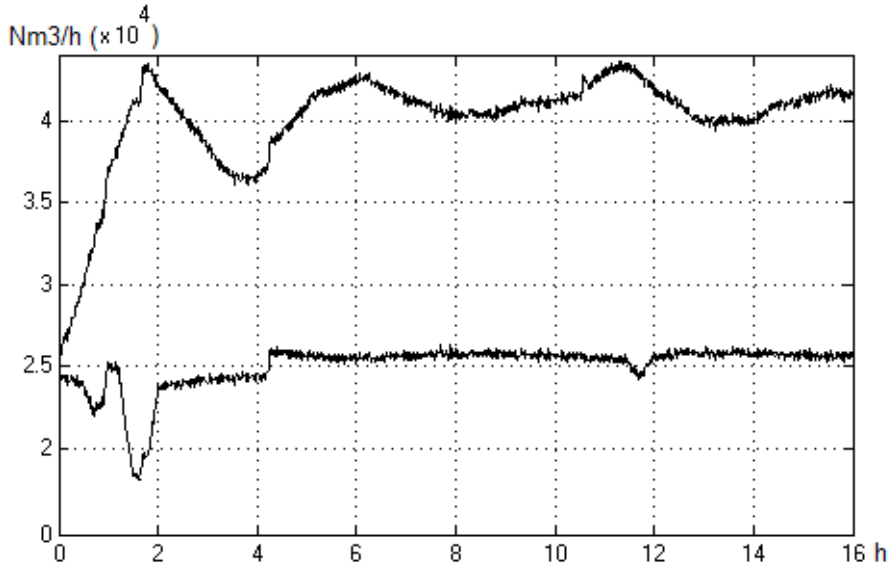

Figure 3.14: Compared air/oxygen flows

30^{th}, 2008). The number of observations was 120 (of 10 minutes). This sample size is calculated with the sampling expression.

$$n = {Z_{0,05}}^2(\frac{\sigma}{\partial})^2 = (1,96)^2(\frac{27,8°C}{5°C})^2 = 118,76 \cong 120 \tag{3.46}$$

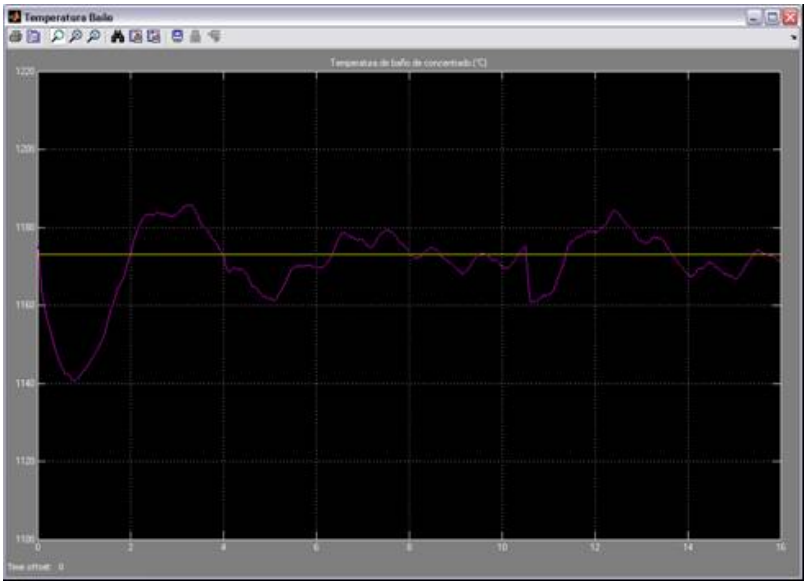

Figure 3.15: Simulated bath temperature

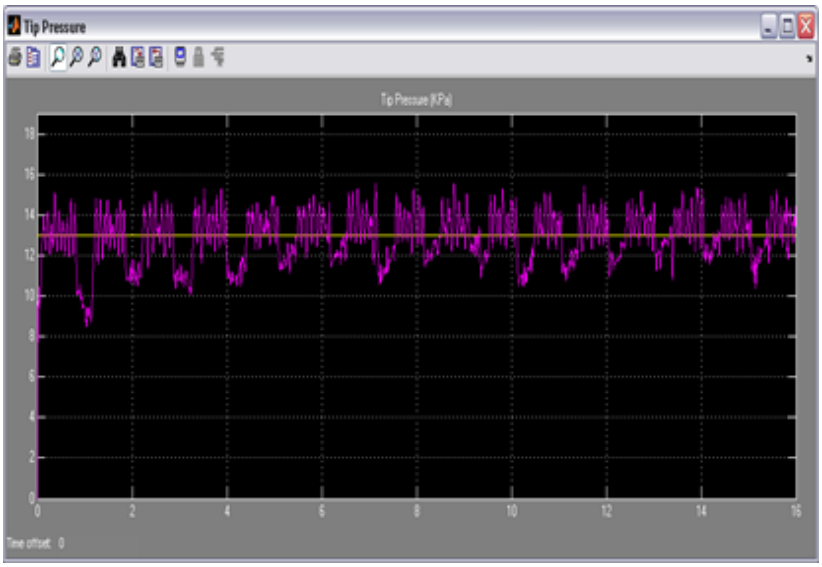

Figure 3.16: Simulated tip pressure

where $Z_{0,05}$ means a confidence interval of 95%, σ is the current population standard deviation, and ∂ is the error of estimation.

This model is validated by comparing simulated and measured real outputs (bath temperature and tip pressure). The mean square relative error between

these two variables are used to evaluate the accuracy of the model:

$$\%e_{rms} = \frac{\sum_{i=1}^{n} \left(\frac{p_i - r_i}{r_i}\right)^2}{n} \times 100 \tag{3.47}$$

where p_i is the simulated data, r_i is the real data and n is the number of samples (120). The error percentages obtained from both output variables are presented in table 6.1.

Table 3.2: Error of simulation model

Variable	Unit	% e_{rms}
Bath temperature	C	0,0068 %
Tip Pressure	KPa	1,6509 %

The comparison of simulated an real temperature is presented in figure 3.17. This comparison is obtained by the same process inputs.

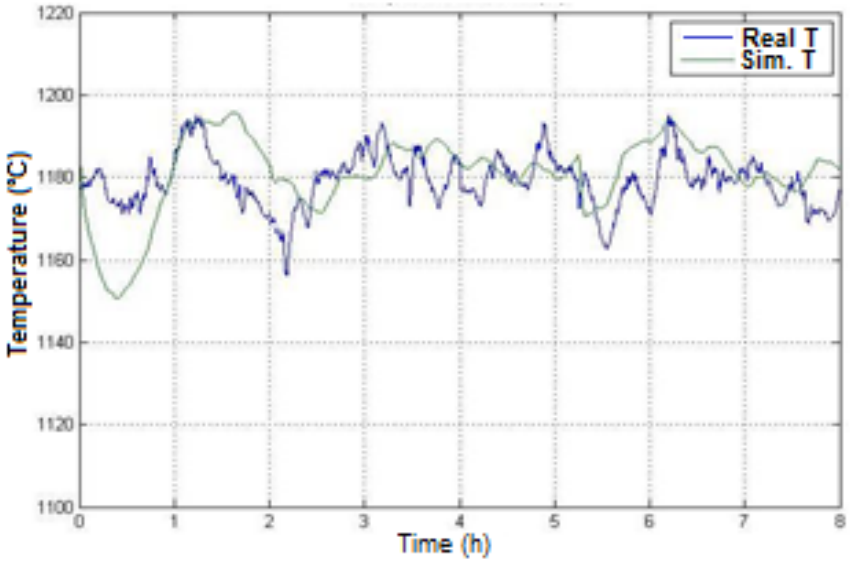

Figure 3.17: Real and simulated temperature

The simulated tip pressure is compared with respect to the real output in figure 3.18.

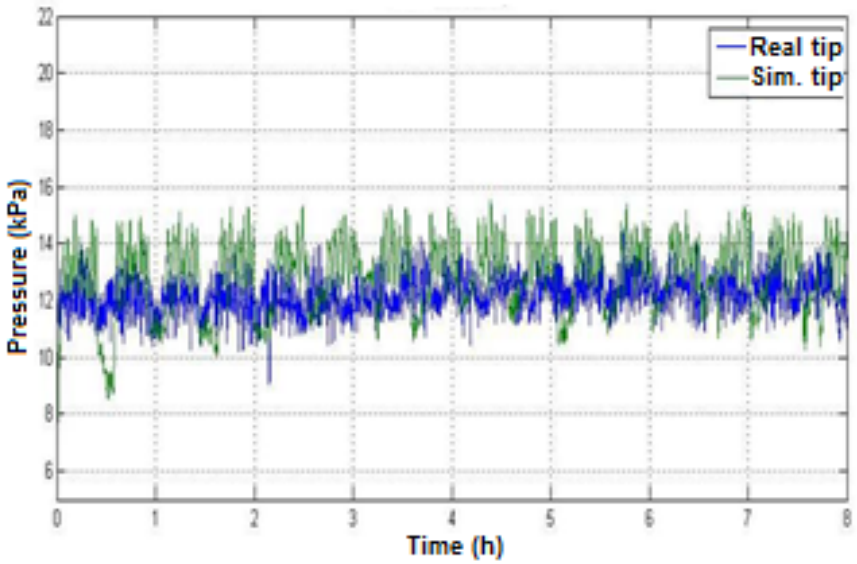

Figure 3.18: Real and simulated tip pressure

3.5 Concluding remarks

In this chapter the copper smelting process has been mathematically modeled. This analysis is focused on thermodynamics aspects of oxidation and reduction reactions as well as mass and energy balance within the Isasmelt furnace. The model is later validated by comparing simulated output variables (bath temperature and tip pressure) and real plant data.

This model improves related works in modelling such process and describes the inlet and outlet system conditions. The description of this process has enabled the furnace simulation. The furnace system control has been properly simulated as a reference to make technical comparisons between the current control system and the proposed control design.

Chapter 4

Isasmelt control system

This chapter describes the main components of the Isasmelt furnace control system in its current deployment in the copper production in Peru. This description includes the bath temperature controller and the combustion control subsystem, which is composed of the oxygen and blower air control and the oil flow control. It is also described the lance tip pressure control and the actuators subsystem.

The success of the smelting process is linked to the control of bath temperature, matte grade and slag chemistry. The furnace control system is designed to achieve output temperatures between 1200° and 1250°, a matte grade up to 62-65% with least copper losses (i.e. lower than 8% Cu) and magnetite activity (around 18%) in the slag.

The bath temperature is largely sourced from the concentrate sulphur, but is also added coal and oil fuels to maintain the process heat. The matte composition is controlled by adjusting the oxygen enrichment rate. This regulation, however, affects slag chemistry and bath temperature. Therefore, those factors should be carefully handled during copper smelting.

4.1 Bath temperature controller

The temperature is measured by four thermocouples (TT354-A, B, C and D) located into the bath zone of the Isasmelt furnace (see figure 4.1). They are inserted at various points on the refractory bricks lining. The operator can select

any one of these thermocouples but generally chooses the highest value. This variable in steady operational conditions lies at $1170°C$, however, it normally fluctuates as the bath rises (taphole closed) and falls (tap hole open).

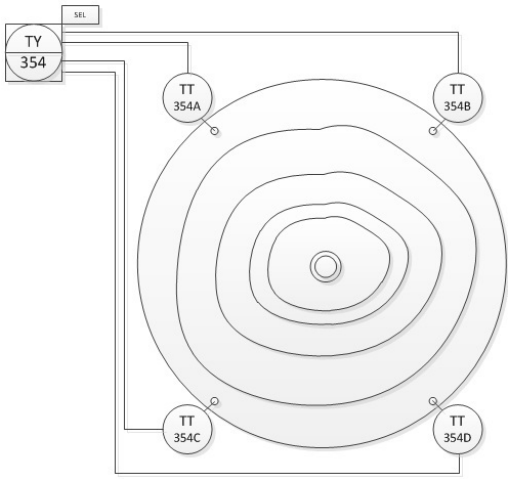

Figure 4.1: Horizontal view of the furnace thermocouples

The design includes a dead-time compensation function to prevent the heat transfer resistance of ceramic sheaths, which surround the furnace thermocouples (see figure 4.2).

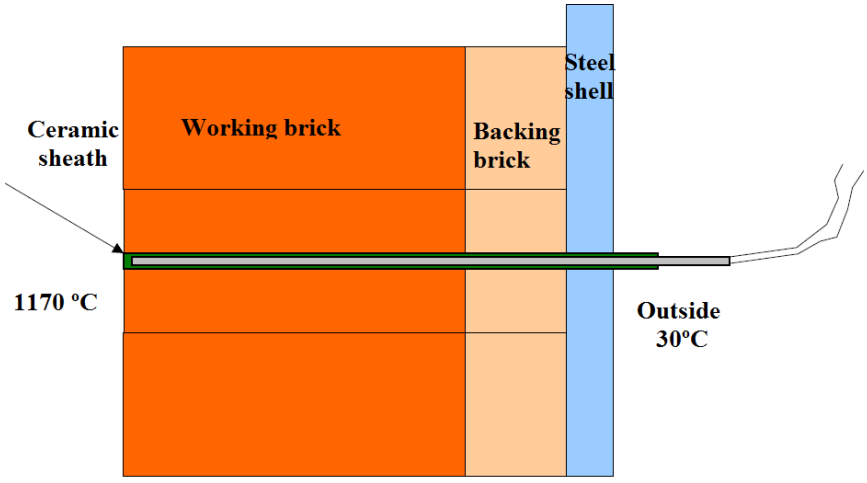

Figure 4.2: Thermocouples placement in the Isasmelt furnace

A PID controller (TIC354) regulates the bath temperature by using a cascade control strategy (see figure 4.3). This controller acts as outer loop within the control structure. The error signal from the temperature controller (by comparing the set point with the temperature process value) is attenuated by a low - pass filter (frequency of 50 rad/s) and transmitted to the main controller (FIC115).

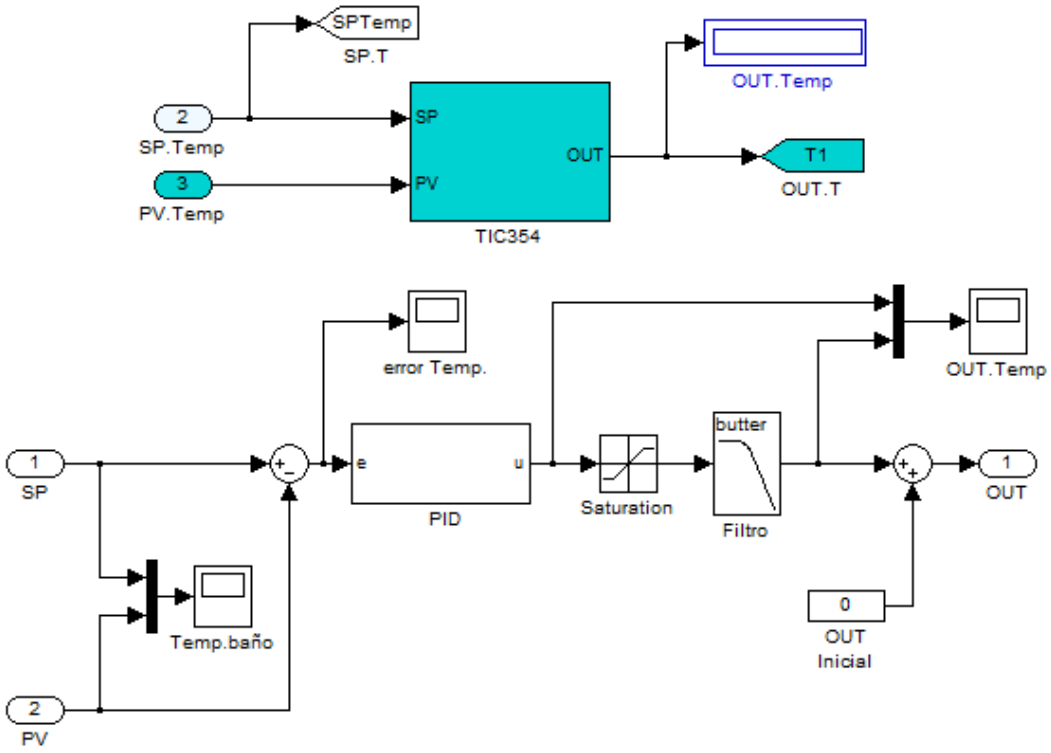

Figure 4.3: PID temperature controller

The specifications for the controller are given as follows: e_{ss}=10°C (with respect to the set point), de/dt=[0 - 3]°C/m (operation controller range). The settling time is not considered among the specifications because of the fixed temperature set-point. However the step model response is equal to 13 s (see figure 4.4).

The primary control loop contains individual dependent PID controllers to regulate oxygen (FIC103), air (FIC113) and oil flow rates (FIC123) in secondary loop. The master controller remotely fixes the set points of those components as intermediate process variables to control the furnace bath temperature (see figure

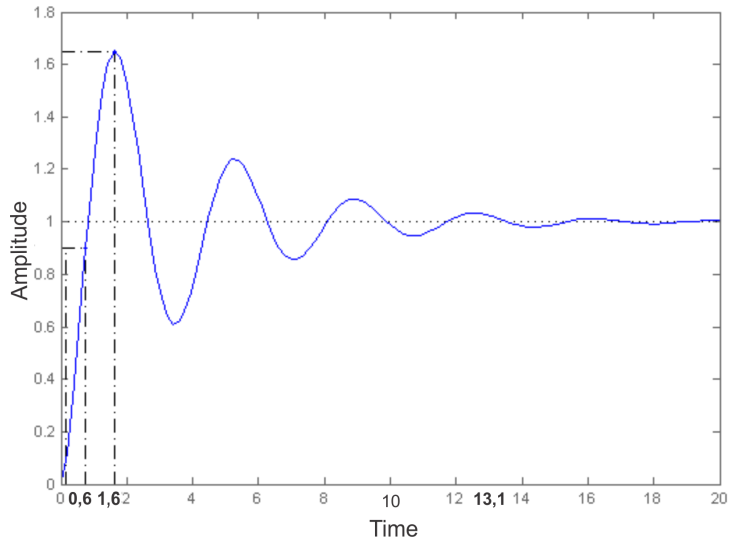

Figure 4.4: Specifications

4.5).

The overall process transfer function is given in 4.1. The coefficients are obtained by applying steady state values to bath temperature ($\bar{T} = 1170°C$ or $1443K$) and associated process variables: $\dot{w}_{N_2} = 24068,93Nm^3$, $\dot{w}_{conc} = 151t/h$ and $\dot{h} = 1,7m$.

$$\Delta T(s) = \frac{\gamma_1 \Delta \dot{w}_{oxy}}{s + b/\dot{h}} + \frac{0,21K\Delta q_{air}}{s + b/\dot{h}} + \frac{\gamma_2 \Delta q_{oil}}{s + b/\dot{h}} - \frac{\gamma_3 \bar{T} \Delta \dot{w}_{conc}}{s + b/\dot{h}} \tag{4.1}$$

with

$$K = \gamma_1 - 3,76\gamma_4 \bar{T} \tag{4.2}$$

$$K = -3,42.10^{-5} - 3,76(-3,47.10^{-7})1443 = 0,0018\frac{mK}{kg} \tag{4.3}$$

and

$$b = \gamma_3 \bar{\dot{w}}_{conc} + \gamma_4 \bar{\dot{w}}_{N_2} \tag{4.4}$$

$$b = -3,47.10^{-7}151 - 2,133.10^{-9}24068,93 = 0,0001 \tag{4.5}$$

Substituting 4.3 and 4.4 in 4.1 becomes:

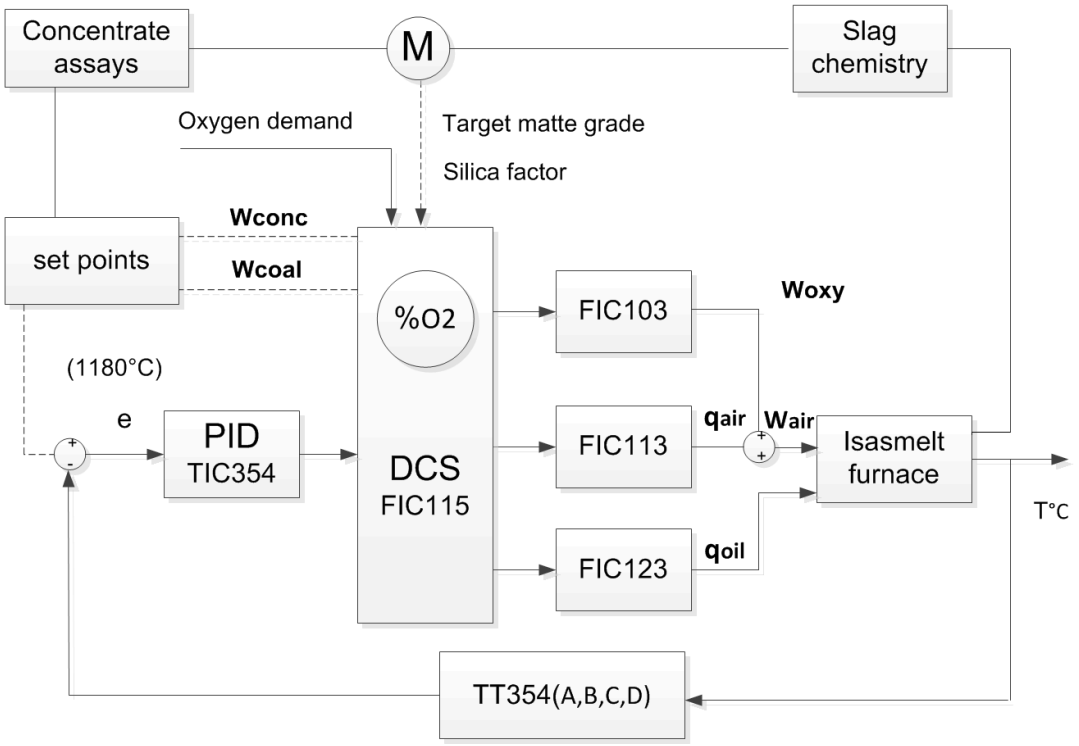

Figure 4.5: Control diagram

$$\Delta T(s) = \frac{\gamma_1 \Delta \dot{w}_{oxy}}{s + b/\dot{h}} + \frac{0,000378 \Delta q_{air}}{s + b/\dot{h}} + \frac{\gamma_2 \Delta q_{oil}}{s + b/\dot{h}} - \frac{\gamma_3 \bar{T} \Delta \dot{w}_{conc}}{s + b/\dot{h}} \tag{4.6}$$

4.2 Combustion control subsystem

The concentrate feeding is established according to the production schedule. The feed rate is manually regulated by the furnace operator (approximately 162 t/h). The sulfur contained in the chalchopyrite is burnt to maintain the process heat (over 1100°C). If the sulphur content is not enough to sustain this temperature, coal and eventually extra fuel oil are also added into the mixture. The coal feed rate is mainly used for coarse thermal regulation, while fuel oil supplement is required for fine temperature control (see figure 4.7).

The temperature control is dependent upon the effective oxygen flow rate Vode et al. [2008]. The oxygen mass comes from the enriched air injected through an Isasmelt lance. The oxygen enrichment means a pre-determined percentage oxy-

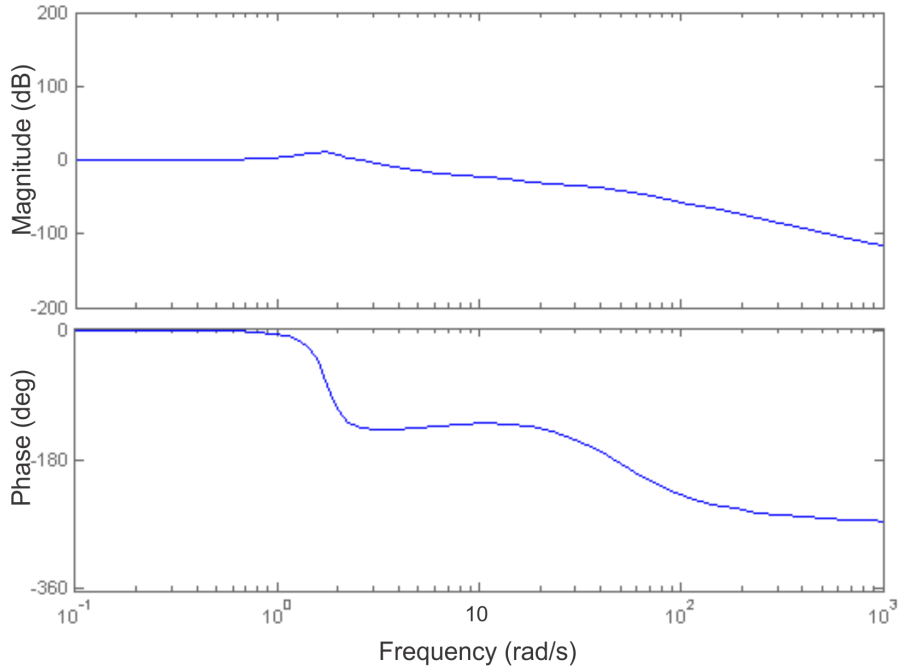

Figure 4.6: Bode diagram

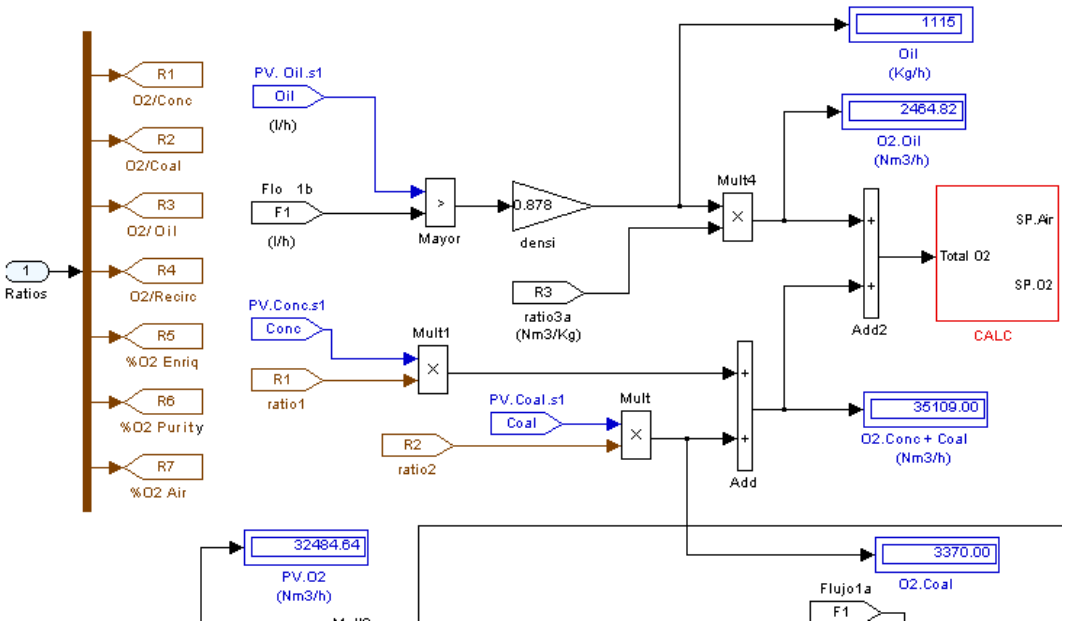

Figure 4.7: Slave control design

gen content within the blown air, which is adjusted by adding industrial oxygen. Then, the resulting mass flow contains a lower relative volume of nitrogen.

The oxygen-enrichment rate is manipulated (sometimes manually by the operator) to attain the desired bath temperature Zhi-xiang et al. [2010]. This operation is critical but very frequent during the furnace operation. The bath temperature can be increased by carrying away less heat to the off gas system. However, high temperature deviations lead to high rates of brick wear.

The flow rates of oxygen and blown air (also called combustion air) are controlled by individual PID control loops (FIC230113 and FIC230103 respectively). These controllers have remote set points determined by the DCS main control. The estimation is based on oxidizing or combustion requirements of copper concentrate and coal or fuel oil (see figure 4.8).

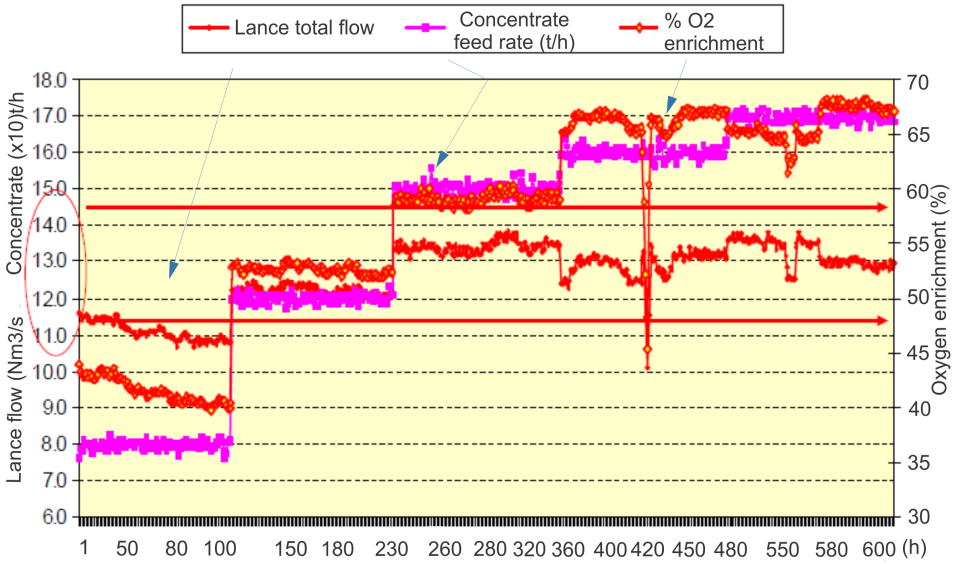

Figure 4.8: Concentrate smelting

Before the feeding charge is introduced into the furnace, the total demand of oxygen is directly settled by calculating concentrate and coal feed rates Arthur and Hunt [2005a], Arthur [2006]. This index logic uses the concentrate and coal feed rate values as a feed forward index to directly set the total oxygen demand. The oil oxygen is also added using the cascade set point of the combustion oil controller.

$$\frac{\Delta T(s)}{\Delta q_{oil}} = \frac{\gamma_2}{s + b/h} \tag{4.7}$$

The oxygen ratios to concentrate, coal and oil (and reverts) as well as the percentage of oxygen enrichment ($\%0_2$) and purity factors are used to estimate the oxygen demand of the smelting process. The ratios are multiplied by their respective feeding rates to calculate such values (for example: oxygen/oil ratio by oil flow rate).

The mate grade (range of 60-65%) and slag composition (range of 32-34%) are dependent upon this calculation. An algorithm is incorporated into the main control to periodically make adjustments of the $\%O_2$ enrichment rate, which is based on periodic mate and slag samples (taken approximately once an hour). However, due to time delays, corrections are not timely executed Errington et al. [1997].

This procedure is based on chemistry analysis of periodical samples of mate and slag (taken approximately once an hour). However, this method is not fast enough to make necessary air ratio adjustments. The relationship between air ratio and temperature deviation required faster calculation to take a corrective action.

This calculation is compensated by the signal of the PID temperature controller. This schema is depicted in figure 4.9.

$$\Delta \dot{w}_{oxy} = \frac{\gamma_3 \bar{T}}{\gamma_1} \Delta \dot{w}_{conc} \tag{4.8}$$

The transfer function establishes an interaction between the bath temperature and the industrial oxygen. This dynamic relation in terms of little variations is given as follows.

$$\frac{\Delta T(s)}{\Delta \dot{w}_{oxy}} = \frac{\gamma_1}{s + b/h} \tag{4.9}$$

The transfer function describes this interaction between bath temperature and blown air. The oxygen-enriched air is injected into the furnace through a vertical lance, which is submerged in the slag bath. The depth of immersion is set automatically by the lance tip pressure.

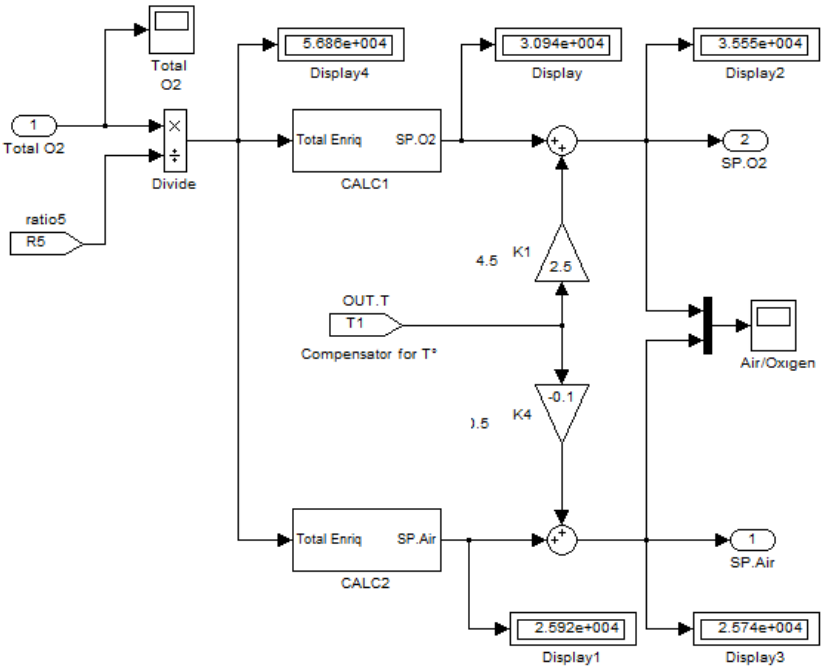

Figure 4.9: Compensation function for oxygen demand

$$\frac{\Delta T(s)}{\Delta q_{air}} = \frac{0,000378}{s + b/h} \tag{4.10}$$

The PID algorithm is composed of three terms: the P term (proportional to the error), the I term (proportional to the integral of the error) and the D term (proportional to the derivative of the error). This expression is described in equation 4.11.

$$u(t) = k_c[e(t) + \frac{1}{T_i}\int_0^t e(\tau)d\tau + T_d\frac{de(t)}{dt}] \tag{4.11}$$

where $u(t)$ is the control signal, k_c is the proportional gain, e is the control error ($e = y_{sp} - y$), T_i is the integral time and T_d is the derivative time.

The PID controllers are tuned by the Ziegler and Nichols method. This technique is based on process information by taking an open-loop step response. The constants a and L are used as index to determine the PID parameters Åström and Hägglund [2006]. These constants are given by the intersections between the tangent to the slope and the coordinate axes (see figure 4.10).

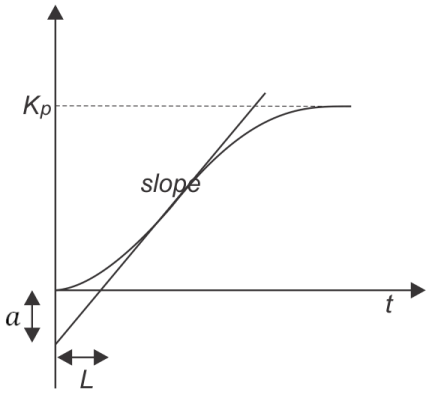

Figure 4.10: Characterization of open-loop step response

The constants are contrasted by using a closed loop tuning method. An estimate of the period T_p is also given in table 4.1.

Table 4.1: Constants for Ziegler-Nichols step response method

Controller	ak_c	T_i/L	T_d/L	T_p/L
P	1			4
PI	0,9	3		5,7
PID	1,2	2	L/2	3,4

The parameters are detailed in table 4.2.

Table 4.2: Parameters of PID controllers

Type	K_p	K_i	K_d
Temperature	10	5	0,1
Oxygen	5,2	3,8	0,005
Air	5,3	3	0,01
Oil	6,3	3	0,01
Lance	8	0,1	0

4.3 Tip pressure controller

The lance tip is a main component of the furnace control system. The tip pressure is used as a measurement method to automatically control the lance depth in

the furnace bath (with respect to the molten bath). Furthermore, it provides the necessary reference to calculate the bath height. This variable is helpful to regulate the bath temperature of the smelting process.

The tip pressure controller automatically adjusts the position of the lance during the smelting process. This mechanism is regulated by a PID controller (PIC230139) in closed loop. The operator establishes an initial position of the lance (called normal operating depth of immersion). The position setup is closely to the set point (generally around 12.5 to 13.5kPa).

The pressure signal is filtered and sent to the DCS logic control. In this block, a pulse width modulation (PWM) either a raise or a lower signal is generated Rodriguez et al. [2012]. The output is sent to the PLC of the speed regulator composed of a motor/gearbox mechanism, which finally determines the spear position and, therefore, the tip pressure (see figure 4.11).

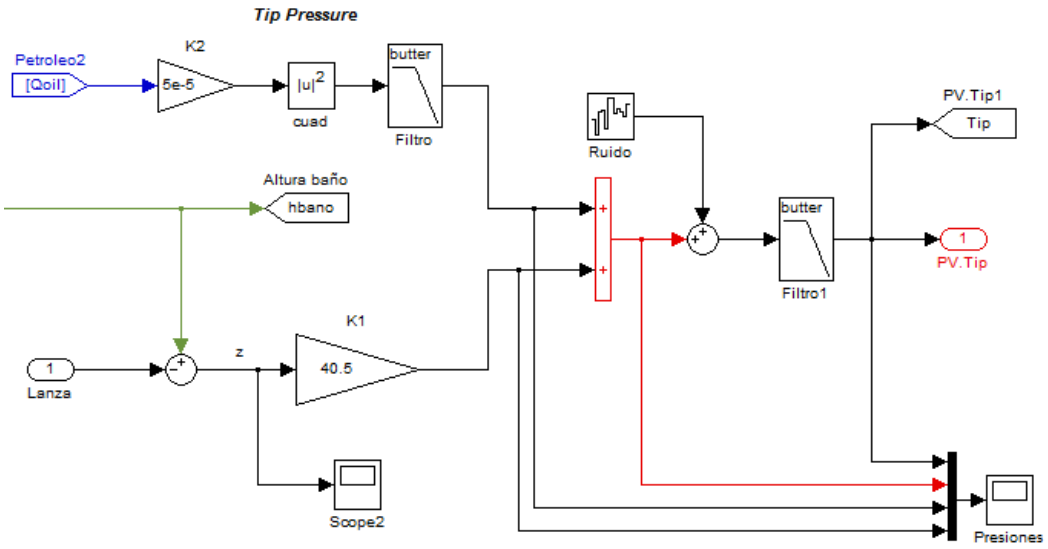

Figure 4.11: Tip pressure controller

The control diagram in figure 4.12 presents the components of the furnace control system.

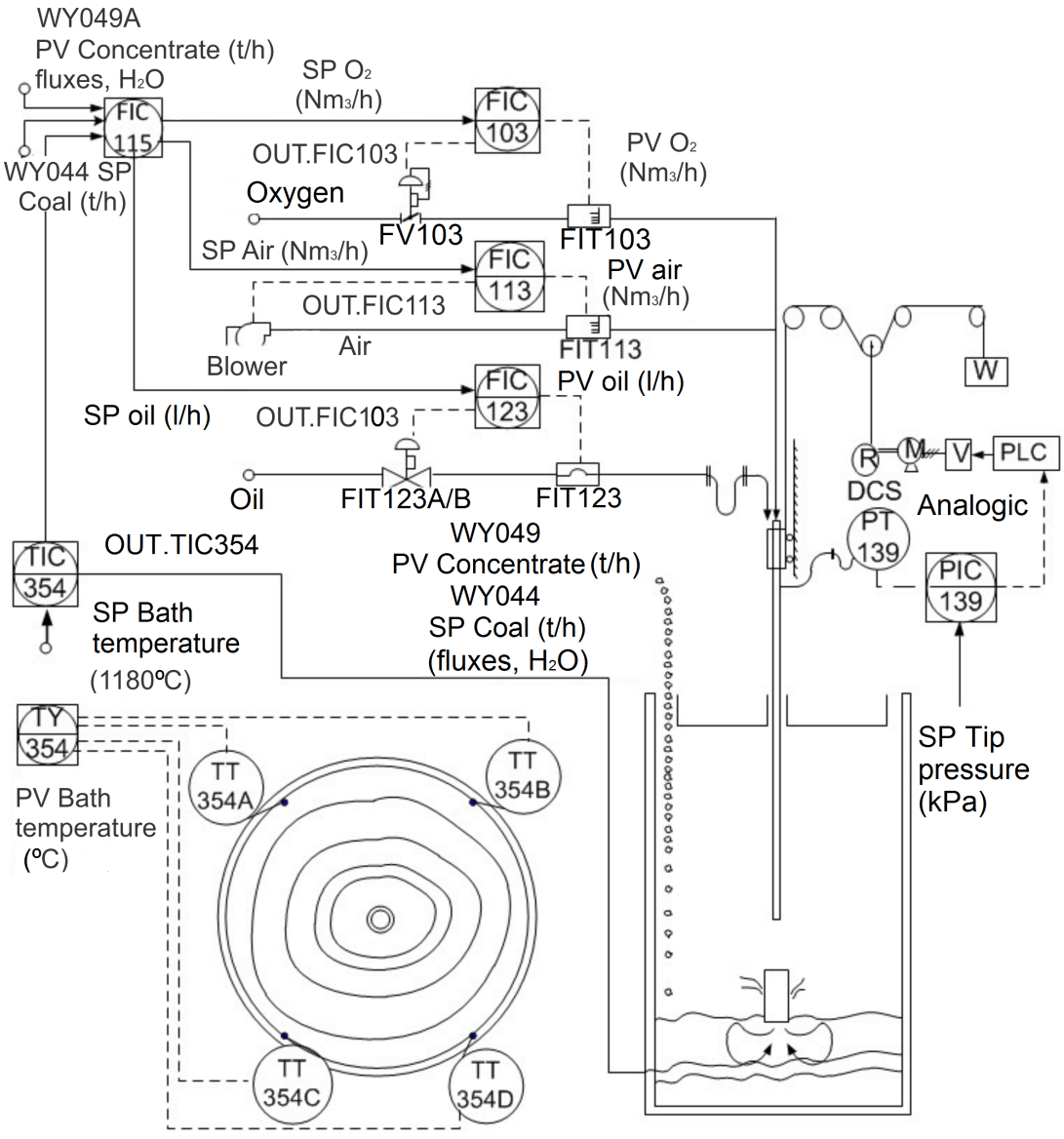

Figure 4.12: Control diagram of the Isasmelt furnace

4.4 Actuators subsystem

The actuator subsystem is mainly composed of inlet guide vane (IGV) valves, which regulate the mass flow of oxygen, blower air and fuel oil. The regulation of such valves responds to their respective controllers. The blower is designed to operate continuously during the furnace operation. However, the flow mass is regulated by opening the relief valve (blow-off valve) air flow to ensure the process requirements.

The oxygen flow is zero when the set point is established at 21%. The operator can select an oxygen enrichment percentage different from 21%, then the oxygen valve is gradually opened until the oxygen enrichment set point is satisfied (see figure 4.13). The total air set point is controlled by the air valve in order to reduce the air flow and comply with 46,800 Nm3/h total flow. The enrichment is calculated by a balance of air and oxygen flows and the respective oxygen compositions at a maximum of 25% O2.

Figure 4.13: Oxygen valve

The oil valve is manipulated via a split range control setup (see figure 4.14) ; that means lower flows are achieved by manipulating one valve only, in case of higher flow demand the second valve is then adjusted to achieve the desired flows.

The block diagram in Simulink of this control structure is given as follows.

Figure 4.14: Oil valve

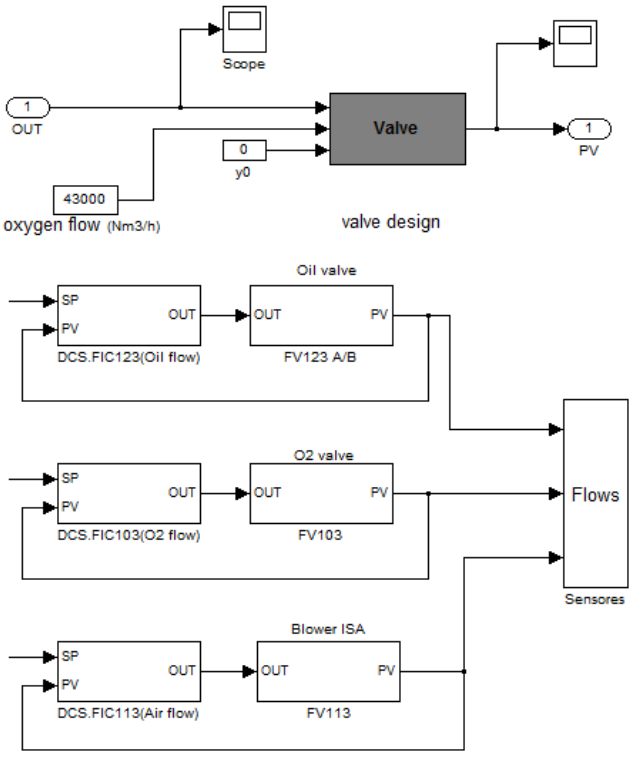

Figure 4.15: valves design

4.5 Concluding remarks

This chapter has described the bath temperature controller and the combustion control subsystem of the Isasmelt furnace. The bath temperature is regulated in cascade mode by a PID controller as outer loop. The control strategy includes the oil flow, air flow and flow rate controllers in outer loop. The flow rates are all manipulated by the operator to attain the temperature set point.

The Isasmelt copper smelting process has been simulated using inlet and outlet process variables. This plant has been modeled based on its mass and energy balance. The simulation model describes the furnace control system and the controlled plant, that are properly validated by stored data from an Isasmelt smelter in southern Peru.

The control settings are critically dependent upon the close regulation of the oxygen-enriched air. The calculation base is the oxygen demand of concentrate, coal and oil feed rates. The temperature is controlled by adjusting the oxygen-enrichment (represented by the N_2/O_2 ratio) and the oil burn rate. The adjustments are also based on sampling essays of the molten material.

The mate grade (range of 60-65% Cu) and slag composition (silica range content of 32-34%) are main parameters to regulate oxygen ratios. However, the current method introduces slow time constants and long time delays, forcing frequently (manual) operator interventions to better control the bath temperature. Such manual regulation generates large deviations up to $30°C$.

Chapter 5

Proposed control system

This chapter describes the proposed control design to regulate the furnace bath temperature. The proposed changes are focused on better control the state variables of copper smelting; also called intensive properties, that describe the thermodynamic equilibrium of this system. That means the bath temperature within the furnace, the matte grade of molten sulfides ($\%Cu$), the silica ($\%SiO_2$) slag content.

The content includes a detailed analysis of the proposed fuzzy controller (i.e. procedures for generating fuzzy rules and control commands). The controller presents basic and extended models to regulate the oxygen enrichment rate ($\%O_2$). The oxygen/nitrogen ratio will be automatic controlled instead of the current manual mode (based on feed recipe calculations).

It is also presented a sampling-based neural network predictor for forecasting the copper (%Cu) and silica ($\%SiO_2$) contents in the molten material. The control action is feedback with this prediction to timely adjust oxygen ratios. The objective is to reduce the operator over-activity and remove dead time (from sampling assays), which lead to temperature deviations up to 30°C.

The proposed control model is shown in figure 5.1. The oxygen enrichment rate and the forecasting of molten composition are manipulated in automatic mode, unlike the current control design where those parameters are manually regulated.

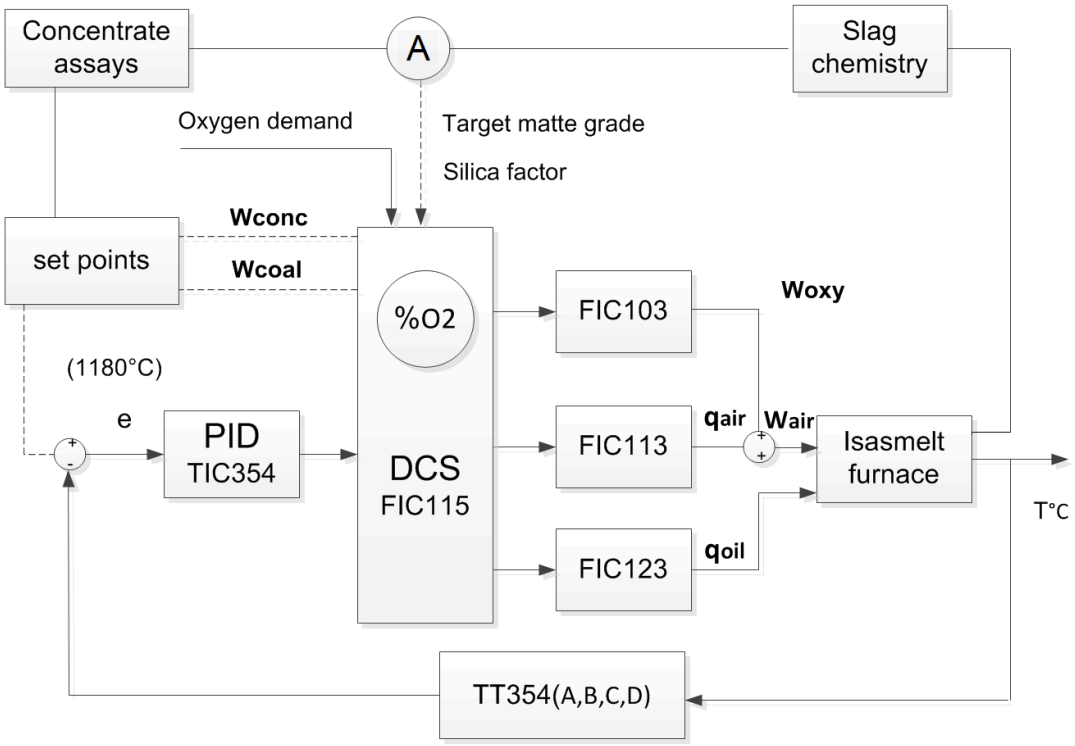

Figure 5.1: Control diagram

5.1 Fuzzy controller

The fuzzy controller is designed to regulate the oxygen enrichment rate ($\%O_2$) and the oil feed rate (see figure 5.1) as the best human operator of the Isasmelt process. The base of rules for this controller is created from past control operations of furnace operators. Their performance has been analyzed to determine the model reference.

The pursued objective of this controller is to closely emulate the best human operator in the steady state zone. The controller should maintain the mixture of combustion air and oxygen content in presence of external events. The better regulation of oxygen enrichment rate should improve the bath temperature control.

5.1.1 Human operator selection

The method consists of initially selecting the best furnace operation as a model reference. The rules should be created based on this expertise, this means knowledge and practical experience in setting-up and regulating the oxygen enrichment rate. The logic of decision making is supported by a set of rules during the furnace operation.

The procedure is as follows: first, the summary of knowledge and skills required for the furnace operation, given by the Australian National Training Authority [2005] are divided into two groups *knowledge* (k_i) and *skills* (s_i). Each group is displayed on a two-dimensional table (E_k for knowledge and E_s for skills), one row for each expertise and in the same order for each column.

Knowledge components (or skills) are compared each other (row versus columns) to establish their importance level (1=equal or more important and 0=less important or matched by itself). The resulting elements of each row are added to obtain the weight-value w_{ei} for each expertise E_k (or E_s) by dividing the row sum $c_i = \sum_{j=1}^{12} e_{ij}, (i = 1, 2, ...12)$ by the amount of the column sum $C = \sum_{i=1}^{12} c_i$.

This expression is given by:

$$w_{ei} = \frac{c_i}{C}, (i = 1, 2, ..., 12) \tag{5.1}$$

The record score for each operator is obtained in multiplying the weight-value by the evaluation score for each expertise topic q_i, using a scale qualification from 1 to 5, to get the preliminary results as is represented as follows:

$$Q_i = w_{ei}.q_i, i = 1, 2, ..., 12 \tag{5.2}$$

It is also added the experience criteria that consists in evaluating the operator's performance in dealing with the oxygen enrichment rate, and therefore, the bath temperature. This criterion is expressed as the inverse of the difference between temperature standard deviations reached by operators in their shift work (σ_i) and the reference standard deviation (σ_T).

The statistical parameters are estimated using stored data during normal operations. Finally, the outcomes are multiplied by heuristic factors (0,6 for exper-

tise and 0,4 for operation performance respectively) according to the expression (5.3) in order to select the best human operator:

$$R_i = 0,6\overline{x}_i + 0,4\frac{\sigma_T}{(\sigma_i - \sigma_T)} \tag{5.3}$$

where i=1, 2, 3, 4 (i.e. the furnace operators).

After selecting the best human operator as a rule-based model, in next sections the basic structure/design of the proposed fuzzy controller is presented, i.e. knowledge base, inference engine, fuzzyfication and defuzzyfication interfaces Ristic and Jestenic [2012].

5.2 Fuzzy rules

The proposed controller, depending of its internal design (basic of alternative model), can apply a base of rules to regulate the oxygen enriched air. In spite of this difference, the fuzzy controller presents common features to finally generate the crisp composite output. The design specifications are detailed in table 5.1.

Table 5.1: Controller specifications

Mandani's inference method	
AND (method)	Min
OR (method)	Max
Implication	Min
Agregation	Max
Defuzzification	Centroid

The temperature function is analyzed under different operating circumstances as concentrate feeding, slag tapping, tap hole close/open or moisture fluctuations, determining the operator's response, that means control actions repeatedly used to keep the furnace temperature controlled or to quickly rise or reduce strong temperature changes.

The operating conditions are ordered depending upon their temperature level (too hot or too cold). The control responses to such conditions according to the

furnace operation manual are summarized as follows:

Temperature too hot: turn any oil off first, reduce average oxygen rate, reduce coal, increase feed moisture value (check moisture first), check feed systems chutes and belts, check feed assays, check magnetite level/metallurgy, check condition of thermocouples and check weighers.

Temperature too cold: put more oxygen on (within limit of low lance cascade set point), increase oil flow, increase average oxygen rate, increase coal, decrease moisture valve, check assays, check metallurgy, check thermocouple consistency and check weighers.

5.2.1 Basic model of fuzzy rules

The inputs of the basic control model are the bath temperature (°C), the temperature rate of change (°C/s) and the feed of copper concentrate (t/h). On the other hand, the model outputs are the percentage of oxygen enrichment ($\%O_2$) and the flow rate of fuel oil (l/h). The model inputs/outputs are put into right and left side respectively as is shown in figure 5.2.

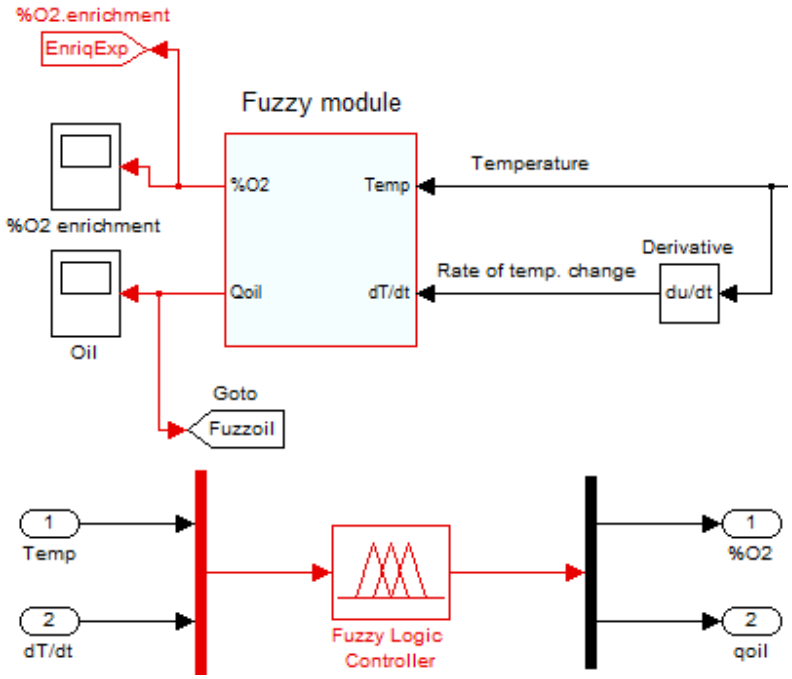

Figure 5.2: Fuzzy control schema

The domain of discourse, also called the universe of discourse is the set of input/output model variables. This declarative part specifies the range of relevant values for each linguistic variable. The discretization of this domain by the fuzzyfication functions is detailed in table 5.2 and the categories for specifying the control rules are described in table 5.3.

Table 5.2: The universe of discourse

Variable	Unit	Scale	Division	Function
Temperature	°C	[1150 - 1210]	7	Gauss
dTemperature	°C/s	[-80 - 80]	3	Triangular
Concentrate	t/h	[120 - 180]	3	Trapezoidal
% O_2 enrich	%	[60 - 70]	7	Triangular
Oil	l/h	[0 - 2000]	3	Triangular

Table 5.3: Linguistic terms

Name	Description
NN	Very cold
N	Cold
ZN	Slightly cold
Z	Ideal temperature
ZP	Slightly hot
P	Hot
PP	Very hot

The concentrate feeding (initially applied as an input) is discarded due to the high computational cost and large number of rules Havl [2006], Hilera and Martínez [2000]. The features of input/output variables based on this practical experience are presented in table 5.4.

Table 5.4: Features of input/output variables

Type	Variable	Range	MF	Function	Parameters
Input	Temperature	$[1100 - 1240]$	NN	Gaussian	[0.909, 1100]
			N		[0.909, 1123]
			ZN		[0.909, 1147]
			Z		[0.909, 1170]
			ZP		[0.909, 1193]
			P		[0.909, 1217]
			PP		[0.909, 1240]
	dTemperature	$[-80 - 80]$	N	Triangular	[-144, -80, -16]
			Z		[-64, 0, 64]
			P		[16, 80, 144]
Ouput	$\%O_2$	$[60 - 70]$	NN	Triangular	[58,33; 60; 61,67]
			N		[60; 61.67; 63,33]
			ZN		[61,67 63,33 65]
			Z		[63,33; 65; 66,67]
			ZP		[65; 66,67; 68,33]
			P		[66,67; 68.33; 70]
			PP		[68,33; 70; 71,67]
	Oil	$[0 - 2000]$	Z	Triangular	[-667; 0; 341,3]
			ZP		[-5,29; 690; 1548]
			P		[934; 1511; 2000]
			PP		[1542; 2000; 2670]

where MF means membership function.

The fuzzy variables are described by mapping crisp points in U to fuzzy sets in U (fuzzyfier), and by mapping fuzzy sets in V to crisp points in V (defuzzyfier). The knowledge base is built considering the furnace operation of the first six months of 2008 as shown in table 5.5.

The initial inference matrix are simplified by Pareto's principle. This approach consists of taking into account the most frequently-occurring rules scenarios (20% of the rules explains 80% of the whole process), instead of taking all possible operating range. This method enables the prioritization of rules so that redundancy is also removed without affecting the overall performance of the fuzzy controller (in comparison with usual redundancy thresholds). Then, the summary of candidate rules are ordered and classified by an algorithm:

Table 5.5: Rules

Rule	Temperature	dTemp	$\%O_2$	Oil
1	N	N	PP	PP
2	NN	Z	PP	P
3	N	P	PP	ZP
4	N	Z	ZP	ZP
5	ZN	Z	Z	Z
6	Z	N	N	Z
7	Z	P	P	Z
8	ZP	Z	ZN	Z
9	P	Z	N	Z
10	P	N	NN	Z
11	PP	Z	NN	Z
12	P	P	NN	Z

Procedure Selection(C, g(.)) %*The rule set and operating range will be searched.*
C = 0; %*Initialize the rule set as an empty set.*
while C $\neq$ 0 do; %Rules searching
s = min,max g(t), t $\in$ T; %*s The Pareto's range within the operating interval T is computed (based on Pareto's principle.)*
Initialize candidate rule x; %*first rule candidate is initialized.*
RC = x $\in$ s $\leq$ g(s); % *Rules candidates are defined.*
Select x, at random, from the RCL;
x = x $\bigcup$ C; %*Rules are included in rule set.*
Update the rule set C;
end while;
end selection;

Table 5.6 describes the base of rules of the fuzzy controller. The rows represent the 7 possible states of the bath temperature, while the columns represent the 3 possible states of its rate of change. The sub-columns represent the possible ranges of oxygen enrichment and oil flow rates to be injected into the lance.

Table 5.6: Fuzzy control rules

		dTemperature					
		N		Z		P	
		$\%O_2$	Oil	$\%O_2$	Oil	$\%O_2$	Oil
Temperature	PP			NN	Z		
	P	NN	Z	N	Z	ZN	Z
	ZP			ZN	Z		
	Z	N	Z			P	Z
	ZN			Z	Z		
	N	PP	PP	ZP	ZP	PP	ZP
	NN			PP	P		

The membership functions of the temperature and the oxygen enrichment rate are described in figure 5.3.

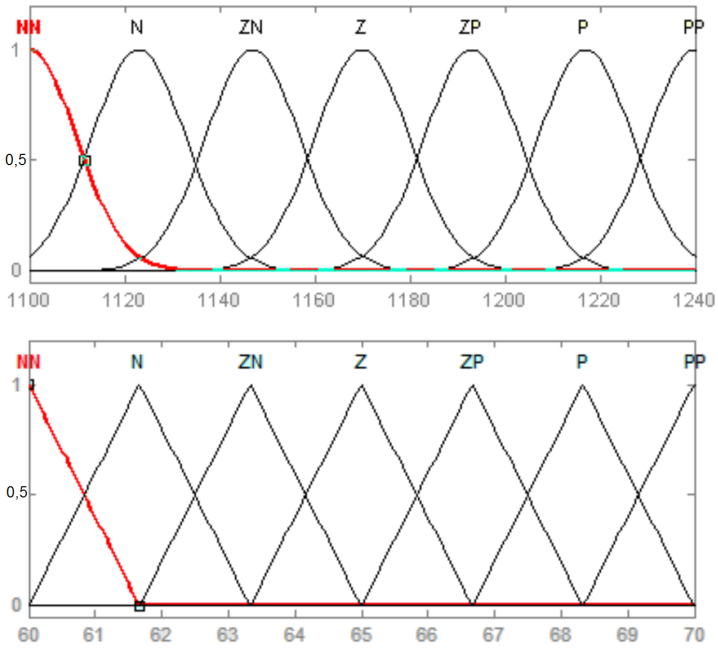

Figure 5.3: (top) Temperature input variable, (down) $\%O_2$ enrichment rate

5.2.2 Extended fuzzy control model

In this section an extended fuzzy control model has been described. This design is helpful to understand the impacts of coal feed into the fuzzy basic controller. The inputs of the alternative model are the temperature error (°C) and the derivative of temperature (°C/s). The outputs are the percentage of oxygen enrichment ($\%O_2$), the coal feed (t/h) and the flow rate of fuel oil (l/h). The membership functions are summarized in table 5.7 and the rules are also presented in table 5.8.

Table 5.7: Membership functions

Name	Temp. error	dTemp.	Oil	O_2	Coal
NN	very cold				
N	cold	negative		low	low
ZN	slightly cold				
Z	ideal temp.	constant	no-flow	normal	normal
ZP	slightly hot		low-flow		
P	hot	positive	middle flow	high	high
PP	very hot		high flow		

Table 5.8: Fuzzy Control Rules

		dTemperature								
		N			Z			P		
		O_2	*Oil*	*Coal*	O_2	*Oil*	*Coal*	O_2	*Oil*	*Coal*
Temperature error	PP	N	Z	N				N	Z	N
	P				Z	Z	Z			
	ZP	Z	Z	Z				Z	Z	N
	Z				Z	ZP	Z			
	ZN	Z	P	Z				Z	ZP	Z
	N				ZN	P	Z			
	NN	P	PP	P				P	PP	Z

The membership function of this alternative model are depicted in figure 5.4.

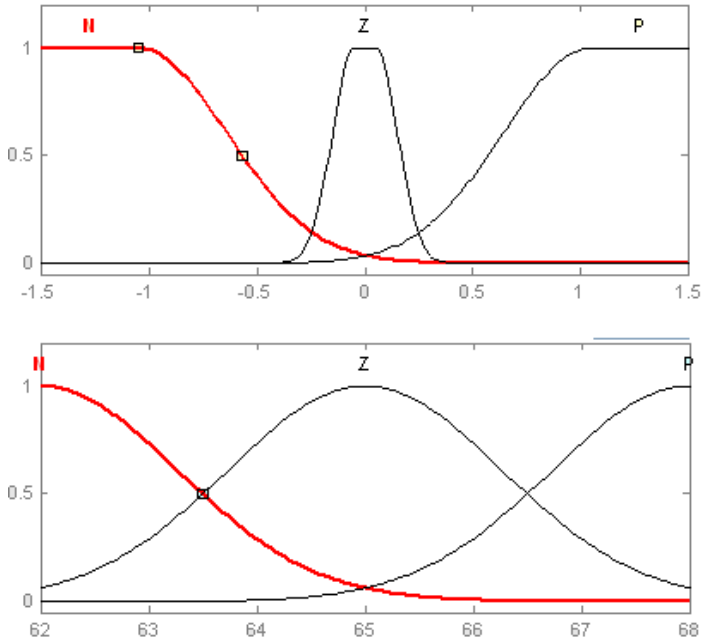

Figure 5.4: Membership function of alternative model

The fuzzy functions are described by their spectral distribution curves that can be interpreted as membership functions (3D view of the membership functions) in figures 5.5, 5.6 and 5.7.

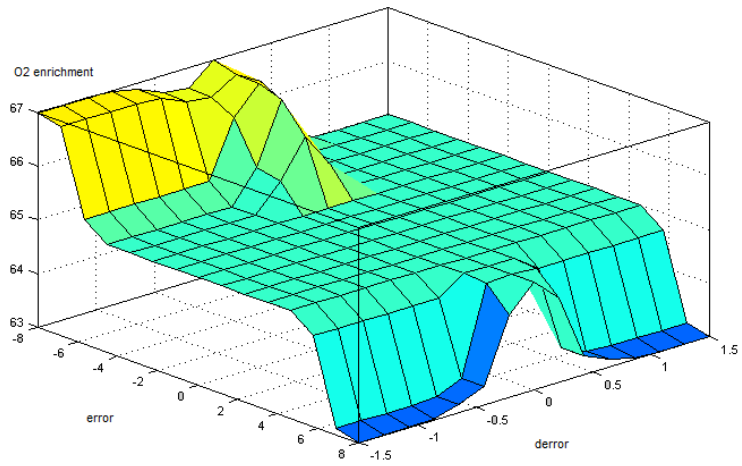

Figure 5.5: Membership function of alternative model

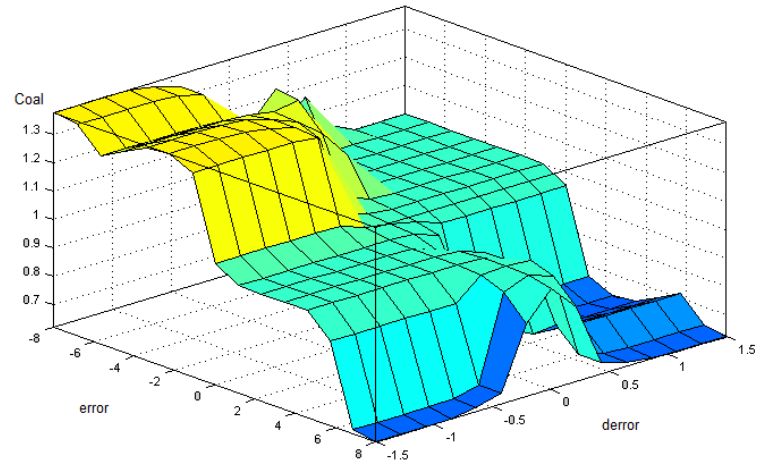

Figure 5.6: Membership function of alternative model

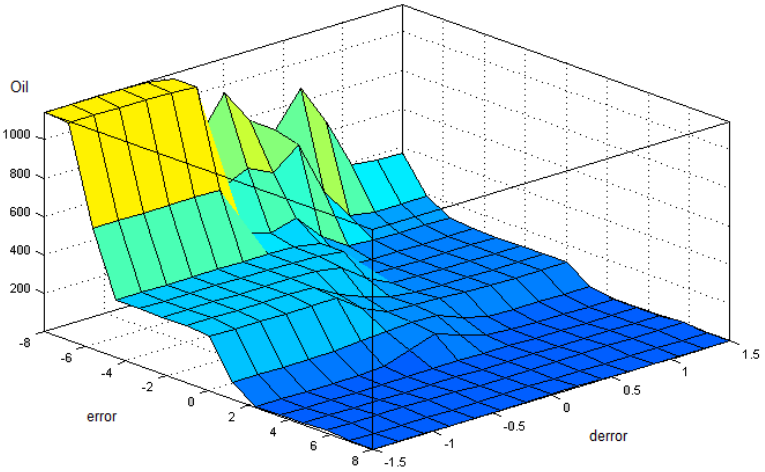

Figure 5.7: Membership function of alternative model

5.3 Metallurgical predictive module

Te actual tapping composition is obtained with a large delay, which causes an extremun difficulty on its control. This delay has motivated the design of a metallurgical predictive module for forecasting the tapping composition (or molten material). This model is composed of two neural networks: one for the matte grade (see figure 5.8) and the other for the silica content (see figure 5.9).

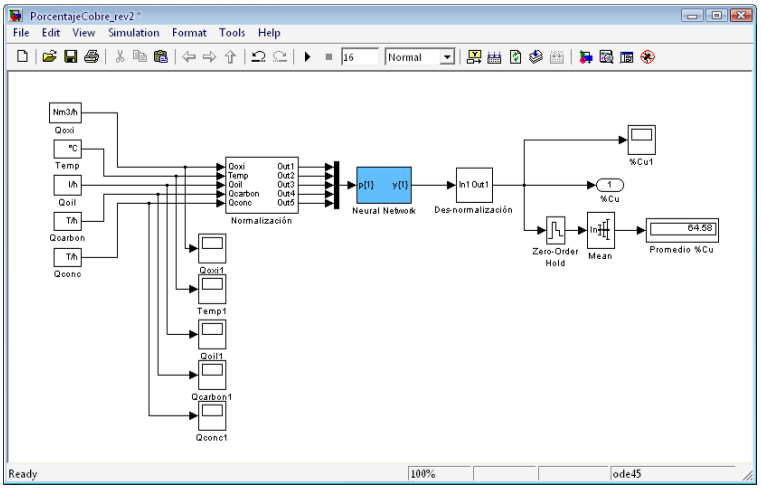

Figure 5.8: Copper predictor submodule

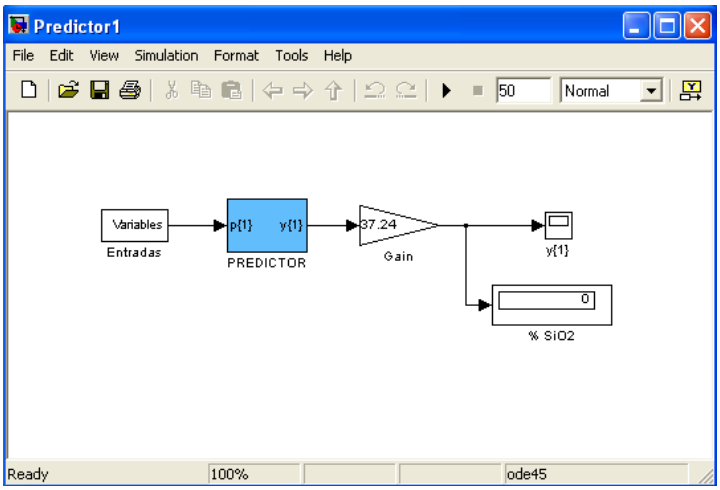

Figure 5.9: Silica predictor submodule

The process variables are firstly analyzed to be used as possible inputs for the predictive module. This analysis consists of taking into consideration their influence on the molten material composition, that means matte grade ($\%Cu$) and silica content ($\%SiO_2$). The stored data of periodical molten samples is applied to find such correlation.

The copper content ranges between 60% and 65% (higher matte grade produces important losses of copper in the slag) and the silica percentage between 32% and 34%. This prediction timely allows calculating the correct oxygen ratios Wei-hua et al. [2007].

5.3.1 Analysis of process variables

The analysis of process variables comprises main variables as bath temperature, concentrate and coal feed, oxygen and oil flow rates, silica and coquina fluxes.

Bath temperature: this variable is critical within the smelting process, because oxidation reactions are only possible under high temperatures, which range between 1180 °C and 1200 °C. At these high temperatures the copper concentrate can be smelted with less slag and lower magnetite concentration.

Concentrate feed: the average of concentrate feed ranges from 38 to 57 tons per hour. The copper content (mostly composed of chalcopyrite) bears between 20-30% at the early phase of smelting. The concentrate becomes a molten sulfide phase richer in copper than the original composition.

Coal feed: the basic smelting operation is auto-thermal, that means the process heat is maintained by the sulfur of the chalcopyrite. However, the smelting temperature is regulated by coal addition to quickly raise the bath temperature, when the sulfur content is not enough to sustain the smelting reactions.

Oxygen flow rate: this element is added onto the blown air to enhance chemical reactions inside the furnace. The average value on a normal day of operation ranges between 28,000 Nm^3/h and 33,160 Nm^3/h. This variable is dependent upon the percentage of oxygen enrichment and the oxygen purity, which determine the general features of the air mixture.

The percentage of oxygen enrichment directly enables the enriched air composition, and therefore, the combustion air. The operation point must be set between 60-67%. However this proportion can be adjusted according to the target matte grade. This adjustment is performed in accordance to sampling-based slag chemistry.

Oil flow: the oil flow is normalized between 0 and 1000 liters/hour. This fuel is used to make fine adjustments to the bath temperature between ± 5°C.

On the other hand the fixed carbon in coarse coal grains survives through the oxidizing reaction to serve later as reductant for magnetite and copper oxide.

Silica: this flux is used to control the chemistry composition of the slag, because it reduces the copper losses in the slag.

Coquina flux: this material neutralizes the oxides which are present in the slag and lowers the fusion point. It also allows the separation of arsenic from the matte to the slag.

Figure 5.10 describes the influence of input variables on the matte grade ($\%Cu$). The legend of the elements is presented in the figure 5.11

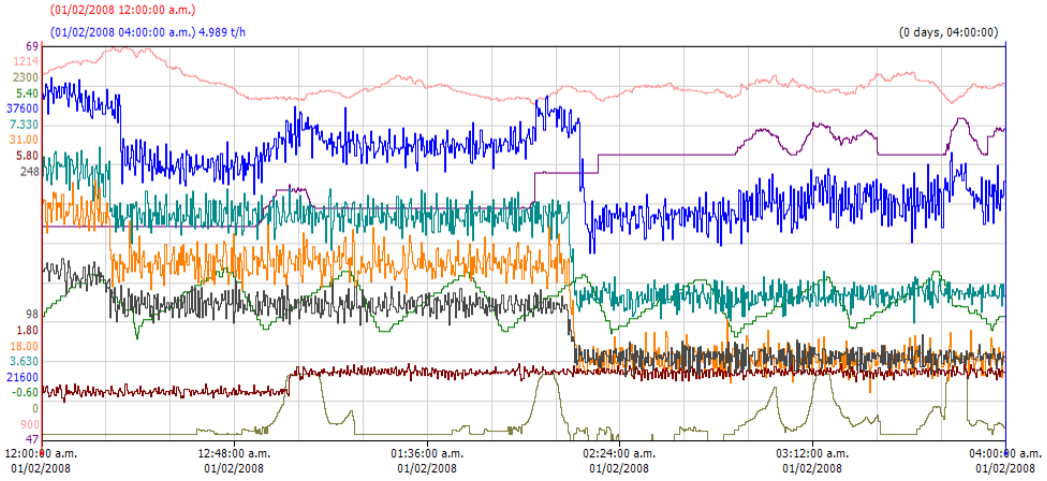

Figure 5.10: Behavior of input variables and their influence on matte grade

Tag Name	Description	Server	Color	Units	Minimum	Maximum	IO Address	Time Off...
FY230103	% O2 in Enriched Air	172.17.32.18		%	47	69	\\172.20.0.32\FSGateway\Delt...	0:00:00.000
TI230354A	Bath Temperature 750 mm North	172.17.32.18		°C	900	1214	\\172.20.0.32\FSGateway\Delt...	0:00:00.000
TI230354B	Bath Temperature 750 mm South	172.17.32.18		°C	900	1214	\\172.20.0.32\FSGateway\Delt...	0:00:00.000
TI230354C	Bath Temperature 1250 mm North	172.17.32.18		°C	900	1214	\\172.20.0.32\FSGateway\Delt...	0:00:00.000
TI230354D	Bath Temperature 1250 mm South	172.17.32.18		°C	900	1214	\\172.20.0.32\FSGateway\Delt...	0:00:00.000
FIC230123	Lance Combustion Oil Flow	172.17.32.18		l/h	0	2300	\\172.20.0.32\FSGateway\Delt...	0:00:00.000
ZI230273A	Lance Position	172.17.32.18		m	-0.60	5.40	\\172.20.0.32\FSGateway\Delt...	0:00:00.000
FIC230103	Lance Oxygen Flow Controller	172.17.32.18		Nm3/h	21600	37600	\\172.20.0.32\FSGateway\Delt...	0:00:00.000
WIC220042	Coquina / flux Bin 2 Feed Rate (dry tonnes/ Hr)	172.17.32.18		t/h	3.630	7.330	\\172.20.0.32\FSGateway\Delt...	0:00:00.000
WIC220043	Silica Bin 3 Feed Rate (dry tonnes/ Hr)	172.17.32.18		t/h	18.00	31.00	\\172.20.0.32\FSGateway\Delt...	0:00:00.000
WIC220044	Coal Bin 4 Feed Rate (dry tonnes/ Hr)	172.17.32.18		t/h	1.80	5.80	\\172.20.0.32\FSGateway\Delt...	0:00:00.000
WIC220045	Concentrate Bin 5 Feed Rate (dry tonnes/ Hr)	172.17.32.18		t/h	32.5	82.5	\\172.20.0.32\FSGateway\Delt...	0:00:00.000
WIC220046	Concentrate Bin 6 Feed Rate (dry tonnes/ Hr)	172.17.32.18		t/h	32.5	82.5	\\172.20.0.32\FSGateway\Delt...	0:00:00.000
WIC220047	Concentrate Bin 7 Feed Rate (dry tonnes/ Hr)	172.17.32.18		t/h	32.5	82.5	\\172.20.0.32\FSGateway\Delt...	0:00:00.000
WI220049	Total Dry Concentrate Feed Rate	172.17.32.18		t/h	98	248	\\172.20.0.32\FSGateway\Delt...	0:00:00.000

Figure 5.11: Active Factory's legend

Figures 5.12 and 5.14 present the influence of input variables on the silica (SiO_2) composition. The legend of the elements is described in figures 5.13 and 5.15 respectively.

- From 09:00:00 pm 01/12/2007 to 01:30:00 am 02/12/2007.
- From 09:00:00 pm 02/12/2007 to 01:30:00 pm 02/12/2007.
- From 04:00:00 pm 05/12/2007 to 08:00:00 am 05/12/2007.
- From 12:30:00 pm 05/12/2007 to 05:30:00 pm 05/12/2007.

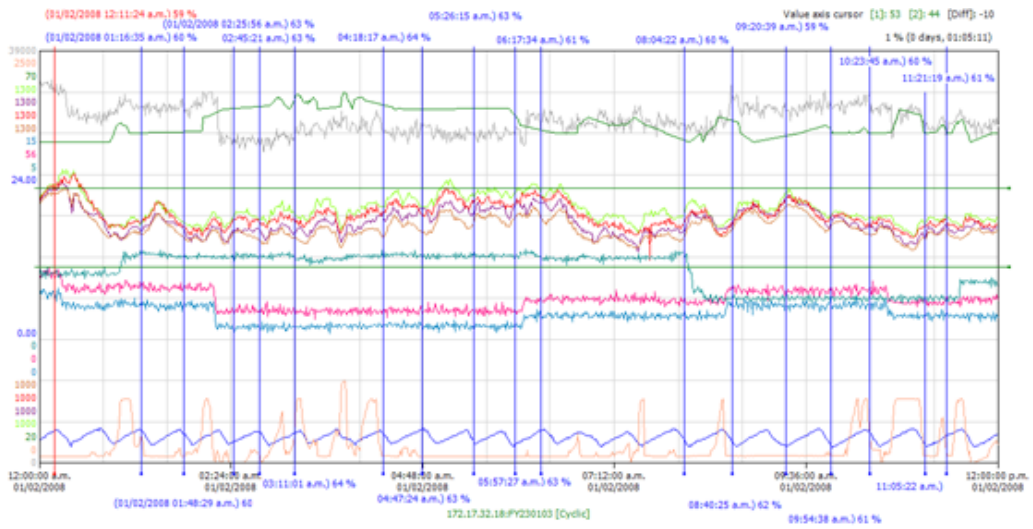

Figure 5.12: Behavior of input variables and their influence on the silica composition

The observing periods run from 26/01/2008 to 03/02/2008 as shown as follows:

- From 04:00:00 on 26/01/2008 to 08:00:00 on 26/01/2008
- From 05:30:00 on 31/01/2008 to 10:30:00 on 31/01/2008
- From 12:00:00 on 01/02/2008 to 16:00:00 on 01/02/2008
- From 00:00:00 on 01/02/2008 to 12:00:00 on 01/02/2008

FIC230103	Lance Oxygen Flow Controller	172.17.32.18	Nm3/h	0	39000
FIC230103SP	Lance Oxygen Flow Set Point	172.17.32.18	Nm3/h	0	39000
FY230103	% O2 in Enriched Air	172.17.32.18	%	35	70
TI230354A	Bath Temperature 750 mm North	172.17.32.18	°C	1000	1300
TI230354B	Bath Temperature 750 mm South	172.17.32.18	°C	1000	1300
TI230354C	Bath Temperature 1250 mm North	172.17.32.18	°C	1000	1300
TI230354D	Bath Temperature 1250 mm South	172.17.32.18	°C	1000	1300
WI220048	Transfer Conveyor Weight Indicator	172.17.32.18	t/h	0	650
WI220049	Total Dry Concentrate Feed Rate	172.17.32.18	t/h	0	350
WIC220042	Coquina / flux Bin 2 Feed Rate (dry tonn...	172.17.32.18	t/h	0	15
WIC220043	Silica Bin 3 Feed Rate (dry tonnes/ Hr)	172.17.32.18	t/h	0	56
WIC220044	Coal Bin 4 Feed Rate (dry tonnes/ Hr)	172.17.32.18	t/h	0	5
ZI230273A	Lance Position	172.17.32.18	m	0.00	24.00

Figure 5.13: Active Factory's legend

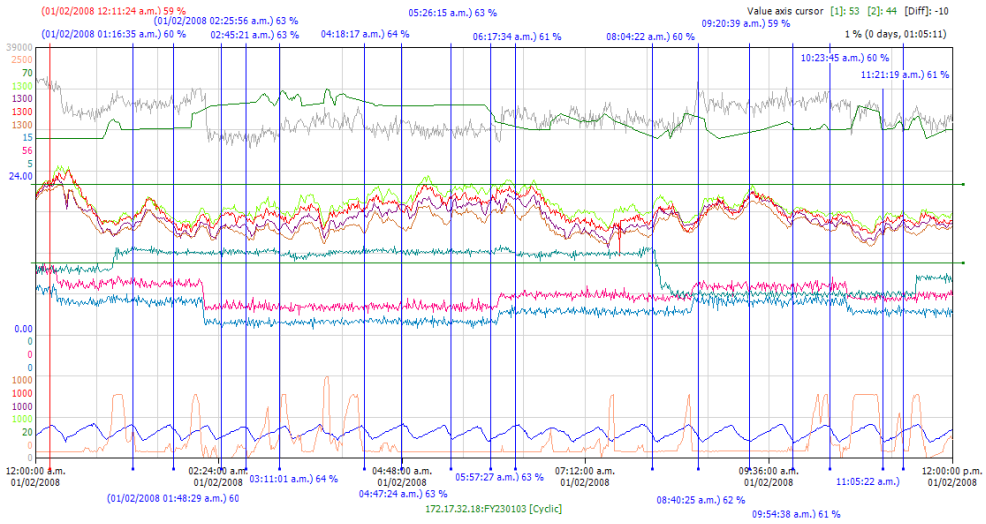

Figure 5.14: Process variables behavior

- From 12:00:00 on 03/02/2008 to 05:30:00 on 03/02/2008

After analyzing the real operation, it can be concluded that copper content is influenced by the bath temperature and by flow rates of oxygen (and indirectly by the percentage of oxygen enrichment), as well as the feed of concentrate ($\dot{w}_{conc}$) and coal ($\dot{w}_{coal}$).

On the other hand, the silica content in the slag (SiO_2) is dependent upon the oxygen enrichment and the oxygen ($\dot{w}_{oxi}$) flow rates as well as oil flows(q_{oil}), as well as the concentrate ($\dot{w}_{conc}$) and coal feeds ($\dot{w}_{coal}$).

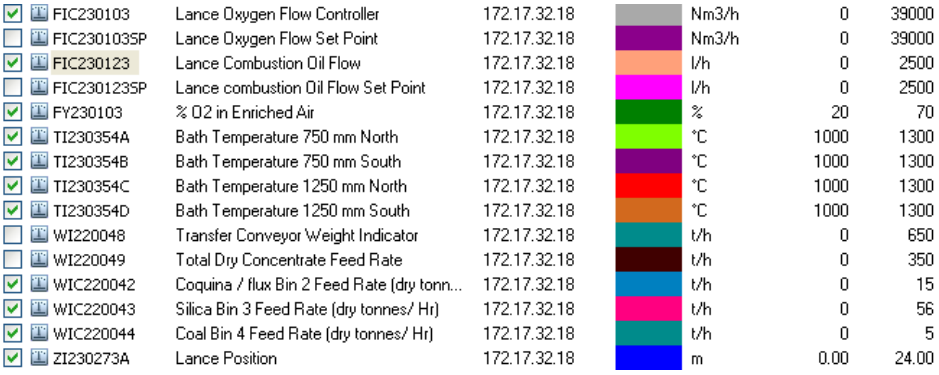

FIC230103	Lance Oxygen Flow Controller	172.17.32.18	Nm3/h	0	39000
FIC230103SP	Lance Oxygen Flow Set Point	172.17.32.18	Nm3/h	0	39000
FIC230123	Lance Combustion Oil Flow	172.17.32.18	l/h	0	2500
FIC230123SP	Lance combustion Oil Flow Set Point	172.17.32.18	l/h	0	2500
FY230103	% O2 in Enriched Air	172.17.32.18	%	20	70
TI230354A	Bath Temperature 750 mm North	172.17.32.18	°C	1000	1300
TI230354B	Bath Temperature 750 mm South	172.17.32.18	°C	1000	1300
TI230354C	Bath Temperature 1250 mm North	172.17.32.18	°C	1000	1300
TI230354D	Bath Temperature 1250 mm South	172.17.32.18	°C	1000	1300
WI220048	Transfer Conveyor Weight Indicator	172.17.32.18	t/h	0	650
WI220049	Total Dry Concentrate Feed Rate	172.17.32.18	t/h	0	350
WIC220042	Coquina / flux Bin 2 Feed Rate (dry tonn...	172.17.32.18	t/h	0	15
WIC220043	Silica Bin 3 Feed Rate (dry tonnes/ Hr)	172.17.32.18	t/h	0	56
WIC220044	Coal Bin 4 Feed Rate (dry tonnes/ Hr)	172.17.32.18	t/h	0	5
ZI230273A	Lance Position	172.17.32.18	m	0.00	24.00

Figure 5.15: Active Factory's legend

5.3.2 Neural network architecture

The metallurgical predictor for forecasting the molten composition consists of two neural networks, which are supported by a feed forward architecture. The matte grade predictor has the bath temperature, the oxygen flow and the feeding of oil, concentrate and coal as inputs and the silica predictor has the bath temperature, the oxygen enrichment rate and the feeding of oil, concentrate and coal as inputs.

The number of layers (including hidden layers) and neurons pro layer have been determined by stored data from bath temperature and oxygen enrichment rate and oil feed during normal operation (see figures 5.16 and 5.17). The architecture is based on a back-propagation algorithm and a logsig transfer function (because the output values are all positive).

The model has been trained (on the training set) for 5000 and 10000 epochs, which was enough for the cleaning error (correction to the net inputs) to stabilize the model. After training, weights associated with the best performance (in terms of hit rate) on the validation set have been selected and applied to get the suitable configuration.

The neural network is initially trained with 32 input/output data (the standard sample of molten material) from January 26th to February 1st, 2008. However, the analytical comparison with real data has been not favorable because the copper content of matte composition are below 40%.

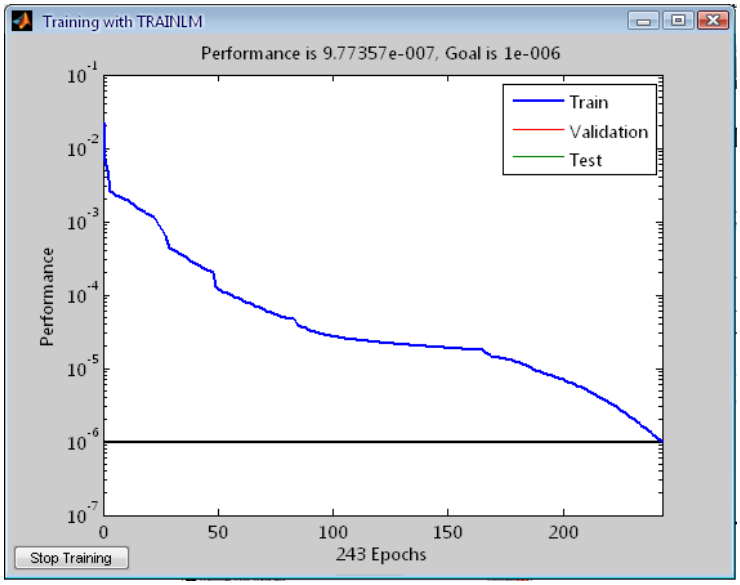

Figure 5.16: Neuronal network training using optimal parameters-1

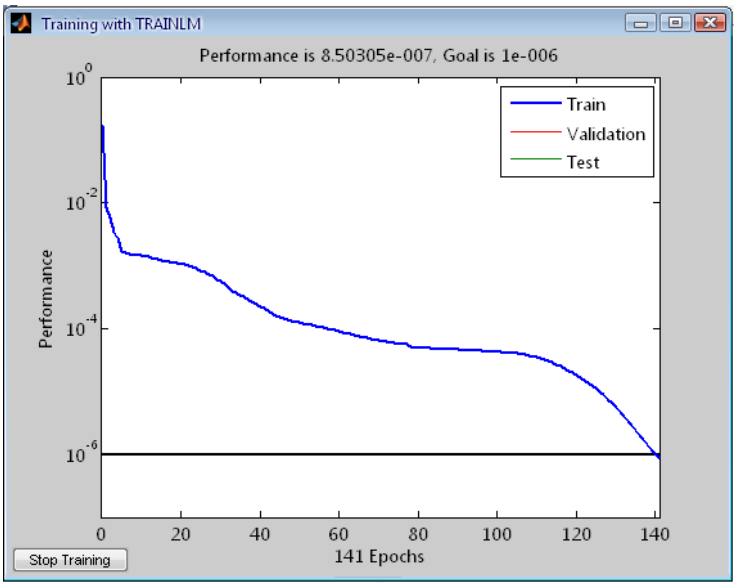

Figure 5.17: Neuronal network training using optimal parameters-2

The data used to train the neural network is previously arranged taking into account the averages of input/output variables during the furnace operation. The chemical register comprises sample analysis of molten material between successive casting operations. The reports establish the content of %Cu in the matte and

%SiO2 in the slag.

The tests are performed using different network settings (number of hidden layers, number of neurons, transfer functions and training parameters). The model responses are also analyzed in order to establish the optimal configuration. The features of the neural networks structure is presented in next paragraph.

In this step, after setting the parameters of the neural network and have got its training data, there is found a reference frame to make analytic comparisons between the predicted data and the real operation values. This analysis includes eight-hour periods under normal operation. The results are graphically depicted in figures 5.18 and 5.19.

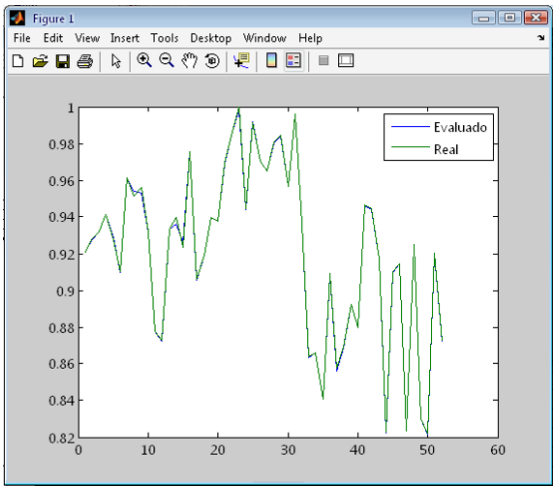

Figure 5.18: Copper predictor

For this reason it is chosen a 52 sample size of input/output data. The neural network of the predictive module reduces the output error in comparison to the real system. The copper percentage also achieves acceptable results. The essays are depicted in figures 5.20 and 5.21. The predictor module for the percentage of SiO_2 is tested with different values are within the real percentage range.

The test for the simulation model in real time is performed for assessing the performance of the system with data directly obtained from the industrial server of the process. Besides to verify the proper operation, it allowed adjusting the important parameters of the control system. Sampling time is one of the critical variables and this module allowed determining the optimal value.

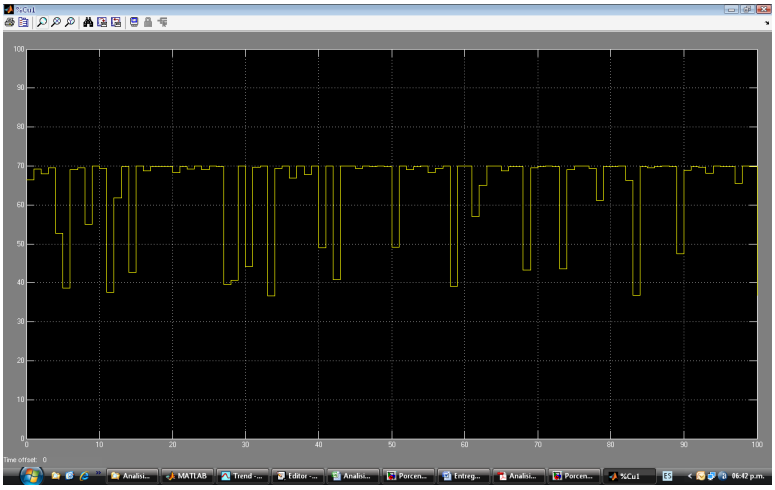

Figure 5.19: Copper prediction (Test 1)

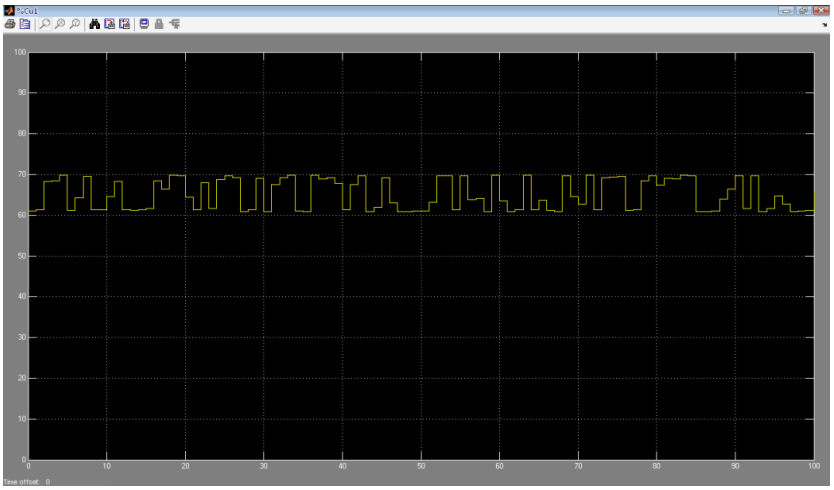

Figure 5.20: Copper prediction (Test 2)

The predictor presents the following features:

- Feedforward backpropagation network.
- Normalization of input data.
- First hidden layer with 10 neurons and logsig transfer function.
- Second hidden layer with 20 neurons and logsig transfer function.

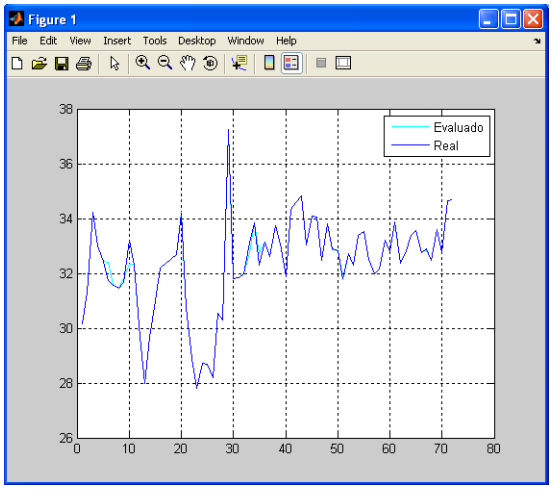

Figure 5.21: Silica predictor

- Third hidden layer with one neuron and logsig transfer function.
- Training type is trainlm.

5.4 Concluding remarks

In this section, a proposed control structure to regulate the furnace bath temperature has been proposed. This model is composed of a fuzzy module for adjusting the ratio oxygen/nitrogen and a metallurgical predictor for forecasting the molten composition. The oxygen enriched air is regulated by a fuzzy controller instead of using a manual regulation. The fuzzy controller emulates the best furnace operator by manipulating the oxygen enrichment rate and the oil feed in order to control the bath temperature.

For designing the fuzzy controller, a human model has been selected taking into account the operator's practical experience in dealing with the furnace temperature (and taking into account good practices from the Australian Institute of Mining and Metallurgy) to have a valid reference for understanding the whole process and better regulate the oxygen enrichment rate.

This structure is complemented by a neural network based predictor, which estimates measured variables of molten material as copper (%Cu) and silica ($\%SiO_2$) contents. The metallurgical predictor takes into account stored data

from sample essays (previously explained in subsection 3.3.1). The forecasting of matte and slag composition removes process dead times caused by sampling assays.

Chapter 6

Discussion and results

This chapter reports the results of a comparative analysis between the current control system and the proposed control design. The comparison is performed by evaluating the furnace bath temperature. In testing such controllers, performance indexes and productivity based indexes have been applied. The simulated plant used in this experiment is an Isasmelt furnace from a Peruvian smelter.

6.1 Comparative analysis between the current and the proposed control systems

After validating the furnace simulation, current and proposed control systems are compared in dealing with the molten bath temperature; that means, the model output (or controlled variable). This evaluation is performed in off-line (with stored process data) and on-line modes (with real process variables).

Temperature values reached by current control system and proposed control design are also tested. The mean square relative error and the standard deviation of process values are considered as measures for comparative purposes. The mean square relative error is defined as:

$$\%e_{rms} = \sqrt{\frac{\sum_{i=1}^{N} \left(\frac{T_{PV_i} - T_{SP_i}}{T_{SP_i}}\right)^2}{N}} \times 100 \tag{6.1}$$

where T_{PV_i} is the temperature process value (measured value), T_{SP_i} is the temperature set point (desired value) and N: is the number of samples.

In off-line mode, the simulated system has been evaluated using concentrate feed as disturbance input. This variable has been processed under normal operating conditions (see figure 6.1).

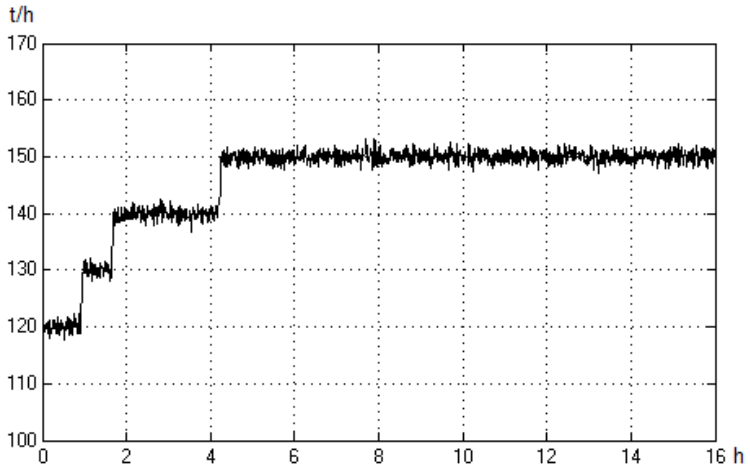

Figure 6.1: Concentrate feed as disturbance input

The proposed controller reduces the mean square relative error in approx. 55% and also the standard deviation in 58% against current PID controller (see table 6.1). The results indicated that the proposed controller achieves a better performance in regulating the molten bath temperature than the current control system.

Table 6.1: Off-line Comparison of Controllers

Type	$e_{rms}(\%)$	$\sigma(°C)$
PID controller	0,653	25,5
Fuzzy controller	0,289	10,8

In order to perform on-line tests, historical and live data from the Isasmelt plant is accessed using the OPC toolbox (see figure 6.2). The simulation is carried out with real process variables (concentrate and coal feed, oil, oxygen and air flows, percent of oxygen enrichment, tip pressure and bath temperature values).

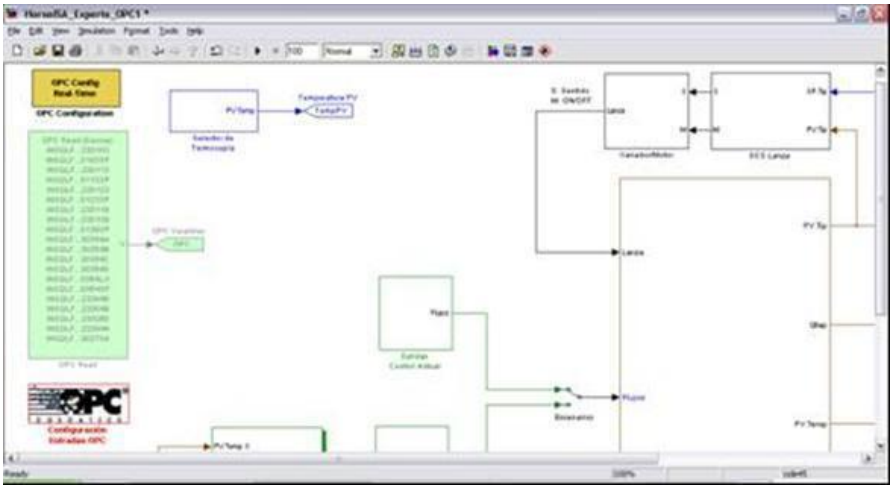

Figure 6.2: OPC toolbox

The process data has been identified with tag numbers to test the connectivity of the distributed control system (see figure 6.3). Then, a GUI/Simulink based interface is built, so that the OPC server could be integrated within the Matlab model. This application includes an user interface to place the model inputs (see figure 6.4).

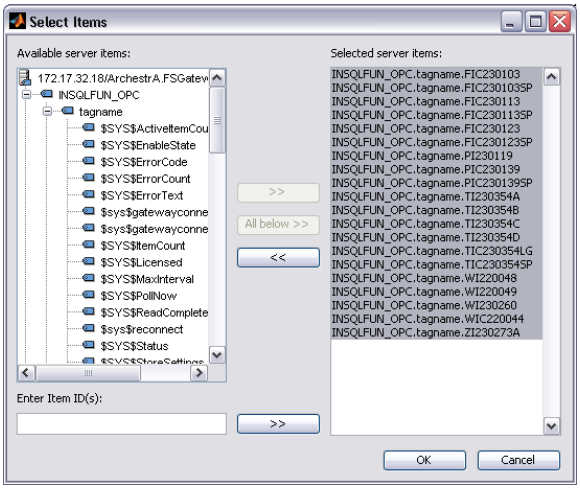

Figure 6.3: none

The model is on-line tested using different gain values (k_1) in function of concentrate feed. This constant is 3.52e-3 if the concentrate flow ranges between

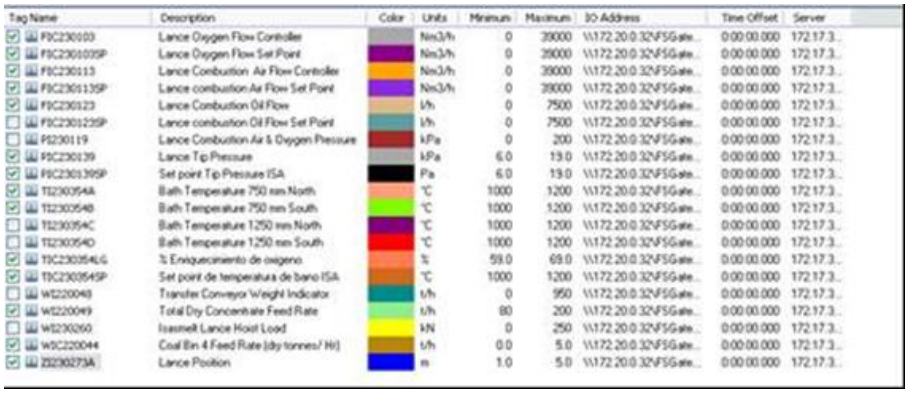

Figure 6.4: Tags of process variables

[120 - 140] t/h and 3.47e-3 if it ranges between [140 - 165] t/h. However, small adjustments of this model could be performed according to concentrate composition.

The OPC server requires some changes to establish the server connectivity. The fuzzy controller block is modified by adjusting scales of error (°C), the derivative of error (°C/s) and the percentage of oxygen enrichment from [60 - 70]% to [57 - 68]%. The OPC application allows to analyze the simulation with real input variables.

The setups of OPC changes are presented in figures 6.5, 6.6, 6.7 and 6.8.

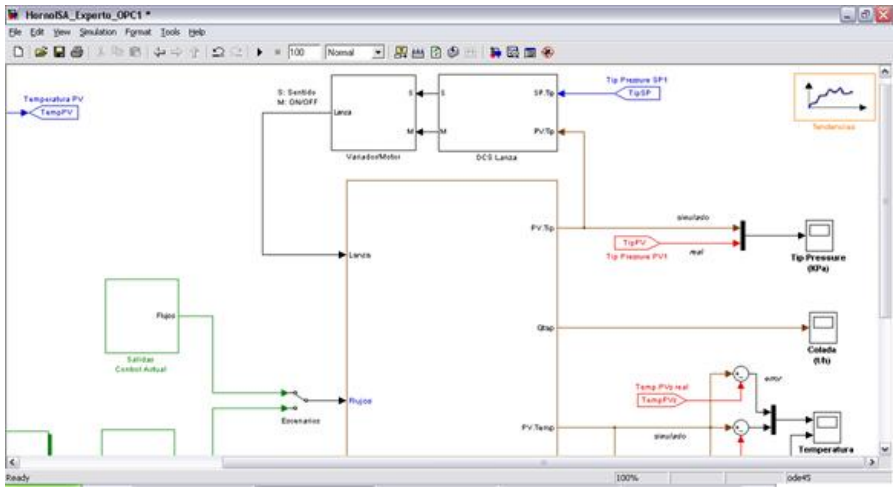

Figure 6.5: OPC platform

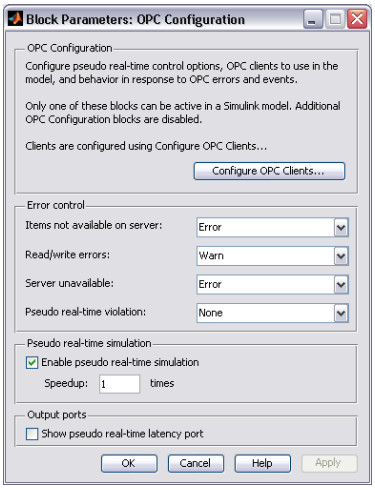

Figure 6.6: Parameters of OPC setting

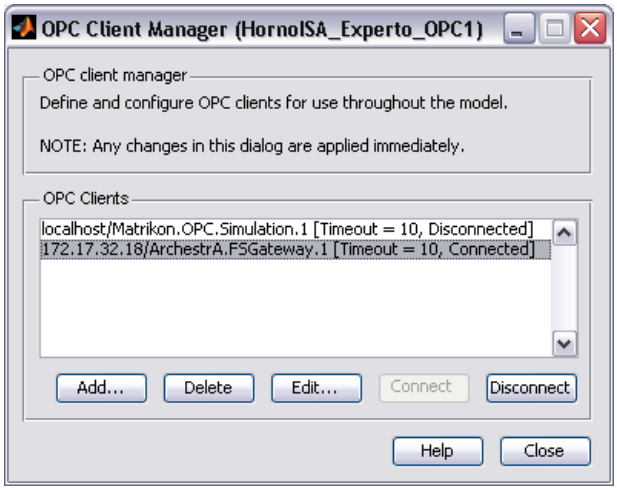

Figure 6.7: OPC address for tests

The table 6.2 presents the summary of the comparison results between the current control system and the control design.

Behavior comparison of molten bath temperature using PID and fuzzy controllers are graphically presented in figures 6.9 and 6.10.

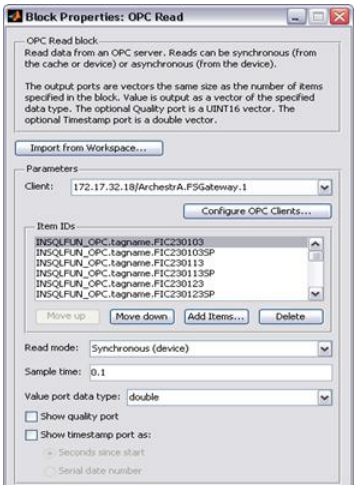

Figure 6.8: OPC tags

Table 6.2: On-line comparison of controllers

Test	PID controller using thermocouples average (e_{rms})	PID controller using control thermocouple(e_{rms})	Fuzzy controller (e_{rms})
1	2,2440%	1,1580%	0,2588%
2	1,859%	0,7924%	0,2162%
3	1,291%	0,2138%	0,1286%

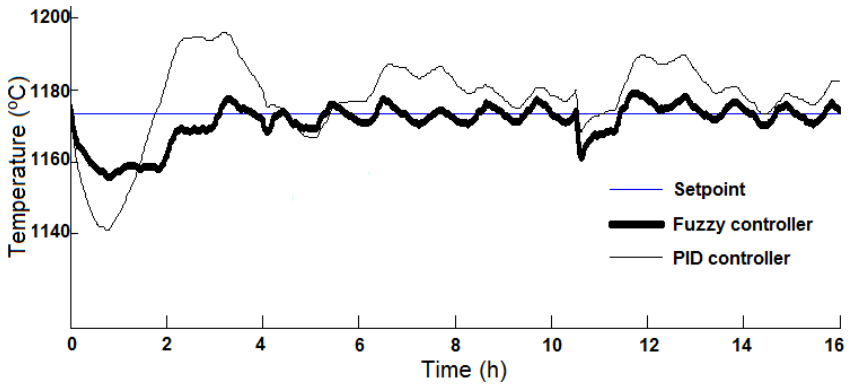

Figure 6.9: Comparison of PID and fuzzy temperature controller

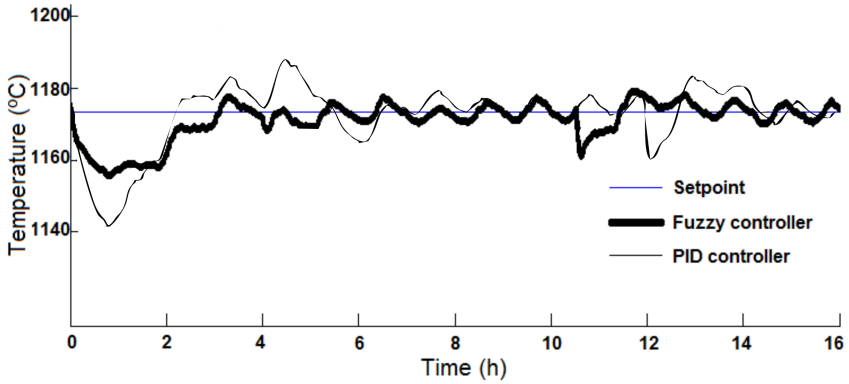

Figure 6.10: Comparison of PID and fuzzy temperature controller

6.2 Analysis of the extended fuzzy controller

In this section, the extended fuzzy based controller, described in subsection 5.2.2, is compared to the current PID controller in regulating the molten bath temperature. The controlled variable is regulated by modifying the percent of oxygen enrichment ($\%O_2$), the coal feed (t/h) and the flow rate of fuel oil (l/h) (see figure 6.11).

The proposed fuzzy controller reduces the standard deviation of the furnace temperature in approx. 61% (on average from 24,23°C to 9,33°C) in comparison to current PID controller. Forecasting of the furnace tapping composition (Cu in matte and SiO_2 in the slag) is helpful to reach this improvement.

Table 6.3: Comparison of controllers

Test	Standard deviation σ	
	PID controller (°C)	Fuzzy controller (°C)
1st test	24,3	8,2
2nd test	20,4	10,6
3rd test	28	9,2

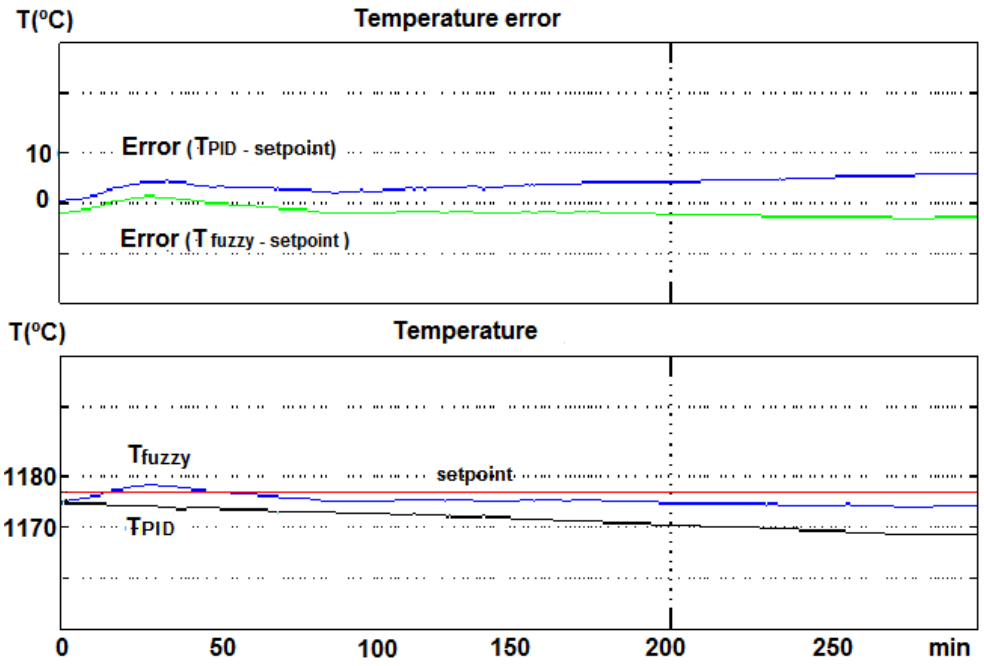

Figure 6.11: Simulated temperature

6.3 Holistic indexes

Indexes provide quantitative and reliable references in industrial processes. They should be measurable, reachable, relevant, reliable, comparable and contextually appropriate. In control theory, indexes are used to evaluate the control performance and help to move design features toward a desired pattern Lavaei et al. [2010].

However, the main disadvantage of conventional indexes is the difficulty of linking control performance and process efficiency, and therefore to convert such ratios into economic measures. This kind of methods are usually not enough to determine the impact of the control design and operation on productivity growth (see figure 6.12).

The differences between the temperature set point and the reached values from both controllers are calculated by the mean square relative error (6.2) and the dispersion of these values by the standard deviation (σ). In addition to these performance measures, single indexes based on the process productivity are

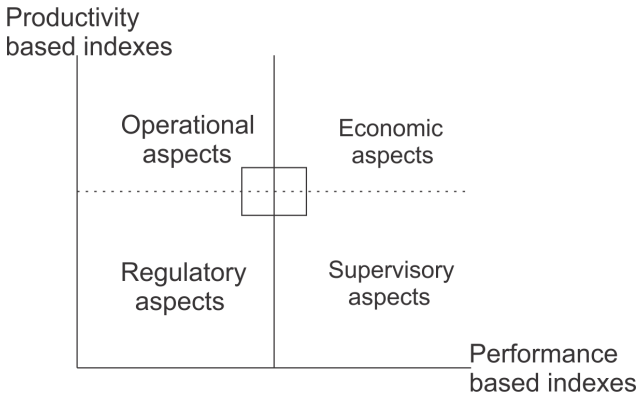

Figure 6.12: Performance/productivity indexes

proposed. Those indexes are the time efficiency and the energy consumption by copper smelting.

Time efficiency (TE) is an index of the furnace operation availability (6.2). It is calculated by dividing the cumulative stopover time of furnace operations over a six month period (stopovers are caused by high temperature oscillations due to poor control).

The energy consumption is a productivity based index that is defined as the ratio of tons of smelted concentrate to 1 ton of required resources such as coal (6.3) and fuel oil (6.4). These indexes based on the energetic usage evaluate productivity effects of the control precision. A typical issue occurs when the control fails to maintain the process heat above 1100°C, coal and eventually oil undergo a rapid increase in temperature due to their intensive energy release.

$$TE = \frac{stopover}{six\_month} = \frac{stopover(h)}{4380(h)} \tag{6.2}$$

$$\frac{t_{conc}}{t_{coal}} = \frac{\sum_{i=1}^{N} \frac{\left(t_{conc}/h\right)_i}{\left(t_{coal}/h\right)_i}}{N} \tag{6.3}$$

$$\frac{t_{conc}}{l_{oil}} = \frac{\sum_{i=1}^{N} \frac{\left(t_{conc}/h\right)_i}{\left(l_{oil}/h\right)_i}}{N} \tag{6.4}$$

where t represents tonnes, h hours and l liters.

Summary of performance and productivity indexes are shown in table 6.4. Fuzzy controller regulated better the molten bath temperature and resulted more efficient than the current PID controller. It followed the set point of temperature more closely and made a better use of energetic resources like coal and oil.

Table 6.4: Indexes of Operation

Index	PID Controller	Fuzzy Controller
Performance Measurement		
Mean square relative error of temperature (erms)	0,7214% (on-line average lecture)	0,2012%(on-line average lecture)
Standard deviation (σ)	27,8°C	11,1°C
Productivity Criteria		
Hours of plant stopover per hour of operation (TE)	0,00103	$8{,}447.10^{-4}$
Tonnes of smelted concentrate per liter of oil (TCO)	0,4397	0,5672
Tonnes of smelted concentrate per ton of coal (TCC)	151,47	171,345

The fuzzy controller closely follows the temperature setpoint (reducing e_{rms} in 72% and σ in 60% with respect to conventional control) and makes a better use of energetic resources like coal (6.5) and oil (6.6).

$$\Delta P = \frac{P_2 - P_1}{P_1}(100) = \frac{171,35 - 151,47}{151,47}(100) = 13\% \tag{6.5}$$

$$= \frac{0,57 - 0,44}{0,44}(100) = 29\% \tag{6.6}$$

In absolute terms, if the plant operates at full capacity for a year to produce 1.200.000 tonnes of copper concentrate, instead of using about 8.000 tonnes of coal by the current control, will only require 7.000 tonnes of coal by the proposed fuzzy control. This analysis indicates that reduction of energetic resources by control improvement clearly increases the productivity rate.

6.4 Concluding remarks

In this chapter, the comparative analysis of the conventional control system and the proposed control design has been presented. The oxygen enriched air has been manipulated by fuzzy rules instead of using static feed recipe calculations. The proposed control schema presents better performance in regulating the molten bath temperature than the current control model.

The bath temperature has presented a better regulation under normal operating conditions. Forecasting of furnace tapping composition (Cu in matte and SiO_2 in the slag) is helpful to reach this improvement. The mean square relative error of temperature error is reduced from 0,7214% to 0,2012% (72%) and the temperature standard deviation from 27,8°C to 11,1°C (approx. 60%).

The productivity based indexes for control assessment better links operational improvements to monetary aspects. Such indexes establish a lower consumption of raw materials (13%) and energy supply (29%). Another conclusion is that productivity based indexes provide a fair information about the control efficiency and complement performance based indexes.

Chapter 7

Conclusions and future works

7.1 Conclusions

In this thesis dissertation, contributions to the study and design of advanced controllers and their application to smelting furnaces have been discussed. For this purpose, this kind of metallurgical plants has been described in detail. The case of study is a copper smelter located in south Peru, which yearly produces about 1200000 tonnes of copper concentrate.

The hypotheses are as follows: a) The control structure design based on Gibbs rule phase determines the number of freedom (or state variables) identified by the process analysis b) Control system improvements are addressed to regulate the state variables of thermodynamic equilibrium b) The flow rates of oxygen enriched - air is better regulated by a fuzzy controller than using current recipe calculations (therefore, the temperature controller reduces the standard deviations of the furnace temperature) c) Productivity based indexes provide fair information about operating controllers in industrial context and d) Performance based indexes are complementary to productivity based indexes.

The smelting process within the Isasmelt furnace has been modeled in chapter 3. The mathematical representation is based on first principles; that means, mass and energy dynamic balances. This model describes the reaction mechanisms of copper concentrate in presence of oxygen-enriched air. This model has been simulated on a Matlab-Simulink platform (previously validated by comparing real and simulated output variables: bath temperature and tip pressure) as a

reference to make technical comparisons between the current and the proposed control systems.

This auto-thermal process, maintained by the sulfur of the chalcopyrite, is regulated by the DCS control logic using a cascade strategy: an outer loop with a PID temperature controller and inner loops composed of PID controllers to regulate the flow rates of oxygen, air (also known as combustion air) and eventually fuel oil (see chapter 4). The ratios of oxygen to concentrate and coal (or oil) is individually set through preset recipe calculations. This algorithm is then based on the oxygen demand of main components. However, such ratios can be adjusted after analyzing the molten material, taking into account the target matte grade and the silica content of bath slag. This method unfortunately introduces long time delays which leads to large temperature deviations in range between 15°C and 30°C from the set point, which causes refractory brick wear and lance damage, and subsequent higher costs of production.

This limitation to regulate the bath temperature is the starting point to this research. This analysis is focused on better control the state variables of copper smelting; also called intensive properties, that describe the thermodynamic equilibrium of this system: bath temperature, matte grade (% Cu), silica composition in the slag ($\%SiO_2$) and partial pressure (or SO_2 pressure). The proposed control structure includes a fuzzy controller to determine the percentage of oxygen enrichment (%O2) and the oil flow rate, instead of using the current calculation method. The controller alternatively manipulates such ratios to closely attain the temperature set point (see chapter 5).

The fuzzy controller emulates the best furnace operator by manipulating the oxygen enrichment rate and the oil feed in order to control the bath temperature. The human model is selected taking into account the operator' practical experience in dealing with the furnace temperature (and taking into account good practices from the Australian Institute of Mining and Metallurgy). This fuzzy module is complemented by a predictive model designed using neural network architecture. The prediction determines the mate grade (range of 60-65%Cu) and slag composition (range of $32-34\%Si_O$) under normal operating conditions. This mechanism removes time delays generated by the chemistry analysis of every tap. The oxygen ratios are adjusted in time based on the prediction of the molten

material. This application provides an optimal control of the tapping flow along with the fuzzy controller.

To systematically evaluate the furnace operation behavioral indexes related to energy costs and productivity have been proposed. Those indexes are used along to traditional performance based indexes. This analysis is performed using stored data from the Isasmelt plant. The proposed control system achieves a consistent mean square relative error reduction of 72% between measured values and the temperature set point and standard deviation of approx. 60% (from 27,8°C to 11,1°C). Productivity indexes establishes a lower consumption of raw materials (13%) and energy supply (28%), using the proposed control system in comparison to the current model (see chapter 6).

The initial hypotheses are supported by thermodynamic criteria. The current study proposes a control structure to regulate the (independent) variables, also called intensive properties, that specify the thermodynamic equilibrium of the system. Therefore, the first task of this research is addressed to identify such variables.

The predictive model is successfully designed using neural network architecture. The prediction determines the mate grade (range of 60-65%Cu) and slag composition (range of $32 - 34\%$ SiO_2) under normal operating conditions. This mechanism removes time delays generated by the chemistry analysis of every tap. The oxygen ratios are adjusted in time based on the prediction of the molten material. This application provides an optimal control of the tapping flow along with the fuzzy controller.

The hypothesis about productivity based indexes provide fair information about operating controllers (proving the third hypotheses in this research), considering that performance based indexes are addressed on assessing the controller behavior. for example, productivity indexes establishes a lower consumption of raw materials (13%) and energy supply (28%), using the proposed control system in comparison to the current model. This information is not possible to obtain by current measuring methods.

7.2 Contributions

The contributions are summarized as follows:

- Advanced control techniques for furnace operation.
- Fuzzy controller for regulating the oxygen-enrichment rate.
- Design of a metallurgical predictor to remove time delays from this smelting process measurements.
- Mathematical modeling of the Isasmelt copper smelting process.
- Introduction of holistic indexes based on productivity criteria to evaluate the controller performance.
- Define thermodynamic criteria to improve thermal processes regulation. The (independent) variables, also called intensive properties, that specify the thermodynamic equilibrium of the system.
- Development of an algorithm to reduce implicit failures in semantic structure and rules redundancy in designing fuzzy controllers.
- Generalization of the proposed control system to smelting processes.

The first contribution is the introduction of advanced control techniques on the Isasmelt operation. A fuzzy controller to emulate the best furnace operator by manipulating the oxygen enrichment rate and the oil feed in order to control the bath temperature and a metallurgical neural network based predictor.

The second contribution is the use of fuzzy controller to better regulate the oxygen-enrichment rate (represented by the N2=O2 ratio) and the oil burn rate in the furnace. This method is widely extended in metallurgical furnaces.

The third contribution is a predictive model for forecasting the composition of molten material; that means, the matte grade ($\%Cu$) and silica percentage (SiO_2) in the slag. The neural network-based model takes into account stored data from sample essays. This application allows to remove dead times from chemistry sampling analysis. The predictive model together with the fuzzy logic

based controller better regulate the oxygen enriched air and therefore the furnace temperature. Publication related to this contribution: [Simulation of fuzzy and PID temperature control within an Isasmelt copper furnace. Transactions on Control Systems, 2013].

The fourth contribution is the modelling of copper smelting process in order to be simulated. This overview, based on first principles techniques, improves previous efforts to represent this process. This simulation, through the Matlab/Simulink software, is validated using stored data from an Isasmelt smelter in southern Peru. The whole plant simulation has been uploaded to the MATLAB website (www.mathworks.com).

The fifth contribution is the introduction of holistic indexes based on productivity criteria (like time efficiency or energetic usage such as coal and fuel oil) to evaluate the impact of control designs in addition to performance single indexes. Publication related to this contribution: [Holistic indexes for productivity control assessment, applied to the comparative analysis of PID and fuzzy controllers within an Isasmelt furnace. Transactions on Industrial Informatics, 2013].

A six contribution is the proposed methodology to design a control structure based on thermodynamic criteria. That means, the application of the Gibbs phase rule to identify (independent) variables, also called intensive properties, that specify the thermodynamic equilibrium and the use of IA techniques to control such variables. Publication related to this contribution: [Mejoras de estructuras de control basadas en criterios de equilibrio termodinámico. Revista Iberoamericana de Informática y Control, 2013].

Another contributions are the development of an algorithm to reduce implicit failures in semantic structure and to remove rules redundancy, the pragmatic integration of conventional and advanced control techniques for critical variables in the copper smelting process and the generalization of the proposed techniques to pyro-metallurgical processes.

7.3 Future works

There are several lines of research arising from this work which should be pursued; unexpected events' modeling within the furnace as for example accumulated accretions. This kind of events can lead to copper losses. On the other hand, the fuzzy model to determine the percentage of oxygen enrichment ($\%O_2$) and the oil flow rate is developed using Mandani's fuzzy system.

A line of research which is partially explored in this research is the predictive control technique. The cascade control strategy has been modified by introducing a model predictive controller as outer loop instead of using a PID controller. The inner loop is kept by using current PID controllers to regulate oxygen enriched air and fuel oil.

There is a possible research line to regulate this process using Takagi Sugeno's fuzzy theory, or an expert system to govern the set of PID controllers.

The distributed control system is another topic in which the theory of hardware collaborative could be tested to improve control systems of complex metallurgical processes (as copper smelting process).

The indexes based on productivity can be compared to each other in order to evaluate a control system; however there is not an optimal reference to establish a comparison and determine how close to this level the controller works.

Appendix 1 - Isasmelt model

The mathematical model for describing the Isasmelt temperature has been developed by using operation data from the real plant. The process values associated to the equation terms are the flow rates of oxygen and nitrogen, the feed rates of concentrate and fuel oil, and the bath temperature within the furnace. The tags to identify these variables in the DCS are detailed in table 1.

Table 1: Tags for parametric estimation in the DCS

Variable	Sensor
Oxygen flow rate	FIC103
Nitrogen flow rate	FIC113
Oil feed rate	FIC113
Concentrate feed rate	WY049
Bath temperature	TIC354

In order to determine the parametric vectors, it has chosen a sample size of 4320 records around the steady state operation; that is: $\dot{w}_{N_2} = 24068,93 Nm^3$, $\dot{w}_{conc} = 151 t/h$ and $\bar{T} = 1170°C$. This procedure has allowed to avoid sampling bias Hubert and Vandervieren [2007].

The data has been statistically treated as an approximately normal distribution, because of the central theorem, which states that, a large number of random variables is approximately normally distributed Jung [2003]. The mean and the standard deviation are, therefore, the most useful measures to study the process variables.

The sampling data has been analyzed to detect the presence of outliers. That is, unusually small or large numerical values distant from the rest of data points.

In this analysis, the outliers have been identified by using the box-plot diagram. This method graphically indicates such points outside the bounded figure. The block contains a data set of values between the lower (Q_1) and upper quartile (Q_4).

The box-plot of the group of process variables is shown in figure 1 and the temperature box-plot is presented in figure 2.

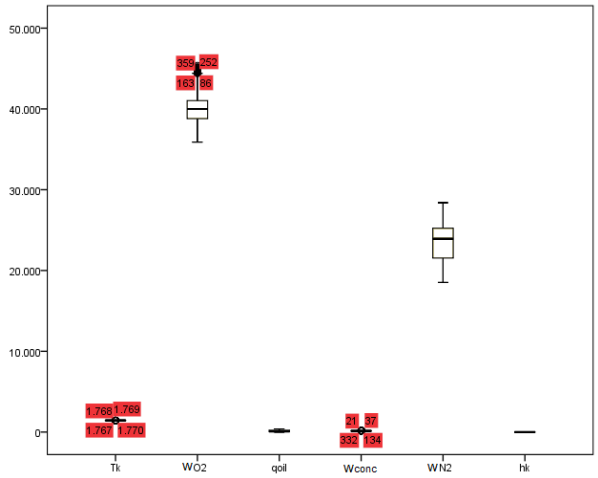

Figure 1: Box-plot of process variables

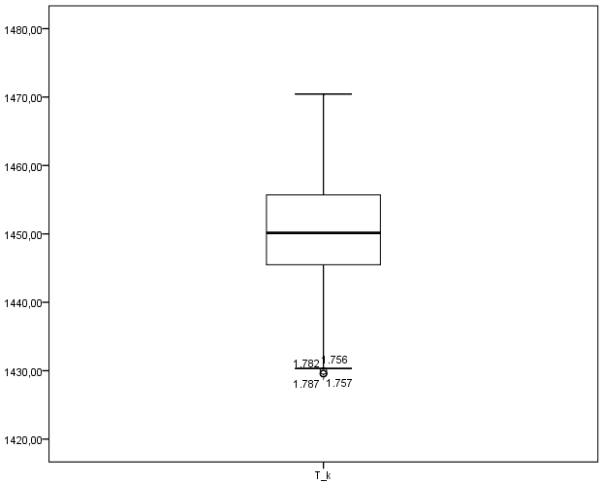

Figure 2: Box-plot of the temperature

The operations to obtain the temperature dynamics are described as follows:

$$\Delta T_{k+1} = T_{k+2} - T_{k+1} \tag{1}$$

$$\Delta T_k = T_{k+1} - T_k \tag{2}$$

Then

$$\Delta T_{k+1} - \Delta T_k = T_{k+2} - T_k \tag{3}$$

The valid observations have been used to get the model constants on the right side of the equation 4.

$$\begin{aligned} \frac{T_{(k+2)} - T_{(k)}}{10s} = \gamma_1 \left[\frac{w_{O_2(k+1)} - w_{O_2(k)}}{h_{(k)}} \right] + \gamma_2 \left[\frac{q_{oil(k+1)} - q_{oil(k)}}{h_{(k)}} \right] \\ - \gamma_3 \left[\frac{\bar{w}_{conc}(T_{(k+1)} - T_{(k)}) - \bar{T}(w_{conc(k+1)} - w_{conc(k)})}{h_{(k)}} \right] \\ -\gamma_4 \left[\frac{\bar{w}_{N_2}(T_{(k+1)} - T_{(k)}) - \bar{T}(w_{N_2(k+1)} - w_{N_2(k)})}{h_{(k)}} \right] \end{aligned} \tag{4}$$

The numerical values are introduced in a statistics processor to calculate the parameters.

k	T_k	w_{O2}	q_{oil}	w_{conc}	w_{N2}	h_k	f1	f2	f3	f4	f5		
	(kelvin)	(Nm3/h)	(l/h)	(t/h)	(Nm3/h)	(m)	x_1	x_2	x_3	x_4	y	$\bar{T}$	1443
1	1468,07	43832,25	0,00	165,20	27121,04	1,18	48,19777	0	49,868479	31030,52	0,11781006	$\bar{w}_{N2}$	24068,93
2	1468,63	43888,89	0,00	165,19	27137,00	1,18	-362,4382	0	1462,2347	389694,53	0,03950195	$\bar{w}_{conc}$	151,00
3	1469,25	43460,08	0,00	166,32	27446,16	1,24	-530,3438	0	1698,5833	267142,56	0,04030762	ts	10,00
4	1469,03	42803,49	0,00	167,80	27679,12	1,25	-38,07944	0	-1102,8282	-638954,15	0,08864746		
5	1469,65	42755,80	0,00	166,78	27114,11	1,31	539,6264	0	1512,2967	-109816,83	-0,0071167		
6	1469,91	43461,25	0,00	168,12	27010,31	1,31	310,5812	0	-2359,9012	209783,06	-0,06088867		
7	1469,58	43867,26	0,00	166,02	27205,86	1,31	-124,6936	0	-2167,5566	232059,80	-0,04462891		
8	1469,30	43704,26	0,00	164,08	27420,75	1,31	38,36049	0	-407,08032	-454932,29	-0,00450439		
9	1469,14	43754,40	0,00	163,73	27011,39	1,31	202,5061	0	-2425,5448	161003,30	0,0222168		
10	1469,26	44019,14	0,00	161,52	27155,22	1,31	-235,58	0,00	5337,55	258224,79	0,06804199		
11	1469,36	43711,17	0,00	166,35	27387,48	1,31	-397,71	0,00	-2750,59	21085,21	0,03895264		
12	1469,94	43191,25	0,00	163,79	27396,91	1,36	-66,75	0,00	-469,07	-302561,94	-0,06550293		
13	1469,75	43100,39	0,00	163,37	27114,70	1,36	-3,25	0,00	-1234,38	106315,43	-0,11685791		
14	1469,28	43095,97	0,00	162,26	27222,77	1,36	37,18	0,00	3890,05	-59122,26	-0,15093994		
15	1468,58	43146,60	0,00	166,00	27178,73	1,36	178,90	0,00	1918,33	-180214,79	-0,11502686		
16	1467,77	43390,19	0,00	167,89	27022,10	1,36	250,08	0,00	1946,64	-71667,36	-0,05181885		
17	1467,43	43730,57	0,00	169,77	26960,26	1,42	52,50	0,00	-2874,69	211814,92	0,04732666		
18	1467,26	43804,88	0,00	166,97	27170,92	1,42	-279,10	0,00	4029,77	162612,12	0,09046631		
19	1467,90	43409,67	0,00	170,85	27319,71	1,45	-20,02	0,00	-669,36	-205667,56	0,07696533		
20	1468,16	43380,70	0,00	170,15	27109,17	1,48	342,30	0,00	-1171,82	-210455,62	0,11209717		
21	1468,67	43886,74	0,00	168,90	26885,03	1,48	228,90	0,00	-5263,72	302701,02	0,06367188		
22	1469,28	44225,15	0,00	163,44	27184,98	1,46	-368,30	0,00	-4927,61	315673,49	0,06021729		
23	1469,31	43686,35	0,00	158,44	27504,56	1,41	-486,48	0,00	-3076,05	-27542,40	0,11297607		
24	1469,88	43000,83	0,00	155,38	27468,07	1,41	-167,26	0,00	8638,03	-341132,34	0,03873291		
25	1470,44	42765,23	0,00	163,75	27125,83	1,41	194,82	0,00	3471,78	-65948,42	-0,1526123		
26	1470,27	43039,64	0,00	167,16	27064,25	1,41	198,66	0,00	-2164,75	34851,81	-0,15686035		
27	1468,91	43319,35	0,00	165,19	27120,92	1,48	143,16	0,00	1744,54	36934,52	-0,05489502		
28	1468,70	43531,09	0,00	167,00	27162,27	1,48	310,36	0,00	-1679,10	-226376,82	-0,04445801		
29	1468,36	43990,09	0,00	165,32	26935,91	1,48	17,56	0,00	3048,21	337965,03	-0,0220459		
30	1468,26	44016,06	0,00	168,45	27284,06	1,48	-444,56	0,00	-649,57	136134,74	0,04078369		
31	1468,14	43358,58	0,00	167,80	27425,50	1,49	-129,44	11,38	-3124,80	-478619,55	0,03260498		

Figure 3: Process variables

Then, the coeficients are estimated using least squares method (multiple linear regresion).

Dependent Variable: F5_Y
Method: Least Squares
Date: 03/02/13 Time: 22:14
Sample (adjusted): 1 4319
Included observations: 4319 after adjustments

Variable	Coefficient	Std. Error	t-Statistic	Prob.
F1_X1	-3.42E-05	2.94E-06	-11.64185	0.0000
F2_X2	-0.000745	0.000134	-5.564042	0.0000
-F3_X3	-3.47E-07	2.98E-07	-1.162790	0.2450
-F4_X4	-2.13E-09	2.79E-09	-0.763261	0.4453

R-squared	0.038891	Mean dependent var	-0.000791
Adjusted R-squared	0.38223	S.D. dependent var	0.056908
S.E. of regression	0.055809	Akaike info criterion	-2.932824
Log likelihood	6337.434	Schwarz criterion	-2.926924
Durbin-Watson stat	0.502810	Hannan-Quinn criter.	-2.930741

Figure 4: Statistic report

The expression finally becomes as

$$T_{k12} = T_k + t_s[f_{1k}f_{2k} - f_{3k} - f_{4k}]\Gamma \tag{5}$$

where $t_s = 10s$ and

$$\Gamma = \begin{bmatrix} \gamma_1 \\ \gamma_2 \\ \gamma_3 \\ \gamma_4 \end{bmatrix} = \begin{bmatrix} -3,4236 \times 10^{-5} \\ -7,4544 \times 10^{-4} \\ -3,4662 \times 10^{-7} \\ -2,1333 \times 10^{-9} \end{bmatrix} \tag{6}$$

The predicted output is presented in figure 5.

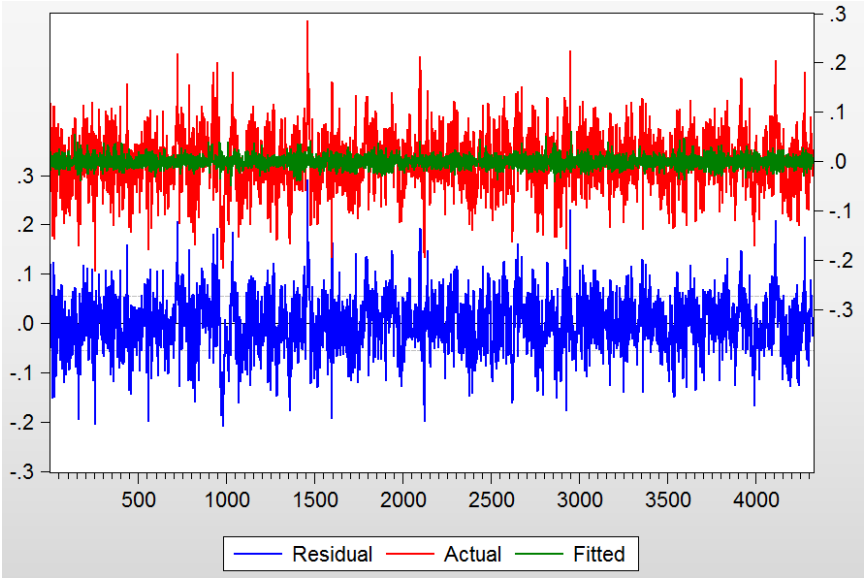

Figure 5: Predicted output

Appendix 2 - Reverts fuzzy controller

In this appendix, it is explored as a future line of research the use of lower cost materials to regulate the bath temperature. The recycled material of molten concentrate is analyzed, because of its influence into the heating system. The design is addressed to emulate the performance of a human operator in dealing with waste material.

This application is described as triangular functions (see figure 6). The negative slope depicts the start and the end of casting positions at bottom right and at top left respectively. The second scenario corresponds to the lance position (when is raising) represented by positive sloping curve.

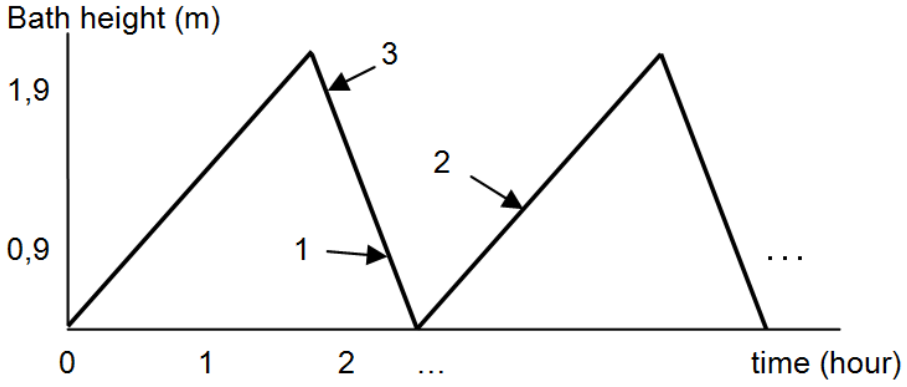

Figure 6: Representation of working scenarios

The rules are defined under normal conditions in different scenarios: at the start or out of casting as well as the lance hoist within the furnace.

The inference mechanism of this rule-based control system is initially performed by 75 rules. However, this structure is finally simplified to 27 rules based on the Pareto's criterion. That means, 20% of the rules which explains 80% of the most important working scenarios (see table 2). Mamdani's max-min composition algorithm as inference mechanism. The defuzzification strategy used for this controller is the gravity center criterion Chiu and Chang [2012].

Table 2: Description of the Working Scenarios

Scenario	Meaning	Conditions to be satisfied
1	Out of casting	H is N and Mov is N
2	Lance hoist	H is Z and Mov is P
3	Start of casting	H is P and Mov is N

The inference matrix obtained from the base of rules involves the bath temperature and its variation rate for each working scenario (see table 3).

Table 3: Initial Inference Matrix

Scenario	T / dT	MN	N	Z	P	MP
1	MN	Fn4	Fn2			
	N				Fn2	Fn1
	Z	Fn3				
	P			0	Fp1	Fp1
	MP			Fp1	Fp1	Fp2
2	MN	Fn3				
	N	Fn2	Fn1	0	0	Fp1
	Z			0	Fp1	
	P			0	Fp2	Fp2
	MP					Fp3
3	MN	Fn3	Fn1			
	N	Fn2				
	Z	Fn2				
	P	Fn1			Fp1	
	MP	0		Fp2	Fp2	Fp3

In this fuzzy model the minimum implication method is used. That means, the fuzzy logic controller truncates the output membership functions at the value

of the corresponding rule weights Santos [2011]. Fuzzy rules operate using a series of "IF", "AND" and "THEN" statements, i.e. as follows:

- Literally: IF the third defined scenario (start of casting) is active, AND the temperature is almost 10°C below the set point, AND the temperature sharply tends to drop, THEN the recycle flow change must be reduced in 2 tph.
- Furthermore, IF the third scenario is replaced by another working scenario, represented by the bath height and lance drive and given by fuzzy rules as follows: IF H is P AND Mov is P AND T is MN AND dT is MN THEN VRev is Fn2

Table 4: Validated Inference Matrix

Scenario	T / dT	MN	N	Z	P	MP
1	MN	Fn4	Fn3	Fn2	Fn1	0
	N	Fn3	Fn2	Fn1	Fn2	Fn1
	Z	Fn3	Fn1	0	0	Fp1
	P	Fn2	0	0	Fp1	Fp1
	MP	Fn1	Fp1	Fp1	Fp1	Fp2
2	MN	Fn3	Fn2	Fn1	Fn1	0
	N	Fn2	Fn1	0	0	Fp1
	Z	Fn1	0	0	Fp1	Fp2
	P	0	0	0	Fp2	Fp2
	MP	0	Fp1	Fp1	Fp2	Fp3
3	MN	Fn3	Fn1	Fn1	0	0
	N	Fn2	0	0	0	0
	Z	Fn1	0	0	0	Fp1
	P	0	0	0	Fp1	Fp2
	MP	0	Fp1	Fp2	Fp2	Fp3

Table 4 shows the comparison of the human operator commands with respect to the fuzzy controller actions (maximum errors of 0,5 tons per hour, as the practical sensor resolution is of 0,5 tons). That means a maximum recycle flow error of 2,7% according to:

$$error \triangleq \frac{resol.}{recycleflow} = \frac{0,5}{18,3} = 0,027 \tag{7}$$

Figures 7 and 8 depict the proposed controller commands for the recycle flow change and the dynamics of the molten bath height during the test operations. This analysis graphically verifies the design consistence and adequate implementation of the control system.

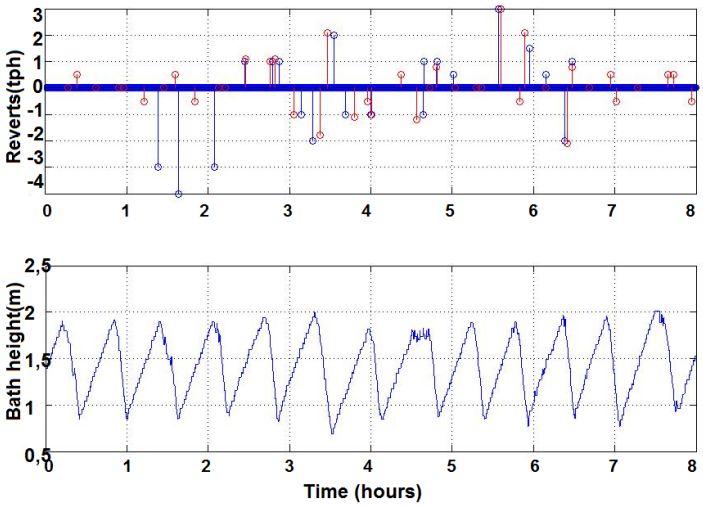

Figure 7: Analysis of reverts and bath height - Test 1

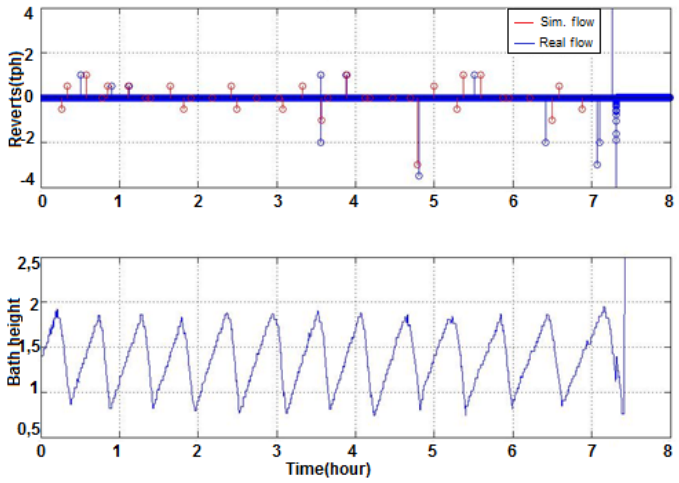

Figure 8: Analysis of reverts and bath height - Test 2

Appendix 3 - Skills and knowledge requirements for furnace operation

In this appendix, the summary of knowledge and skills required for smelting furnace operations are detailed. Those requirements are based on the Metal and Engineering Training Package and on good mining practice.

Required knowledge (k_i):

- Refractory conditions, faults, and routine repair (k_1).
- Starting procedures for the furnace (k_2).
- Metallic charge materials and alloying elements (k_3).
- Weighing procedures and scale types (k_4).
- Correct order of loading of different charge materials (k_5).
- Thermocouple condition monitoring to estimate mate temperature and adjustment mechanism for furnace (k_6).
- Interpretation of matte grade, and quantity of matte in the furnace (k_7).
- Degassing procedures including tablet, lance and other procedures (k_8).
- Close-down procedures (k_9).

- Applicable industry standards (k_{10}).
- Safe work practices and procedures (k_{11}).
- Hazards and control measures associated with operating melting furnaces (k_{12}).

Required skills (s_i):

- Reading and interpreting routine information on written job instructions, specifications, standard operating procedures relevant test data sheets and other standard workplace forms (s_1).
- Following oral instruction (s_2).
- Identifying faults and areas for routine repair of the furnace and performing routine maintenance (s_3).
- Following procedures for starting and closing down the furnace (s_4).
- Deciding on charge materials (s_5).
- Weighing charge materials (s_6).
- Feeding materials into furnace (s_7).
- Measuring metal temperature and correcting as necessary (s_8).
- Sampling for chemical, carbon equivalent and wedge tests (s_9).
- Degassing as necessary (s_{10}).
- Deslagging/drossing (s_{11}).
- Tapping the metal (s_{12}).

Appendix 4 - Model predictive controller

In the alternative control structure, the outer loop of the cascade control strategy (described in section 3.1) has been modified by including a predictive controller instead of the current PID temperature controller. The inner loop is composed of dependent PID controllers to regulate oxygen, air and oil flow rates.

A first-order plus dead-time model is used to linearly approximate the system response.

$$G(s) = \frac{K}{1 - \tau s} e^{-\tau_d s} \tag{8}$$

The plant (including the inner control loop) has been identified by exciting the system with open-loop step inputs (between input and output points) Bordons et al. [2007].

$$Y(s) = \begin{bmatrix} \frac{0{,}0297(1+3074{,}4s)}{1+92065s} e^{-2{,}42s} & \frac{3{,}58(10^{-8})}{s(1+0{,}0018s)} e^{-0{,}0046s} & \frac{0{,}848}{1+40787s} \end{bmatrix} \begin{bmatrix} U_1(s) \\ U_2(s) \\ U_3(s) \end{bmatrix} \tag{9}$$

where U_i represents the manipulated variables, i=1 (oxygen), i=2 (air) and i=3 (oil).

This model has 2 inputs (the bath temperature and its set point) and three outputs which fix setpoints of air, oxygen and oil. The predictive controller is

based on GPC algorithm, which consists of applying a control sequence that minimizes a multistage cost function of the form:

$$J(N) = \sum_{j=d+1}^{d+N} [\widehat{y}(t+j|t) - \omega(t+j)]^2 + \sum_{j=1}^{N} \lambda[\Delta u(t+j-1)]^2 \qquad (10)$$

The control parameters are as follows: range of 0.5 seconds, a time horizon of 15 steps prediction and control horizon of 10 steps. Also, there have been limits to the manipulated variables 0 to $40,000m^3/h$ for the oxygen and 0 to $40,000m^3/h$ for air flows, and 0 to $1,200l/h$ for oil feed.

References

G. Alvear, P. Arthur, and P. Partington. Feasibility to profitability with copper Isasmelt. *Pyrometallurgy I, Proceedings of Copper 2010*, 5:615–630, 2010. 41

P. Arthur and S. Hunt. Isasmelt - 25 years of continuous evolution, Xstrata technology. *M. Nilmani and W. Rankin, Eds., NCS Asociates*, pages 73 – 94, 2005a. John Floyd International Symposium on Sustanaible Developments in Materials Processing. 61

P. Arthur and S. Hunt. Isasmelt - 25 years of continuous evolution. *Australian Institute of Mining and Metallurgy*, pages 73–78, 2005b. John Floyd International Symposium Sustainable Developments in Metals Processing. 35

P. S. Arthur. Isasmelt - 6.000.000 tpa and rising. *The Minerals, Metals and Materials Society. Sohn International Symposium of Metals and Minerals*, 2006. 61

Australian National Training Authority. *Metal and Engineering Training Package (MEM05)*, volume 2. Manufacturing Industry Skills Council, Sidney, Australia, 2005. 73

Carlos Bordons, Manuel R. Arahal, Eduardo F. Camacho, and Jos M. Tejera. Energy saving in a copper smelter by means of model predictive control. *Identification and Control. The Gap between Theory and Practice*, pages 63–85, 2007. 125

Jose Manuel Cano-Izquierdo, Julio Ibarrola, and Miguel Almonacid Kroeger. Control loop performance assessment with a dynamic neuro-fuzzy model

(dfasart). *IEEE Transactions on Automation Science and Engineering*, 9:377–389, 2012. 25

Chunlin Chen, Ling Zhang, and Sharif Jahanshahi. Thermodynamic modeling of arsenic in copper smelting processes. *Metallurgical and Materials Transactions B*, 41B:1175–1185, 2010. 18

Chih-Hui Chiu and Chun-Chieh Chang. Design and development of mamdani-like fuzzy control algorithm for a wheeled human-conveyance vehicle control. *IEEE Transactions on Industrial Electronics*, 59 (11):4443–4455, 2012. 120

R. A. Cockerell, S. Crisafulli, A. G. Hunt, and A. A. Shook. Application of advanced process control to copper smelting. *The Mineral Metals and Materials Society*, 5:655–670, 1999. Copper 99 - Smelting Operations and Advances. 20

P. Coursol and N. Stubina. Arsenic and lead volatilization from molten copper at high oxygen levels. *Metallurgical and Materials Transactions B*, 36B:411–413, 2005. 18

Michel Dussud, Sylvie Galichet, and Laurent P. Foulloy. Application of fuzzy logic control for continuous casting mold level control. *IEEE Transactions on Control Systems Technology*, 6 (2):246–256, 1998. 21

W. Errington, J. Edwards, and P. Hawkins. Isasmelt technology - current status and future development. *The Journal of The South African Institute of Mining and Metallurgy*, 79(5):161–167, 1997. 62

Gang Feng. A survey on analysis and design of model-based fuzzy control systems. *IEEE Transactions on Fuzzy Systems*, 14(5):676–697, 2006. 24

T. J. Harris. Assessment of control loop performance. *Canadian Journal of Chem. Eng.*, 67(10):856–861, 1989. 24

P. Havl. Overview of automatic control of glass furnaces. *Ceramics - Silikáty*, 50(1):51–55, 2006. 76

J. R. Hilera and V. J. Martínez. *Redes neuronales artificiales. Fundamentos, modelos y aplicaciones*. Editorial Alfaomega Ra-Ma, 2000. 76

Zhennan Hong, Yifa Sheng, Junhong Li, Masao Kasuga, and Liang Zhao. Development of ac electric arc-furnace control system based on fuzzy neural network. *Proceedings of the 2006 IEEE International Conference on Mechatronics and Automation*, pages 2459–2464, 2006. 24

M. Hubert and E. Vandervieren. An adjusted boxplot for skewed distributions. *Proc. Amer. Math. Soc.*, 1(52):822–824, 2007. 113

Zhao Hui, Chen Fa-zheng, and Zhao Zhuo-qun. Study about the methods of electrodes motion control in the eaf based on intelligent control. *2010 International Conference on Computer, Mechatronics, Control and Electronic Engineering*, pages 68–71, 2010. 23

Mohieddine Jelali. *Control System Performance Monitoring*. Fakultät für Ingenieurwissenschaften, Abteilung Maschinenbau und Verfahrenstechnik der Universität Duisburg-Essen, 2010. 9, 24

Jiang Jing and Zhang Xuesong. Research on fuzzy-pid control algorithm from the temperature control system. *3rd IEEE International Conference on Computer Science and Information Technology (ICCSIT)*, 4:152–155, 2010. 23

S. T. Johansen. Mathematical modeling of metallurgical processes. *Proceedings of the 3rd International Conference on CFD in the Minerals and Process Industries*, pages 5–12, 2003. 20

Shao Jung. *Mathematical Statistics*. Springer, New York, 2003. 113

Tak Seng Kho. Microelement distribution during matte smelting. *Dissertation submitted in fulfillment of the requirements for the degree of Doctor of Philosophy in Engineering. School of Civil & Chemical Engineering*, RMIT University, 2006. 36

Michael J. King. The evolution of technology for extractive metallurgy over the last 50 yearsis the best yet to come? *Journal of the Minerals, Metals, and Materials Society*, 59(02):21–25, 2007. 16

J. Lavaei, S. Sojoudi, and A. G. Aghdam. Pole assignment with improved control performance by means of periodic feedback. *IEEE Transactions on Automatic Control*, 55(1):1082–1087, 2010. 102

Gibum Lee, J. H. Heo, and Moon G. Joo. Weighing control of alloy metal for electric arc furnace by fuzzy system. *Second International Conference on Future Generation Communication and Networking Symposia*, 1 (9-11):44–48, 2008. 21

Wang Lei, Sun Hui, Cui Ming-yuan, Yang Hong, and Wang Qiong. The simulation study on temperature control system of nitriding electric-furnace based on fuzzy-pid control. *2009 First International Worshop on Education Technology and Computer Science*, pages 361–365, 2009. 23

C. S. Li and C. Y. Lee. Self-organizing neuro-fuzzy system for control of unknown plants. *IEEE Transactions on Fuzzy Systems*, 11(1):135–150, 2003. 24

Zenghuan Liu, Likong Li, Lu Wen, and Guangxiang He. Analysis of heating furnace temperature control system based on expert fuzzy control. *2009 International Conference on Measuring Technology and Mechatronics Automation*, 2:542–545, 2009. 23

I. M. MacLeod, W. Harlen, R. A. Cockerell, and S. Crisafulli. Temperature control of a copper Isasmelt plant. *Australian Journal of Instrumentation and Control*, 10:10–20, 1995. 19, 42

D. McKee. P9l process controlthe optimisation of mineral processes by modelling and simulation. *Australian Mineral Industry Research Association*, 1:21–25, 1999. 15

Vicente Milans, Jorge Villagr, Jorge Godoy, and Carlos Gonzlez. Comparing fuzzy and intelligent pi controllers in stop-and-go manoeuvres. *IEEE Transactions on Control Systems Technology*, issue: 99:1–9, 2011. 23

S. Mitra and Y. Hayashi. Neuro-fuzzy rule generation: Survey in soft computing framework. *IEEE Transactions on Neural Network*, 11(3):748–768, 2000. 24

Un-Chul Moon and Kwang Y. Lee. Hybrid algorithm with fuzzy system and conventional pi control for the temperature control of tv glass furnace. *IEEE Transactions on Control Systems Technology*, 11 (4):548–554, 2003. 21

Un-Chul Moon and Kwang Y. Lee. A practical multiloop controller design for temperature control of a tv glass furnace. *IEEE Transactions on Control Systems Technology*, 15 (6):1137–1142, 2007. 20

A. B. Morrow and M. Gajaredo. *Control of copper Teniente smelting units using integrated advanced control technologies*. Editors H. Chan, L. Ryan and S. Kennedy. Process control applications in mining and metallurgical plants, Montreal, 2009. 17

M. Nagamori. Thermodynamic behaviour of arsenic and antimony in copper matte smelting - a novel mathematical synthesis. *Canadian Metallurgical Quarterly*, 40(4):499–522, 2001. 18

M. Nagamori, W. Errington, P. J. Mackey, and D. Poggi. Thermodynamic simulation model of theisasmelt process for copper matte. *Metallurgical and Materials Transactions B*, 5 (6):839–853, 1994. 18, 38

Yuhua Pan and David Langberg. Physical and mathematical modeling investigations of the mechanisms of splash generation in bath smelting furnaces. *Seventh International Conference on CFD in the Minerals and Process Industries*, 2010. 20

Chandrashekhar G. Patil and Mahesh T. Kolte. An approach for optimization of hadnoff algorithm using fuzzy logic system. *Computational Statistics and Data Analysis*, 2 (1):5186–5201, 2008. 21

R. L. Player. Copper Isasmelt. Process investigation. *Mount Isa Mines Limited, Mount Isa*, 22(5):655–670, 1996. 41

M. Pokorny and Z. Buzek. Hybrid numerical and non-numerical artificial intelligence approaches in steel-making monitoring and control. *ISIE 2003. IEEE International Symposium on Industrial Electronics*, 1 (9-11):444–447, 2003. 21

M. Ramírez, R. Haber, V. Pena, and Iván Rodriguez. Fuzzy control of a multiple hearth furnace. *Computers in Industry*, 54(1):105–113, 2004. 23

Karl Åström and Tore Hägglund. *Adavanced PID Control*, pages 158–172. ISA - Instrumentation, Systems and Automation Society, New York, 2006. 63

L. B. Ristic and B. I. Jestenic. Implementation of fuzzy control to improve energy efficiency of variable speed bulk material transportation. *IEEE Transactions on Industrial Electronics*, 59(7):2959–2969, 2012. 74

Jos Rodriguez, Ralph M. Kennel, Jos R. Espinoza, Mauricio Trincado, Csar A. Silva, and Christian A. Rojas. High-performance control strategies for electrical drives: an experimental assessment. *Transactions on Industrial Electronics*, 59(2):812–820, 2012. 65

G. Roghani, Y. Takeda, and K. Itagaki. Phase equilibrium and minor element distribution between feox-sio2-mgo-based slag and cu2s-fes matte at 1573 k under high partial pressure of so2. *Metallurgical and Materials Transactions B*, 31(B):705–712, 2000. 17, 136

S-L.Jämsä-Jounella, R. Poikonen, Z. Georgiev, U. Zuehlke, and K. Halmevaara. Evaluation of control performance: Methods and applications. *Proceeding of the 2002 IEEE lnternational- Conference on Control Applications*, pages 681–686, 2002. 26

M. Santos. Un enfoque aplicado del control inteligente. *Revista Iberoamericana de Automática e Informática Industrial*, 8:283–296, 2011. 121

Mark E. Schlesinger, Mthew J. King, Kathryn C. Sole, and William G. Davenport. *Extractive metallurgy of copper*. El Sevier Ltd. Fith edition, Oxford, 2011. 16, 136

J. C. Shen. Fuzzy neural networks for tuning pid controller for plants with underdamped responses. *IEEE Transactions on Fuzzy Systems*, 9(2):334–342, 2001. 24

A. Steinboeck, K. Graichen, and A. Kugi. Dynamic optimization of a slab reheating furnace with consistent approximation of control variables. *IEEE Transactions on Control Systems Technology*, 19(6):1444–1456, 2011. 42

Philip Thwaites. Process control in metallurgical plants - from an Xstrata perspective. *Annual Reviews in Control*, 31:221–239, 2007. 21

S. Ueda, S. Natsui, H. Nogami, J. Yagi, and T. Ariyama. Recent progress and future perspective on mathematical modeling of blast furnace. *ISIJ Int.*, 50(7): 914–923, 2010. 21

F. Vode, A. Jakli, T. Kokalj, and D. Matko. A furnace control system for tracing reference reheating curves. *Steel Res. Int., Metal Forming*, 79(5):364 – 370, 2008. 59

W. Y. Wang, C. Y. Cheng, and Y. G. Leu. An online ga-based output-feedback direct adaptive fuzzy-neural controller for uncertain nonlinear systems. *IEEE Transactions on Systems, Man, and Cybernetics - Part B*, 34(1):334–345, 2004. 24

Gui Wei-hua, Wang Ling-yun, Yang Chun-hua, Xie Yong-fang, and Pen Xiao-bo. Intelligent prediction model of matte grade in copper flash smelting process. *Transactions of Nonferrous Metals Society of China*, 17:1075–1082, 2007. 84

Yuezhi Yea and Junghui Chen. Diagnosis of closed control loop status using performance analysis based approach. *Industrial and Engineering Chemistry Research*, 44(15):5660–5671, 2005. 24

Fu yong Su and Zhi Wen. Application of fuzzy control technology in temperature setting of regenerative rotary reheating furnace. *2010 Seventh International Conference on Fuzzy Systems and Knowledge Discovery*, pages 1205–1208, 2010. 23

Ling Yun, Chen Gang, and Liu Zhongwei. Design and optimization of integrated controller for vacuum sintering furnace. *2009 International Conference on Energy and Environment Technology*, pages 257–260, 2009. 23

R. Zapata. *Continuous reactor Altonorte smelter*. Editors A. E. M. Warner, C. j. Newman, A. Vahed, D.G. George, P. J. Mackey, A. Warcok. Copper-Cobre 2007 The Carlos Diaz symposium on pyrometallurgy, 2007. 16

Liu Zenghuan, He Guangxiang, and Wang Lizhen. Improvement of heat furnace temperature control system via model free control method. *2010 International Conference on Measuring Technology and Mechatronics Automation*, 2:446–449, 2010. 23

Wen Xiao Zhao. Parametric identification of hammerstein systems with consistency results using stochastic inputs. *IEEE Transactions on Automatic Control*, 55(2):474 – 480, 2010. 43

Mo Zhi, Peng Xiaohong, and Xiao Laisheng. Research and application on two-stage fuzzy temperature control system for industrial heating furnace. *2009 International Conference on Intelligent Computation Technology and Automation*, 2:756–759, 2009. 23

Cui Zhi-xiang, Shen Dian-bang, Wang Zhi, Li Wei-qun, and Bian Rui-min. The theory and practice of copper smelting with oxygen enriched bottom blowing. *China Nonferrous Metallurgy*, 6, 2010. 61

List of Tables

List of Figures